Renal cell carcinoma:
advances in minimally invasive treatments and
outcome prediction.

Stephanie G.C. Kroeze

Renal cell carcinoma:
advances in minimally invasive treatments
and outcome prediction.

Kleine niertumoren:
vooruitgang bij minimaal invasieve behandelingen
en voorspelling van prognose

(met een samenvatting in het Nederlands)

Proefschrift

ter verkrijging van de graad van doctor aan de Universiteit Utrecht
op gezag van de rector magnificus, prof.dr. G.J. van der Zwaan,
ingevolge het besluit van het college voor promoties
in het openbaar te verdedigen op dinsdag 12 juni 2012
des middags te 12.45 uur

door

Stephanie Gerdina Catherina Kroeze

geboren op 20 mei 1983 te Emmen

Promotor: Prof.dr. J.L.H.R. Bosch

Co-promotor: Dr. J.J.M. Jans

Renal cell carcinoma: advances in minimally invasive treatments and outcome prediction.
Cover illustration: Regien M.A. Kroeze
Cover design: Regien M.A. Kroeze

Printed by:

CONTENTS

Introduction to Renal Cell Carcinoma

With a worldwide incidence of approximately 200,000 new cases and a mortality of 102,000 patients each year kidney cancer accounts for approximately 4% of cancer incidence and 2% of cancer mortality.[1-2] The most common type of kidney cancer is renal cell carcinoma (RCC). RCC has several subtypes, of which clear cell RCC (ccRCC, 80%) and papillary RCC (pRCC, 11%) are the most common types. Over the last decades the incidence of RCC has risen, largely due to the widespread use of cross-sectional imaging.[3] Incidentally found renal masses are identified in an estimated 10-41% of all abdominal imaging cases, and have thus become a common radiologic finding.[4-5] While the majority of these incidentally found lesions are small cysts that do not require any treatment, small localized (stage I) tumors are responsible for the greatest increase in incidence of RCC.[3, 6] These tumors currently account for 48-66% of all diagnosed RCCs.[7] Conversely, the relative incidence of more advances stages of RCC has slightly declined.[8]

Radical nephrectomy of the tumor-bearing kidney is the only curative treatment for large renal tumors.[9] The rise in the number of patients with small renal masses (SRMs), defined as tumors smaller than 4 cm, has lead to the development of nephron-sparing treatments. Currently, nephron-sparing surgery is equally effective in cancer control and better in preservation of renal function compared to radical nephrectomy.[10] It has therefore become the gold standard treatment for small renal tumors. In addition to nephron-sparing surgery, several minimally-invasive techniques have been developed, of which cryoablation (CA) and radiofrequency ablation (RFA) are the most commonly applied. These thermoablative techniques employ either freezing or heat to eradicate tumor tissue, and can be applied either percutaneously or by laparoscopy.[11] Treatment options for RCC will be described more thoroughly in **part 2**.

The 5-year survival rate for stage 1 RCC tumors is currently about 93%. Over the years, age-adjusted survival rates have not improved for metastasized RCC (mRCC).[8] Approximately 20% of all RCC patients will present with synchronous metastases, and a further 25% with metachronous metastases within 5 years after initially curative treatment.[8, 12] Median survival of mRCC is 20 months[13] with a 5-year cancer-specific survival rate of approximately 11%.[14] Chances of metastatic development for patients with SRMs are low; as 4.2-7.0% presents with synchronous metastases and 1-8.4% will be diagnosed with metastases within 10 years of follow-up.[15-17] The wide range of survival for different RCC stages and the inability to predict the natural behaviour of RCC in individual patients has resulted in a critical need to find ways to predict patient prognosis and optimize treatment. The aim of this thesis is to make advances in outcome prediction (**part 1**) and the development of minimally invasive treatments of RCC (**part 2**).

Introduction to and scope of part 1: Prognosis and diagnosis of RCC

Prognostic predictors for RCC

There is a substantial difference in survival between the various RCC stages, and individual outcomes remain difficult to predict. This has been the reason to investigate several approaches to improve RCC patient prognostic prediction.[18] Improved individualized prognostication may help improve risk-stratified clinical decision making. Current approaches consist of prognostic markers and nomograms.[19] Many prognostic markers have been found in renal tumor tissue. These biomarkers will be described in **Chapters 2 and 3**. Other markers are localized in the blood, tissue, urine or genes. Several prognostic nomograms have been developed for postoperative prognostic assessment of all stages or localized RCC. These nomograms combine clinical or pathologic features of predictive value, sometimes complemented with biomarkers.[20-22] Although these nomograms are not 100% accurate, their prognostic abilities are better than anatomical staging alone.[18] The most well known nomograms are the UCLA integrated staging system (UISS),[23] tumor stage, size, grade and necrosis (SSIGN) score[24] and the Leibovich prognostic scoring algorithm.[25] Prognostic factors used in these nomograms are the tumor-node-metastasis (TNM) classification, tumor size, Fuhrman grade, presence of tumor necrosis and the ECOG performance status (ECOG-PS). Nomograms can be used in follow-up strategies, although there is currently no consensus on which nomogram would be most adequate.[26] Furthermore, the UISS and Leibovich algorithm are being used for inclusion criteria of phase III trials.[21] While prognostic nomograms are slowly gaining importance in RCC treatment, none of the prognostic markers are used routinely in the clinic. Reasons for this are described in **Chapter 2**. However, it appears that prognostic markers will eventually be important for prediction of tumor response to currently used systemic therapies for mRCC.[27-29]

In addition to postoperative clinical or pathologic features several other factors play a significant role in surgical outcome and long term prognosis. These include patient physical status, advanced age and comorbidities.[30-32] With the increasing incidence of RCC in an elderly population, comorbidities and advanced age are of such importance that they can compete with RCC as the primary cause of death.[32-33] **Chapter 5** describes the effect of severe comorbidities on postoperative complications following surgical treatment of RCC.

Role of percutaneous renal biopsies in diagnosis and prognosis determination

Modalities used for detection of RCC include contrast enhanced CT, ultrasonography and MRI. In addition to these modalities, renal mass biopsy (RMB) is emerging as a valuable diagnostic tool in several situations. Its increased popularity is partly due to the fact that

modern RMB has a diagnostic accuracy of over 90% and complications are limited. One situation in which RMB has become valuable is the diagnosis of indeterminate SRM. When a SRM has been identified on imaging, it is challenging to distinguish malignant from benign SRMs. The majority of SRMs can be classified as benign or malignant by two-phase contrast CT, where malignant masses typically show contrast enhancement. However, enhanced renal lesions are not always malignant, and there are no other CT criteria that are specific in discriminating malignant from benign solid lesions.[34-35] Suspicious lesions on imaging are found to be benign on postoperative histological evaluation in approximately 20% of cases. Several studies have shown that 43 to 65% of patients with benign lesions are being surgically over-treated.[36-37] This inaccurate diagnosis indicates that urologists and radiologists should not solely rely on imaging. An additional characteristic that may distinguish benign from malignant SRMs is the size of the tumor; the smaller the tumor, the higher chance of benign or low grade cases.[36] There are currently no other factors that can be used to distinguish benign from malignant SRMs, or predict the aggressiveness of SRMs. In order to fully diagnose these suspicious lesions, RMB would therefore be a useful addition to imaging.[38] For larger tumors, RMB is usually not of additional value since the majority of these masses are reliably diagnosed as malignant with imaging alone. However, current imaging techniques are still unable to accurately identify benign lesions such as oncocytomas or angiomyolipomas with minimal fat, granulomas or inflammatory lesions,[39-41] in which situation RMB would be of additional use.

Adequate diagnosis using RMB is increasingly important for clinical decision making and prediction of prognosis. Currently, RMB changes the management of the tumor in 40-60% of cases.[42-43] One reason is that a significant number of SRMs are diagnosed in an elderly patient population. These patients quite often have comorbidities that may limit their treatment options. RMB could prevent the need to operate when lesions are benign. Furthermore, for selected patients active surveillance is a possibility. In order to predict the risk of developing metastases, RMB could stratify patients suitable for active surveillance. As discussed in **Chapter 2**, factors such as the Fuhrman grade and histological subtype are important prognostic indicators. The diagnostic accuracy of RMB for Fuhrman grading ranges between 70 and 83%.[44] Histological subtypes can be determined by biopsy in 88 to 100% of cases.[44-45] When tumors are treated with local ablative therapy and therefore no histological specimen is obtained, RMB prior to treatment can provide for these important prognostic indicators. **Chapter 4** describes the technical considerations for currently used modalities used for RMB. While over the years the success rate of RMBs has increased to up to 90%, remaining limitations include technical failure and indeterminate or inaccurate histological diagnosis.[46] In particular the sensitivity of RMB for lesions smaller than 3 cm

appears to be low.[47-49] Therefore, new developments in RMB to increase the diagnostic accuracy remain important.

References

1. Tavani A, La Vecchia C. Epidemiology of renal-cell carcinoma. J Nephrol 1997;10:93-106.

2. Parkin DM, Bray F, Ferlay J, Pisani P. Global cancer statistics, 2002. CA Cancer J Clin 2005;55:74-108.

3. Hollingsworth JM, Miller DC, Daignault S, Hollenbeck BK. Rising incidence of small renal masses: a need to reassess treatment effect. J Natl Cancer Inst 2006;98:1331-4.

4. Carrim ZI, Murchison JT. The prevalence of simple renal and hepatic cysts detected by spiral computed tomography. Clin Radiol 2003;58:626-9.

5. Tsugaya M, Kajita A, Hayashi Y, Okamura T, Kohri K, Kato Y. Detection and monitoring of simple renal cysts with computed tomography. Urol Int 1995;54:128-31.

6. Chow WH, Devesa SS. Contemporary epidemiology of renal cell cancer. Cancer J 2008;14:288-301.

7. Nguyen MM, Gill IS, Ellison LM. The evolving presentation of renal carcinoma in the United States: trends from the Surveillance, Epidemiology, and End Results program. J Urol 2006;176:2397-400; discussion 400.

8. Sun M, Thuret R, Abdollah F, et al. Age-adjusted incidence, mortality, and survival rates of stage-specific renal cell carcinoma in North America: a trend analysis. Eur Urol 2011;59:135-41.

9. Ljungberg B, Hanbury DC, Kuczyk MA, et al. Renal cell carcinoma guideline. Eur Urol 2007;51:1502-10.

10. Lucas SM, Stern JM, Adibi M, Zeltser IS, Cadeddu JA, Raj GV. Renal function outcomes in patients treated for renal masses smaller than 4 cm by ablative and extirpative techniques. J Urol 2008;179:75-9; discussion 9-80.

11. Gill IS, Aron M, Gervais DA, Jewett MA. Clinical practice. Small renal mass. N Engl J Med;362:624-34.

12. Leibovich BC, Han KR, Bui MH, et al. Scoring algorithm to predict survival after nephrectomy and immunotherapy in patients with metastatic renal cell carcinoma: a stratification tool for prospective clinical trials. Cancer 2003;98:2566-75.

13. Motzer RJ, Hutson TE, Tomczak P, et al. Overall survival and updated results for sunitinib compared with interferon alfa in patients with metastatic renal cell carcinoma. J Clin Oncol 2009;27:3584-90.

14. Schrader AJ, Varga Z, Hegele A, Pfoertner S, Olbert P, Hofmann R. Second-line strategies for metastatic renal cell carcinoma: classics and novel approaches. J Cancer Res Clin Oncol 2006;132:137-49.

15. Lughezzani G, Jeldres C, Isbarn H, et al. Tumor size is a determinant of the rate of stage T1 renal cell cancer synchronous metastasis. J Urol 2009;182:1287-93.

16. Chawla SN, Crispen PL, Hanlon AL, Greenberg RE, Chen DY, Uzzo RG. The natural history of observed enhancing renal masses: meta-analysis and review of the world literature. J Urol 2006;175:425-31.

17. Klatte T, Patard JJ, de Martino M, et al. Tumor size does not predict risk of metastatic disease or prognosis of small renal cell carcinomas. J Urol 2008;179:1719-26.

18. Sun M, Shariat SF, Cheng C, et al. Prognostic factors and predictive models in renal cell carcinoma: a contemporary review. Eur Urol 2011;60:644-61.

19. Flanigan RC, Polcari AJ, Hugen CM. Prognostic variables and nomograms for renal cell carcinoma. Int J Urol 2011;18:20-31.

20. Parker AS, Leibovich BC, Lohse CM, et al. Development and evaluation of BioScore: a biomarker panel to enhance prognostic algorithms for clear cell renal cell carcinoma. Cancer 2009;115:2092-103.

21. Tan MH, Li H, Choong CV, et al. The Karakiewicz nomogram is the most useful clinical predictor for survival outcomes in patients with localized renal cell carcinoma. Cancer 2011.

22. Ficarra V, Novara G, Galfano A, et al. The 'Stage, Size, Grade and Necrosis' score is more accurate than the University of California Los Angeles Integrated Staging System for predicting cancer-specific survival in patients with clear cell renal cell carcinoma. BJU Int 2009;103:165-70.

23. Zisman A, Pantuck AJ, Wieder J, et al. Risk group assessment and clinical outcome algorithm to predict the natural history of patients with surgically resected renal cell carcinoma. J Clin Oncol 2002;20:4559-66.

24. Frank I, Blute ML, Cheville JC, Lohse CM, Weaver AL, Zincke H. An outcome prediction model for patients with clear cell renal cell carcinoma treated with radical nephrectomy based on tumor stage, size, grade and necrosis: the SSIGN score. J Urol 2002;168:2395-400.

25. Leibovich BC, Cheville JC, Lohse CM, et al. A scoring algorithm to predict survival for patients with metastatic clear cell renal cell carcinoma: a stratification tool for prospective clinical trials. J Urol 2005;174:1759-63; discussion 63.

26. Ljungberg B, Cowan NC, Hanbury DC, et al. EAU guidelines on renal cell carcinoma: the 2010 update. Eur Urol 2010;58:398-406.

27. Heng DY, Xie W, Regan MM, et al. Prognostic factors for overall survival in patients with metastatic renal cell carcinoma treated with vascular endothelial growth factor-targeted agents: results from a large, multicenter study. J Clin Oncol 2009;27:5794-9.

28. Atkins MB. Treatment selection for patients with metastatic renal cell carcinoma: identification of features favoring upfront IL-2-based immunotherapy. Med Oncol 2009;26 Suppl 1:18-22.

29. Yuasa T, Takahashi S, Hatake K, Yonese J, Fukui I. Biomarkers to predict response to sunitinib therapy and prognosis in metastatic renal cell cancer. Cancer Sci 2011;102:1949-57.

30. de Cassio Zequi S, de Campos EC, Guimaraes GC, Bachega W, Jr., da Fonseca FP, Lopes A. The use of the American Society of Anesthesiology Classification as a prognostic factor in patients with renal cell carcinoma. Urol Int 2010;84:67-72.

31. Bensalah K, Pantuck AJ, Crepel M, et al. Prognostic variables to predict cancer-related death in incidental renal tumours. BJU Int 2008;102:1376-80.

32. Santos Arrontes D, Fernandez Acenero MJ, Garcia Gonzalez JI, Martin Munoz M, Paniagua Andres P. Survival analysis of clear cell renal carcinoma according to the Charlson comorbidity index. J Urol 2008;179:857-61.

33. Kutikov A, Egleston BL, Wong YN, Uzzo RG. Evaluating overall survival and competing risks of death in patients with localized renal cell carcinoma using a comprehensive nomogram. J Clin Oncol 2010;28:311-7.

34. Millet I, Doyon FC, Hoa D, et al. Characterization of Small Solid Renal Lesions: Can Benign and Malignant Tumors Be Differentiated With CT? AJR Am J Roentgenol 2011;197:887-96.

35. Bosniak MA, Rofsky NM. Problems in the detection and characterization of small renal masses. Radiology 1996;198:638-41.

36. Frank I, Blute ML, Cheville JC, Lohse CM, Weaver AL, Zincke H. Solid renal tumors: an analysis of pathological features related to tumor size. J Urol 2003;170:2217-20.

37. Remzi M, Ozsoy M, Klingler HC, et al. Are small renal tumors harmless? Analysis of histopathological features according to tumors 4 cm or less in diameter. J Urol 2006;176:896-9.

38. Eshed I, Elias S, Sidi AA. Diagnostic value of CT-guided biopsy of indeterminate renal masses. Clin Radiol 2004;59:262-7.

39. Bosniak MA, Rofsky NM. Problems in the detection and characterization of small renal masses. Radiology 1996;200:286-7.

40. Silverman SG, Israel GM, Herts BR, Richie JP. Management of the incidental renal mass. Radiology 2008;249:16-31.

41. Willatt J, Francis IR. Imaging and management of the incidentally discovered renal mass. Cancer Imaging 2009;9 Spec No A:S30-7.

42. Maturen KE, Nghiem HV, Caoili EM, Higgins EG, Wolf JS, Jr., Wood DP, Jr. Renal mass core biopsy: accuracy and impact on clinical management. AJR Am J Roentgenol 2007;188:563-70.

43. Wood BJ, Khan MA, McGovern F, Harisinghani M, Hahn PF, Mueller PR. Imaging guided biopsy of renal masses: indications, accuracy and impact on clinical management. J Urol 1999;161:1470-4.

44. Neuzillet Y, Lechevallier E, Andre M, Daniel L, Coulange C. Accuracy and clinical role of fine needle percutaneous biopsy with computerized tomography guidance of small (less than 4.0 cm) renal masses. J Urol 2004;171:1802-5.

45. Leveridge MJ, Finelli A, Kachura JR, et al. Outcomes of small renal mass needle core biopsy, nondiagnostic percutaneous biopsy, and the role of repeat biopsy. Eur Urol 2011;60:578-84.

46. Laguna MP, Kummerlin I, Rioja J, de la Rosette JJ. Biopsy of a renal mass: where are we now? Curr Opin Urol 2009;19:447-53.

47. Lane BR, Samplaski MK, Herts BR, Zhou M, Novick AC, Campbell SC. Renal mass biopsy--a renaissance? J Urol 2008;179:20-7.

48. Lechevallier E, Andre M, Barriol D, et al. Fine-needle percutaneous biopsy of renal masses with helical CT guidance. Radiology 2000;216:506-10.

49.   Wang R, Wolf JS, Jr., Wood DP, Jr., Higgins EJ, Hafez KS. Accuracy of percutaneous core biopsy in management of small renal masses. Urology 2009;73:586-90; discussion 90-1.

Chapter 2

Diagnostic and prognostic tissuemarkers in clear cell and papillary renal cell carcinoma

Stephanie G.C. Kroeze*

Annika M. Bijenhof*

J.L.H.Ruud Bosch

Judith J.M. Jans

(*Authors contributed equally)

Department of Urology, University Medical Center Utrecht, the Netherlands

Abstract

Introduction

Approximately one-third of all Renal Cell Carcinoma (RCC) patients undergoing a nephrectomy face metastatic disease. The availability of novel therapeutics for metastatic patients underscores the importance of identifying patients at risk of recurrence or patients responding well to specific therapies. Unlike clear cell RCC (ccRCC), information on biomarkers for the papillary subtype (pRCC) remains limited. In this review, we identified tissue markers that are differentially expressed between subtypes and may be of diagnostic use. In addition, markers with promising prognostic power for ccRCC and/or pRCC are described and their clinical value is discussed.

Materials and methods

To identify diagnostic markers that differentiate between pRCC and ccRCC a Pubmed search was performed, limited to original articles published in the English language between 1990 and 2009, using the terms *pRCC/papillary RCC/papillary renal cell carcinoma/papillary kidney cancer*, *biomarker/biomarkers*, *protein expression*, *mass spectrometry* and *immunohistochemistry*. Prognostic markers for ccRCC and pRCC were identified using the search terms *kidney cancer*, *renal cell carcinoma*, *prognostic marker*, *biomarker* and *prognosis*. Only markers with independent prognostic value in multivariable analysis were included.

Results

25 proteins are differentially expressed between ccRCC and pRCC, reflecting the molecularly distinct nature of these subtypes. 5 of these proteins were externally validated, which shows their diagnostic potential. Whereas 48 biomarkers with independent prognostic power have been identified for ccRCC patients, only CD44, CA9, p53, Ki67 and PCNA have shown prognostic value in multiple studies. Expression of IMP-3 and VEGF-R2 are independent predictors of survival of pRCC patients, although this is shown in single studies.

Conclusions

So far 5 validated diagnostic markers are able to differentiate between ccRCC and pRCC. Few independent prognostic markers have been identified for pRCC in single studies, compared to numerous biomarkers identified for the more common ccRCC. Despite the abundance of promising markers for ccRCC, their exact role in clinical decision making still needs to be established through validation studies.

Introduction

Renal Cell Carcinoma

The incidence of renal cell carcinoma (RCC) has increased progressively over the last two decades and now accounts for approximately 3% of all cancers.[1] Mortality from RCC represents 2% of all cancer-associated deaths. Radical or partial nephrectomy is considered the only curative treatment.[2-3] Approximately one third of all patients have metastasized disease at time of diagnosis, another third develop local or distant recurrences at later stages. For these patients currently no curative treatment exists. [4-6]

RCC is comprised of a heterogeneous group of subtypes. According to classification by their histological characteristics of which clear cell (ccRCC, 80-90%) and papillary RCC (pRCC, 10-15%) are the two most common forms.[7] The pRCC subtype can be further subdivided into type 1 and type 2. Type 1 pRCCs are generally low grade lesions with a chromophilic cytoplasm and have a favorable disease outcome. Type 2 lesions are typically high grade with a generally eosinophilic cytoplasm and exhibit a higher chance of metastasizing.[8-9]

The importance of biomarkers

After initial RCC diagnosis it is difficult to predict the individual chance of metastatic development or response to the available treatment options. Awareness of the potential importance of biomarkers in predicting these issues is growing progressively. Biomarkers are objective molecular or cellular characteristics of *e.g.* cancer tissue, and may be implemented in clinical practice for diagnostic or prognostic purposes in the development of personalized medicine.

Diagnostic RCC Markers

Histological diagnosis of subtypes of RCC can be a significant challenge since all subtypes may exhibit solid, alveolar, or papillary growth patterns (reviewed in [10]). Diagnosis is particularly challenging with small tumor biopsies from nephron-sparing procedures which are prone to sampling error. In cases where standard histology alone is not sufficient, biomarkers may serve as a tool for the differentiation between RCC subtypes. Diagnostic differentiation is important for several reasons. Firstly, the histological subtypes of RCC appear to be associated with variances in prognosis and survival.[11] Secondly, differentiation between histological subtypes may be important to determine individual chances of optimal treatment response. For example, immunotherapy can have durable responses in a small subset of ccRCC patients but is not effective in pRCC. Also, the standard treatment for advanced RCC with targeted therapies such as tyrosine kinase inhibitors may result in lower clinical responses in pRCC tumors compared to ccRCC tumors.[12] As both targeted therapies

and immunotherapy encompass significant side effects it is important to select for patients who are likely to respond.[13-15] Thirdly, in addition to providing prognostic information, differentially expressed biomarkers may reveal which pathways are affected in the different subtypes and may provide information on the etiology of the disease. Thus, accurate diagnosis of the tumor subtype is important to help design individualized treatments.

Prognostic Markers for ccRCC and pRCC

A major challenge in current kidney cancer research is the prediction of metastatic potential of individual tumors and, related to this, the prognosis of RCC patients. Much effort is directed towards the identification of molecular markers with prognostic value, and comprehensive reviews have appeared describing their potential.[16-17] Although the practical and clinical usefulness remains to be fully established and many markers need to be validated, several promising biomarkers for ccRCC have been identified.

So far, information on biomarkers for the papillary subtype remains limited. This is particularly unfortunate since pRCC is molecularly and pathologically distinct from ccRCC. A subset of prognostic markers for ccRCC may directly apply to pRCC patients as well, but the small number of pRCC patients included in studies often complicates statistically significant statements on their prognostic potential. Given the different molecular causes underlying the various RCC subtypes, it is not surprising that biomarkers can be identified that are specific for pRCC. This review will provide an overview of the currently most promising biomarkers of ccRCC and pRCC.

Materials and Methods

To identify diagnostic molecular markers that are differentially expressed between pRCC and ccRCC, a Pubmed search was performed in the fields 'title' and 'abstract' using the terms 'pRCC/papillary RCC/papillary renal cell carcinoma/papillary kidney cancer' combined with one of the following terms 'biomarker/biomarkers', 'protein expression', 'mass spectrometry' or 'immunohistochemistry' in title or abstract. Included articles were investigated for under- or overexpression of molecular markers in pRCC, significant differences in expression of these markers compared to the ccRCC subtype and for the presence of external validation. Prognostic markers for ccRCC and pRCC were identified through a systematic Pubmed search using the search terms 'kidney cancer', 'renal cell carcinoma', 'prognostic marker', 'biomarker' and 'prognosis'. Only biomarkers with independent prognostic value in multivariable analysis were included. All searches were limited to papers published in the English language between 1990 and 2009. Single case reports were excluded.

Results

Diagnostic RCC Markers

The search resulted in 29 studies that described significantly altered expression of in total 25 proteins in pRCC compared to normal tissue and ccRCCs (Table 1). Most of these were significantly overexpressed in pRCC compared to ccRCC. Furthermore, 8 proteins were demonstrated to be expressed at significantly different levels between type 1 and type 2 pRCC. These included CD10, p53, Mucin 1, E-cadherin, VEGF-R2 and -R3, cytokeratin 20 and 7. The most promising diagnostic markers, based on confirmation of their diagnostic value in multiple studies and external validation, are discussed in more detail below.

Alpha-methylacyl-CoA racemase

Several studies show that alpha-methylacyl-CoA racemase (AMACR) is strongly overexpressed and mRNA levels are increased in almost all pRCC tumors.[18-19] ccRCC tumors show only minor differences in AMACR mRNA abundance compared to normal tissue. AMACR is mainly expressed in hepatocytes and in the epithelium of the renal proximal tubules where β-oxidation of fatty acids takes place.

Cytokeratins

Several cytokeratins (CK) appear to differentiate between pRCC and ccRCC. Multiple studies showed that CK 7 is significantly overexpressed in pRCC compared to ccRCCs.[20-24] Similarly, multiple studies identified CK 8, CK 19 and CK20 overexpression more frequently in pRCC than in ccRCC tumors.[23-24] To gain further evidence that several CK subsets can be used as markers to help differentiate pRCC from ccRCC, a combination of two monoclonal anti-cytokeratin antibodies; CK AE1/AE3, was developed. This combination recognizes CK1-8, 10 and 14-16. Of the pRCC tumors 81.8% (n=8) were positive for CK AE1/AE3 in contrast to 35.5% (n=76) of ccRCC.

In addition, some CKs contain potential diagnostic value to help distinguish between pRCC type 1 and type 2. For example, CK7 was expressed in 80-97% of pRCC type 1 tumors, while a much smaller fraction (<32%) of pRCC type 2 tumors express this protein.[16-20] Other studies revealed that 25% of the pRCC type 2 tumors expressed CK 20. No CK20 expression was observed in pRCC type 1.[19-20]

p53

Wild-type p53 is usually not detectable with immunohistochemical staining due to its short half-life. Mutated p53, on the other hand, can be found in up tot 50% of RCCs. Overexpression of p53 was shown to be significantly more frequent in pRCC compared to

ccRCC.[25] Although p53 could be an excellent diagnostic marker for pRCC, it does not have a prognostic value.

Table 1. Diagnostic markers distinguishing ccRCC and pRCC subtypes

Name	N Total (ccRCC;pRCC)*	P value	External validation	References
ADAM-10 (A Disintegrin And Metallopeptidase 10)	N=104 (82;17)	P<0.0001	No	Gutwein 2009
Alpha-methylacyl-CoA racemase (AMACR)	N=40 (10;10)	P<0.0001	Yes	Takahashi 2003
BD-1 (β defensin-1)	N=46 (23;7)	P<0.001	No	Young 2003
Cdr2 (Cerebellar degeneration-related protein 2)	N=384 (255;48)	P<0.0001	No	Balamurugan 2009
Cldn1 (Claudin-1)	N=318 (278;30)	P<0.001	No	Fritzsche 2008
membranous Cldn7 (Claudin-7)	N=178 (98;80)	P<0.05	No	Li 2008
CXCL-16 (CXC Chemokine ligand 16)	N=104 (82;17)	P<0.001	No	Gutwein 2009
CXR-6 (CXC chemokine receptor 6)	N=104 (82;17)	P<0.001	No	Gutwein 2009
Cytokeratin 7	N=202 (102;44)	P<0.05	Yes	Mazal 2005
Cytokeratin 8	N=86 (15;15)	P=0.008	Yes	Skinnider 2005;
Cytokeratin 19	N=86 (15;15)	P=0.003	Yes	Skinnider 2005;
Cytokeratin 20	N=167 (125;20)	P<0.0001	No	Langner 2004
ET-1 (Endothelin-1)	N=183 (125;30)	P<0.001	No	Herrmann 2007
GOLPH2 (Golgi membrane protein 2	N=104 (83;16)	P<0.001	No	Fritzsche 2008
IGFBP-5 (Insulin-like growth factor-binding protein 5)	N=22 (13;6)	P<0.05	No	Cheung 2005
IGF-IR (Insulin-like growth factor-I receptor)	N=180 (137;20)	P<0.001	No	Schips 2004
Matriptase	N=168 (123;14)	P<0.05	No	Jin 2006
MRP-1/CD9 (Motility-related protein 1)	N=108 (66;13)	P<0.05	No	Kuroda 2001
PV (Parvalbumin)	N=46 (23;7)	P<0.001	No	Young 2003
P53 (Protein 53)	N=184 (134;20)	P<0.0001	Yes	Zigeuner 2004
SCHIP1 (Schwannomin-interacting protein 1)	N=94 (66;16)	P<0.001	No	Osunkoya 2009
Cytosolic STC2 (Stanniocalcin 2)	N=108 (85;17)	P<0.05	No	Meyer 2009
VEGF-C	N=166 (135;31)	P=0.002	No	Bierer 2008
VEGF-D	N=166 (135;31)	P=0.04	No	Bierer 2008
VDR (Vitamin D Receptor)	N=204 (52;35)	P<0.05	No	Liu 2006

* VEGFR-2 is a prognostic marker for pRCC

Prognostic Markers for ccRCC

Table 2 lists the 48 tissue markers that are currently described to have independent prognostic value for ccRCC patients. Although promising in these retrospective studies, only CD44, CA9, p53, Ki67 and PCNA have shown prognostic value for ccRCC in multiple studies. This means that many of these biomarkers currently need to be externally validated. A majority of the identified biomarkers play a pivotal role in biological processes including apoptosis, cell cycle, cell migration, and angiogenesis. Because of the high number of available prognostic markers for ccRCC, only the best described biomarkers, subdivided in each of these biological processes, are described in more detail below.

Apoptosis

Several ccRCC biomarkers have an inhibitory effect on apoptosis. Examples include p53, Livin and Survivin.[25-28] Enhanced tumor progression and recurrences may be a consequence of overexpression of anti-apoptotic proteins. Although p53 overexpression is not common in ccRCC, it is indicative for a poor prognosis. An important problem related to p53 as a biomarker is the heterogeneous expression within tumors. Therefore, sampling errors may occur resulting in unreliable predictions.[25]

Cell cycle and proliferation

Many studies have been performed investigating the expression of Ki67, a marker for proliferating cells, in cancer. Overexpression of Ki67 independently predicts survival of RCC patients (p≤0.04).[29-31] p27 and p21 are important components of the cell cycle machinery and a low expression of these proteins is associated with a poor cancer specific survival and progression free survival (p=0.0001 and p=0.004, respectively).[32-34] A high nuclear expression of p21 in the primary tumor is associated with a better prognosis for patients with non-metastatic disease, making this a promising marker for patients undergoing a nephrectomy with curative intent.[34]

Angiogenesis and vasculogenesis

More than 80% of all sporadic RCCs harbour a mutated *VHL* gene.[35] VHL is a tumor suppressor protein responsible for the oxygen-dependent degradation of the transcription factor HIF under normoxic conditions. Inactivation of VHL results in accumulation of HIF. This induces transcription of many genes, thereby stimulating processes including angiogenesis, erythropoiesis and glucose metabolism. Proteins that are upregulated by HIF include CA9 and VEGF. Given the importance of these proteins in the aetiology of kidney cancer, much effort has been directed towards determining their prognostic significance. Expression of CA9 (p=0.014), VEGF (p=0.01) (both downstream HIF targets) and VHL (p=0.046) appear to be of important prognostic value, although external validation remains to be performed .[30,36,37]

Prognostic Markers for pRCC

The expression levels of 10 proteins were found to be related to the prognosis of pRCC. Only 2 (IMP-3 and VEGF-R2) had independent prognostic value as determined by multivariable analysis. This was shown in single studies and external validation is yet to be performed.

IMP-3

IMP-3 induces insulin-like growth factor-II expression through which it promotes proliferation of tumor cells.[38] In a study with 254 pRCC patients, tumor expression of IMP-3 was shown to be an independent prognostic marker.[39] Following multivariate analysis correcting for stage and grade, expression of IMP-3 resulted in a 10 times higher chance to develop metastases after surgery and patients were twice more likely to die from the disease (p<0.001). However, IMP-3 expression was detected in only 10.2% of pRCCs, limiting its value for use in clinical practice.

VEGF-R2

VEGF is a growth factor that plays a key role in blood vessel formation by promoting endothelial cell proliferation, differentiation and migration. VEGF-R2 is also known as

KDR/Flk-1 and is the receptor mediating most of the cellular responses of VEGF. High VEGF-R2 levels were significantly related to a poor prognosis for type 1 and type 2 pRCC patients. Furthermore, multivariable analyses indicated that the prognostic value of VEGF-R2 expression in pRCC was independent of histological variables.[40] As the prognostic value of this receptor was investigated in only one study and pRCC was not compared to ccRCC, validation in additional studies is warranted.

Future perspectives and clinical application

Tissue biomarkers are expected to play an important role in future determination of diagnosis, prognosis and treatment regimens. Many markers have been identified with potential diagnostic and/or prognostic relevance for RCC. Expression levels of several markers may be indicative of a poor prognosis in all RCC histological subtypes. These may merely reflect enhanced cell growth (e.g. Ki67), metastatic potential through enhanced migration, or reduced levels of apoptosis (e.g. Bcl2). Whereas many markers with independent prognostic value for ccRCC patients exist, information on independent prognostic markers for pRCC remains limited. The relatively small number of pRCC patients may explain the lag in identification of markers specific for this subtype.

In addition, markers specific for tumor (sub)type are important. This is especially apparent in ccRCC where mutations in the Von Hippel-Lindau (VHL) gene underlie the majority of kidney tumors.[35] The VHL protein is an important player in the hypoxia response pathway, and several proteins in this pathway (e.g. CA9) have been identified as biomarkers for ccRCC. It is conceivable that more or better biomarkers for pRCC become available once more knowledge is obtained on the molecular defects underlying this disease.

Despite their promising potential, none of the identified biomarkers are used routinely in the clinic. An important factor delaying translation of the here described biomarkers to the clinic is the lack of external validation from independent datasets. Given the large number of studies geared towards identifying appropriate biomarkers, and given the multitude of proteins currently under investigation it is not unlikely that a number of the identified markers are in fact false positives. Required characteristics of good biomarkers are multiple, including a straightforward analysis and interpretation and a strong prognostic power (concordance index, CI).

Table 2. Markers predicting survival of RCC patients

Name	Survival	References	P Value
Apoptosis			
Bcl-2	CSS	Phuoc 2007	P=0.04
MMP-9	CSS	Kawata 2007	P=0.003
Livin	PFS, CSS	Haferkamp 2008	P=0.045
p53	CSS, PFS, OS	Shiina 1997; Zigeuner 2004; Cho 2005; Phuoc 2007; Klatte 2009	P<0.02
Survivin	PFS, CSS	Parker 2006; Byun 2007	P=0.012
TRAIL-R2 and TRAIL	CSS	Macher-Goeppinger 2009	P=0.01
XIAP	CSS	Mizutani 2007	P<0.05
Cell cycle			
Cyclin A	DFS	Aaltomaa 1999	P=0.0002
EBAG9	CSS	Ogushi 2005	P=0.049
EMA	OS	Bamias 2003	P=0.018
Ki67	CSS DFS OS	de Riese 1993; Aaltomaa 1997; Klatte 2009; Bui 2004; Paul 2004; Rioux-Leclercq 2000; Rioux-Leclercq 2001; Rioux-Leclercq 2004; Tollefson 2007; Dudderidge 2005; Visapaa 2003; Kirkali 2001; Visapaa 2003; Kirkali 2001	P<0.04
KIT	OS	Zhang 2009	P=0.0005
p21	CSS	Weiss 2007	P=0.0004
p27	CSS, PFS	Haitel 2001; Migita 2002	P=0.0001
pRb	PFS	Haitel 2001	P=0.002
PTHrP	PFS	Iwamura 1999	P=0.011
PCNA	OS	Delahunt 1993; Morell-Quadreny 1998	P<0.05
RXRα	CSS	Obara 2007	P<0.05
VHL	CSS	Di Cristofano 2007	P=0.046
Cellular migration			
bFGF	CSS	Horstmann 2005	P=0.04
CXCL16	OS	Gutwein 2009	P=0.033
CXCR3	DFS	Klatte 2008	P=0.04
PDGFR-α	OS	Tawfik 2007	P=0.03
Immune response			
B7-H1	CSS	Thompson 2006	P=0.036
B7-H3	CSS	Crispen 2008	P=0.029
CD24	PFS	Lee 2008	P=0.043
PI3K	OS	Merseburger 2008	P=0.03
TβRII	CSS	Parker 2007	P<0.05
Angiogenesis and vasculogenesis			
CD44	PFS, OS, CSS, DFS	Paradis 1999; Daniel 2001; Rioux-Leclercq 2001; Lim 2008	P<0.05
VEGF	CSS	Yildiz 2004; Minardi 2008	P=0.01
VEGF-D (epithelial)	DFS	Klatte 2009	P<0.001
VEGFR-1	DFS	Klatte 2009	P=0.007
VEGFR-2*	DFS	Klatte 2009	P=0.039
Other processes			
AgNOR	OS	Delahunt 1993	P<0.05
Ca125	OS	Bamias 2003	P=0.021
Ca9	CSS	Bui 2008; Phuoc 2004; Sandlund 2007	P≤0.01
Cadherin-6	OS	Paul 2004	P=0.028
Cathepsin D	OS	Merseburger 2005	P<0.05
Caveolin 1	DFS	Campbell 2003	P=0.03
CDCP1	PFS	Awakura 2008	P=0.042
Claudin-1	CSS	Fritzsche 2008	P=0.095
DCR3	CSS	Macher-Goeppinger 2008	P=0.006
EpCAM	CSS	Seligson 2004	P=0.017
FHIT	OS	Ramp 2002	P=0.014
IDO	CSS	Riesenberg 2007	P=0.016
IMP3**	CSS	Hoffmann 2008; Jiang 2008	P≤0.02
MDR-1	CSS	Mignogna 2006	P<0.05
Na,K-adenosine triphosphatase α1 subunit	CSS	Seligson 2008	P=0.0015
SPM8-2	CSS	Rioux-Leclercq 2004	P=0.001

** IMP3 is a prognostic marker for both ccRCC and pRCC

OS: Overall Survival, DFS: Disease Free Survival, CSS: Cancer Specific Survival, PFS: Progression Free Survival

No single marker currently fulfils all criteria. Therefore, combinations of molecular markers or combinations of markers with clinical and pathological information are expected to form the most promising tool to help guide treatment decision. An example of combining multiple molecular factors is provided by the BioScore.[41] In this model, the prognostic markers Ki67, B7-H1 and survivin are combined resulting in a concordance index (CI) of 0.733-0.752. Kim *et al.* combined expression data of CA9, p53 and vimentin with T stage, M stage and ECOG-Performance Status.[42] This multifactorial model resulted in a CI of 0.79 compared to 0.76 for the University of Los Angeles Integrated Staging System (UISS). Klatte *et al.* describe a nomogram predicting disease free survival combining T stage, ECOG- Performance Status and five molecular markers (Ki67, p53, epithelial and endothelial VEGFR-1 and epithelial VEGF-D) resulting in a CI of 0.838 compared to 0.780 for the UISS.[30]

In addition to building models that predict prognosis of RCC patients, expression of markers may help guide treatment decisions. An important example is the association of CA9 expression and response to IL-2 immunotherapy, suggesting that patients with low CA9 expression would not benefit from IL-2 treatment.[13] A prospective clinical trial (SELECT) (http://www.ClinicalTrials.gov, identifier: NCT00554515) is currently investigating this. Markers indicating the response to TKIs are also being studied (http://www.ClinicalTrials.gov, identifier:NCT00930345).

Conclusions

In conclusion, although many diagnostic and prognostic markers have been identified for both ccRCC and pRCC, their in clinical decision making still needs to be established. Given the differences between pRCC and ccRCC it is conceivable that subtype needs to be taken into account and subtype-specific markers must be incorporated to obtain the most powerful model to predict prognosis.

References

1. Hollingsworth JM, Miller DC, Daignault S, Hollenbeck BK. Rising incidence of small renal masses: a need to reassess treatment effect. J Natl Cancer Inst 2006;98:1331-34.

2. Cambio AJ, Evans CP. Management approaches to small renal tumours. BJU Int 2006;97: 456-60.

3. Robson CJ, Churchill BM, Anderson W. The results of radical nephrectomy for renal cell carcinoma. J Urol 2002;167: 873-75; discussion 876-77.

4. Ljungberg B, Alamdari FI, Rasmuson T, Roos G. Follow-up guidelines for nonmetastatic renal cell carcinoma based on the occurrence of metastases after radical nephrectomy. BJU Int 1999;84: 405-11.

5. Motzer RJ, Bander NH, Nanus DM.Renal-cell carcinoma. N Engl J Med 1996;335: 865-75.

6. Zisman A, Pantuck AJ, Wieder J, Chao DH, Dorey F, et al. Risk group assessment and clinical outcome algorithm to predict the natural history of patients with surgically resected renal cell carcinoma. J Clin Oncol 2002;20: 4559-66.

7. Lopez-Beltran A, Carrasco JC, Cheng L, Scarpelli M, Kirkali Z, et al. 2009 update on the classification of renal epithelial tumors in adults. Int J Urol 2009;16: 432-43.

8. Delahunt B, Eble JN, McCredie MR, Bethwaite PB, Stewart JH, et al. Morphologic typing of papillary renal cell carcinoma: comparison of growth kinetics and patient survival in 66 cases. Hum Pathol 2001;32: 590-95.

9. Allory Y, Ouazana D, Boucher E, Thiounn N, Vieillefond A. Papillary renal cell carcinoma. Prognostic value of morphological subtypes in a clinicopathologic study of 43 cases. Virchows Arch 2003;442: 336-42.

10. Young AN, Master VA, Amin MB. Current trends in the molecular classification of renal neoplasms. Scientific WorldJournal 2006;6: 2505-18.

11. Capitanio U, Cloutier V, Zini L, Isbarn H, Jeldres C, et al. A critical assessment of the prognostic value of clear cell, papillary and chromophobe histological subtypes in renal cell carcinoma: a population-based study. BJU Int 2009;103: 1496-1500.

12. Choueiri TK, Plantade A, Elson P, Negrier S, Ravaud A, et al. Efficacy of sunitinib and sorafenib in metastatic papillary and chromophobe renal cell carcinoma. J Clin Oncol 2008;26: 127-31.

13. Atkins MB. Treatment selection for patients with metastatic renal cell carcinoma: identification of features favoring upfront IL-2-based immunotherapy. Med Oncol 2009;26 Suppl 1: 18-22.

14. Hudes G, Carducci M, Tomczak P, Dutcher J, Figlin R, et al. Temsirolimus, interferon alfa, or both for advanced renal-cell carcinoma. N Engl J Med 2007;356: 2271-81.

15. Motzer RJ, Hutson TE, Tomczak P, Michaelson MD, Bukowski RM, et al. Sunitinib versus interferon alfa in metastatic renal-cell carcinoma. N Engl J Med 2007;356: 115-24.

16. Tunuguntla HS, Jorda M. Diagnostic and prognostic molecular markers in renal cell carcinoma. J Urol 2008;179: 2096-2102.

17. Eichelberg C, Junker K, Ljungberg B, Moch H. Diagnostic and prognostic molecular markers for renal cell carcinoma: a critical appraisal of the current state of research and clinical applicability. Eur Urol 2009;55: 851-63.

18. Tretiakova MS, Sahoo S, Takahashi M, Turkyilmaz M, Vogelzang NJ, et al. Expression of alpha-methylacyl-CoA racemase in papillary renal cell carcinoma. Am J Surg Pathol 2004;28: 69-76.

19. Chen YT, Tu JJ, Kao J, Zhou XK, Mazumdar M. Messenger RNA expression ratios among four genes predict subtypes of renal cell carcinoma and distinguish oncocytoma from carcinoma. Clin Cancer Res 2005;11: 6558-66.

20. Allory Y, Bazille C, Vieillefond A, Molinie V, Cochand-Priollet B, et al. Profiling and classification tree applied to renal epithelial tumours. Histopathology 2008;52: 158-66.

21. Huang W, Kanehira K, Drew S, Pier T. Oncocytoma can be differentiated from its renal cell carcinoma mimics by a panel of markers: an automated tissue microarray study. Appl Immunohistochem Mol Morphol 2009;17: 12-17.

22. Mazal PR, Stichenwirth M, Koller A, Blach S, Haitel A, et al. Expression of aquaporins and PAX-2 compared to CD10 and cytokeratin 7 in renal neoplasms: a tissue microarray study. Mod Pathol 2005;18: 535-40.

23. Skinnider BF, Folpe AL, Hennigar RA, Lim SD, Cohen C, et al. Distribution of cytokeratins and vimentin in adult renal neoplasms and normal renal tissue: potential utility of a cytokeratin antibody panel in the differential diagnosis of renal tumors. Am J Surg Pathol 2005;29: 747-54.

24. Langner C, Wegscheider BJ, Ratschek M, Schips L, Zigeuner R. Keratin immunohistochemistry in renal cell carcinoma subtypes and renal oncocytomas: a systematic analysis of 233 tumors. Virchows Arch 2004;444: 127-34.

25. Zigeuner R, Ratschek M, Rehak P, Schips L, Langner C (2004) Value of p53 as a prognostic marker in histologic subtypes of renal cell carcinoma: a systematic analysis of primary and metastatic tumor tissue. Urology 2004;63: 651-55.

26. Haferkamp A, Bedke J, Vetter C, Pritsch M, Wagener N, et al. High nuclear Livin expression is a favourable prognostic indicator in renal cell carcinoma. BJU Int 2008;102: 1700-1706.

27. Kempkensteffen C, Hinz S, Christoph F, Krause H, Koellermann J, et al. Expression of the apoptosis inhibitor livin in renal cell carcinomas: correlations with pathology and outcome. Tumour Biol 2007;28: 132-38.

28. Parker AS, Kosari F, Lohse CM, Houston Thompson R, Kwon ED, et al. High expression levels of survivin protein independently predict a poor outcome for patients who undergo surgery for clear cell renal cell carcinoma. Cancer 2006;107: 37-45.

29. Bui MH, Visapaa H, Seligson D, Kim H, Han KR, et al. Prognostic value of carbonic anhydrase IX and KI67 as predictors of survival for renal clear cell carcinoma. J Urol 2004;171: 2461-66.

30. Klatte T, Seligson DB, LaRochelle J, Shuch B, Said JW, et al. Molecular signatures of localized clear cell renal cell carcinoma to predict disease-free survival after nephrectomy. Cancer Epidemiol Biomarkers Prev 2009;18: 894-900.

31. Rioux-Leclercq N, Epstein JI, Bansard JY, Turlin B, Patard JJ, et al. Clinical significance of cell proliferation, microvessel density, and CD44 adhesion molecule expression in renal cell carcinoma. Hum Pathol 2001;32: 1209-15.

32. Haitel A, Wiener HG, Neudert B, Marberger M, Susani M. Expression of the cell cycle proteins p21, p27, and pRb in clear cell renal cell carcinoma and their prognostic significance. Urology 2001;58: 477-81.

33. Migita T, Oda Y, Naito S, Tsuneyoshi M. Low expression of p27(Kip1) is associated with tumor size and poor prognosis in patients with renal cell carcinoma. Cancer 2002;94: 973-979.

34. Weiss RH, Borowsky AD, Seligson D, Lin PY, Dillard-Telm L, et al. p21 is a prognostic marker for renal cell carcinoma: implications for novel therapeutic approaches. J Urol 2007;177: 63-68; discussion 68-69.

35. Kim WY, Kaelin WG. Role of VHL gene mutation in human cancer. J Clin Oncol 2004;22: 4991-5004.

36. Di Cristofano C, Minervini A, Menicagli M, Salinitri G, Bertacca G, et al. Nuclear expression of hypoxia-inducible factor-1alpha in clear cell renal cell carcinoma is involved in tumor progression. Am J Surg Pathol 2007;31: 1875-1881.

37. Yildiz E, Gokce G, Kilicarslan H, Ayan S, Goze OF, et al. Prognostic value of the expression of Ki-67, CD44 and vascular endothelial growth factor, and microvessel invasion, in renal cell carcinoma. BJU Int 2004;3: 1087-93.

38. Liao B, Hu Y, Herrick DJ, Brewer G (2005) The RNA-binding protein IMP-3 is a translational activator of insulin-like growth factor II leader-3 mRNA during proliferation of human K562 leukemia cells. J Biol Chem 2005; 280: 18517-24.

39. Jiang Z, Lohse CM, Chu PG, Wu CL, Woda BA, et al. Oncofetal protein IMP3: a novel molecular marker that predicts metastasis of papillary and chromophobe renal cell carcinomas. Cancer 2008;112: 2676-2682.

40. Klatte T, Pantuck AJ, Said JW, Seligson DB, Rao NP, et al. Cytogenetic and molecular tumor profiling for type 1 and type 2 papillary renal cell carcinoma. Clin Cancer Res 2009;15: 1162-69.

41. Parker AS, Leibovich BC, Lohse CM, Sheinin Y, Kuntz SM, et al. Development and evaluation of BioScore: a biomarker panel to enhance prognostic algorithms for clear   cell renal cell carcinoma. Cancer 2009;115: 2092-2103.

42. Kim HL, Seligson D, Liu X, Janzen N, Bui MH, et al. Using tumor markers to predict the survival of patients with metastatic renal cell carcinoma. J Urol 2005;173: 1496- 1501.

Chapter 3

Expression of nuclear FIH independently predicts overall survival of clear cell renal cell carcinoma patients

Stephanie G.C. Kroeze[1,2]
Joost S. Vermaat[3*]
Aram van Brussel[2*]
Harm H.E. van Melick[4]
Emile E. Voest[3]
Trudy G.N. Jonges[5]
Paul J. van Diest[5]
John Hinrichs[5]
J.L.H. Ruud Bosch[1]
Judith J.M. Jans[1,2]

* Authors contributed equally to the manuscript

[1] Department of Urology, University Medical Center Utrecht, the Netherlands
[2] Laboratory of Experimental Oncology, University Medical Center Utrecht, the Netherlands
[3] Department of Medical Oncology, University Medical Center Utrecht, the Netherlands
[4] Department of Urology, St. Antonius Hospital, Nieuwegein, the Netherlands
[5] Department of Pathology, University Medical Center Utrecht, the Netherlands

Abstract

Introduction

The hypoxia inducible factor (HIF) pathway plays an important role in sporadic clear cell renal cell carcinoma (ccRCC) by stimulating processes of angiogenesis, cell proliferation, cell survival and metastases formation. Here, we evaluate the significance of upstream proteins directly regulating the HIF pathway; the prolyl hydroxylases domain proteins (PHD)1, 2 and 3 and factor inhibiting HIF (FIH), as prognostic markers for ccRCC.

Methods

Immunohistochemical marker expression was examined on a tissue microarray containing tumor tissue derived from 100 patients who underwent nephrectomy for ccRCC. Expression levels of HIF, FIH and PHD1, 2 and 3 were correlated with overall survival (OS) and clinicopathological prognostic factors.

Results

HIF-1α was positively correlated with HIF-2α ($p<0.0001$), PHD1 ($p=0.024$), PHD2 ($p<0.0001$), PHD3 ($p=0.004$), FIH ($p<0.0001$) and VHL ($p=0.031$). HIF-2α levels were significantly associated with FIH ($p<0.0001$) and PHD2 ($p=0.0155$). Mutations in the *VHL* gene, expression variations of HIF-1α, HIF-2α and PHD1, 2, 3 did not show a correlation to OS or clinicopathological prognostic factors. Tumor stage, grade, diameter, metastastic disease and intensity of nuclear FIH were significantly correlated to OS in univariable analysis ($p=0.023$). Low nuclear FIH levels remained a strong independent prognostic factor in multivariable analysis ($p=0.009$).

Conclusion

These results show that low nuclear expression of FIH is a strong independent prognostic factor for a poor overall survival in ccRCC.

.

27

Introduction

With a worldwide incidence of approximately 200,000 new cases and a mortality of 102,000 patients each year renal cell carcinoma (RCC) is one of the most lethal genitourinary malignancies.[1] Of all RCC patients approximately 30% will develop local or distant recurrences within 5 years after initial curative treatment.[2] Observational follow-up, succeeded by targeted therapy once metastases are present, remains the postoperative standard of care for these patients. Even with first line therapy, 5 year survival of metastasized RCC (mRCC) is less than 20%.[3] Improvements in identification of patients at risk of developing metastatic disease are therefore important.

Currently available prognostic models for non-metastasized disease, such as the University of California Integrated Staging System (UISS) and Stage, Size, Grade and Necrosis (SSIGN) score, are mainly based on clinical and pathologic variables.[4-5] The most important conventional features are tumor-node-metastasis (TNM) stage, Fuhrman grade[6] and Eastern Cooperative Oncology Group performance status (ECOG PS). Risk stratification with these features is possible, although the described accuracies vary.[7-9] In addition to clinical and pathologic prognostic parameters, tissue biomarkers can play a significant role in predicting prognosis. For example in breast cancer, tissue marker detection for gene expression profiles indicating prognosis and treatment response has become common practice.[10] Since the understanding of molecular pathways underlying RCC has increased dramatically in recent years, the search for prognostic tissue biomarkers has been facilitated.

In clear cell RCC (ccRCC), the molecular hypoxia response pathway, in which hypoxia-inducible factors-α (HIF-1α and HIF-2α) play a central role, is crucial (Figure 1).[11] HIF-α stimulates tumor growth and survival, angiogenesis, metastatic spread and glucose metabolism, amongst others. HIF-α levels are dependent of cellular oxygen levels and presence of the von Hippel-Lindau tumor suppressor protein (pVHL). In normoxia, the prolyl hydroxylase domain proteins (PHD1, PHD2 and PHD3) stimulate HIF-α degradation by enabling its recognition by pVHL by hydroxylation. Factor inhibiting HIF (FIH) adds a further level of control by reducing the transcriptional activity of HIF-α.[12] Approximately 50-70% of sporadic ccRCC cases have *VHL* gene mutations.[13] The subsequent absence of functional pVHL causes an overexpression of HIF-α (both HIF-1α and HIF-2α) independent of oxygen concentrations. Expression of HIF-α and various downstream proteins of the HIF pathway in RCC have been studied for their prognostic value.[14-15] While of great importance for HIF-α regulation, proteins upstream in the HIF pathway have been less extensively investigated in RCC, despite recent reports on associations of levels of these proteins with aggressiveness of other tumor types.[16-18] The aim of this study was to determine whether the upstream

factors of the HIF pathway PHD1, 2 and 3 and FIH have independent prognostic value as tissue biomarker for ccRCC.

Figure 1. The hypoxia pathway. Under normoxic conditions the prolyl hydroxylase domain proteins (PHD-1, PHD-2 and PHD-3) stimulate HIF-α degradation by enabling its recognition by the von Hippel-Lindau protein (pVHL) through hydroxylation. Factor inhibiting HIF (FIH) adds a further level of control by reducing the transcriptional activity of HIF-α, until severe hypoxia occurs. In the presence of hypoxia or VHL mutations, HIF-α accumulates and mediates the transcription of factors stimulating tumor growth and survival, angiogenesis and glucose metabolism, amongst others. Ub: Ubiquitin, HRE: hypoxia response element.
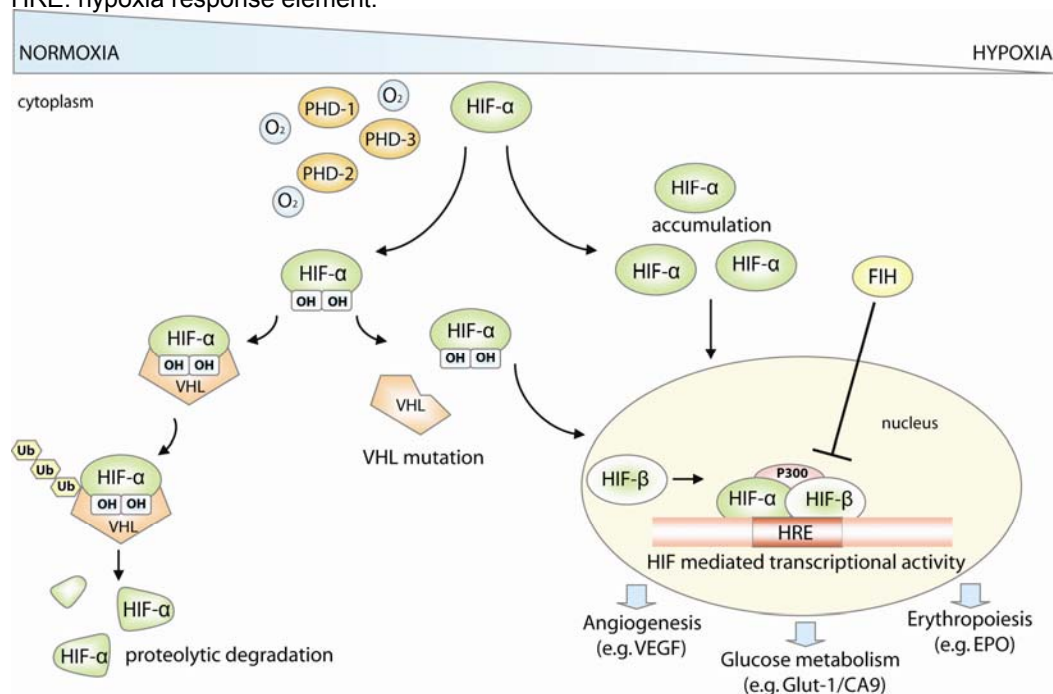
Material and Methods

Patients

This retrospective study included patients who underwent nephrectomy for ccRCC between 1994 and 2006 at the University Medical Center Utrecht (UMCU). The study was carried out in accordance with the ethical guidelines of our institution concerning informed consent about the use of patient's materials after surgical procedures. Patients with von Hippel-Lindau's disease, tuberous sclerosis, Wilms' tumor or RCC subtypes other than ccRCC were excluded. Hereafter, a random ccRCC population of 100 patients was included of which the clinicopathologic characteristics are summarized in Table 1. Patient clinical, pathologic and survival data were obtained by reviewing hospital records and by information from the general practitioner, and included age, sex, 2002 tumor-node-metastasis (TNM) classification, Fuhrman grade, ECOG performance data, primary tumor size, presence of

tumor necrosis and SSIGN score. Tumor stage and grade were determined by one pathologist (TGNJ). Patients were evaluated from time of diagnosis to 10 year follow-up. OS was defined as time from nephrectomy till date of death or last clinical follow-up.

Table 1. Patient Characteristics

Features	Median (Inter-Quartile Range)	N (%)
No. patients		100
Age (y)	64 (54-73)	
Gender		
Female		32 (32)
Male		68 (68)
Overall survival (Months)	55 (22-93)	
Tumor classification		
pT1a		18 (18)
pT1b		14 (14)
pT2		12 (12)
pT3a		17 (17)
pT3b/c		35 (35)
pT4		3 (3)
Fuhrman nuclear grade		
Total		88 (88)
1		12 (12)
2		45 (45)
3		28 (28)
4		3 (3)
Tumor size	7.5 (4.5-10)	
<5cm		26 (26)
≥5cm		74 (74)
Lymph node involvement		
pNx + pN0		90 (90)
pN1+ pN2		10 (10)
Metastases		
Synchronous		17 (17)
Metachronous		18 (18)
Tumor necrosis		
Yes		10 (10)
No		90 (90)
SSIGN Score		
Total		88 (88)
0-1		19 (22)
2		13 (15)
3		3 (3)
4		14 (16)
5		13 (15)
6		6 (7)
7		7 (8)
8		5 (6)
9		3 (3)
≥10		5 (6)
VHL mutation		
Sequencing Completed		37
Yes		16 (43)
Missense		4 (11)
Deletion		11 (30)
Indel		1 (3)
No		21 (57)

Tissue microarray construction

Formalin-fixed paraffin embedded (FFPE) renal tumor material was obtained from the Biobank of the UMCU after approval of the UMCU Institutional Review Board in accordance with Dutch medical ethical guidelines. A tissue microarray (TMA) was constructed by taking 3 cores (1 mm diameter) from each of the 100 cancer specimens and 3 cores from benign renal parenchyma surrounding the tumor and arranging them in a new composite paraffin block using an arrayer (Beecher instruments, Sun Prairy, USA).

Immunohistochemistry

TMA sections (5 μm) were deparaffinised and rehydrated. Immunohistochemistry procedures included antigen retrieval using citrate buffer (pH 6) (FIH, VHL, PHD1 and PHD3) or ethylenediaminetetraacetic acid buffer (pH 9) (PHD2, HIF-1α and HIF-2α). The primary antibodies and their respective dilutions were as follows: VHL (Clone Ig32, BD Biosciences, Temse, Belgium, 1:100), PHD1 (Abcam, Cambridge, UK, 1:100), PHD2 (Abcam, Cambridge, UK, 1:100), PHD3 (Novus Biologicals, Cambridge, UK, 1:400), HIF-1α (BD Biosciences, Temse, Belgium, 1:50), HIF-2α (Abcam, Cambridge, UK, 1:500) and FIH (Novus Biologicals, Cambridge, UK, 1:100). PowerVision (Immunologic, Duiven, the Netherlands) was used as secondary antibody. All reactions were visualized using diaminobenzidine/H_2O_2. Finally, array sections were counterstained with haematoxylin.

Scoring methods

Protein expression was analyzed by a pathologist (PJvD) blinded to other data. Cytoplasmic staining (PHD1, 2, 3, VHL), percentage of positively stained nuclei (PHD1, 2, 3, FIH, HIF-1α, HIF-2α) and nuclear intensity (FIH), were assessed in a semiquantitative fashion. For cytoplasmic and nuclear staining tumors were scored as 0, no intensity; 1, weak; 2; moderate; 3, strong intensity. Percentages of positively stained nuclei were scored as 0, <15%; 1, 15-75%; 2, >75%. The mean score of three cores of a tumor was used for statistical analysis.

DNA extraction and amplification

Tumor tissue was separated from normal kidney on paraffin tissue sections by scratching, guided by H&E staining of adjacent paraffin sections, lysed in Tris/HCl buffer, pH 8.0 with Tween-40 mg/ml proteinase K (2mg/ml) at 56°C o/n. The lysate was boiled for 10' and subsequently cooled down on ice. After 2' centrifugation at 14680 rpm, the DNA concentration of the supernatant was measured using the Isogen Nanodrop Spectrophotometer ND-1000. The DNA was subsequently stored at -20°C. Amplification of

patient tumor DNA was carried out in 25 µl reactions using 1 µg of tumor DNA. Primers used for amplification are listed in Table 2, exon 1 was amplified in two parts.

DNA purification and VHL gene sequencing

Residual primers and single-stranded DNA were removed from PCR products using exonuclease I and Shrimp Alkaline Phosphatase at 37°C for 30 minutes followed by 20' termination at 80°C. Sequencing was carried using the Big Dye system and the primers listed in table 2. Sequencing runs were performed with the Gene-amp PCR system 9600 (Applied biosystems). Sequence reaction products were purified using sephadex columns prior to running them on a 3130x/genetic analyzer (Applied Biosystems, Foster City, USA). Results were analyzed using Mutation Surveyor software (SoftGenetics, LLC., State College, PA, USA v3.24).

Table 2. PCR primers VHL gene

PCR Primers	sequence
Exon 1A Forward	5' GGT-GGT-CTG-GAT-CGC-GGA-GGG-A 3'
Exon 1A Reverse	5' CGC-GAG-TTC-ACC-GAG-CGC-AGC-A 3'
Exon 1B Forward	5' AAC-TGG-GCG-CCG-AGG-AGG-AGA-T 3'
Exon 1B Reverse	5' GGG-CTT-CAG-ACC-GTG-CTA-TCG 3'
Exon 2 Forward	5' TTC-ACC-ACG-TTA-GCC-AGG-AC 3'
Exon 2 Reverse	5' GGT-CTA-TCC-TGT-ACT-TAC-CA 3'
Exon 3 Forward	5' AGC-CTC-TTG-TTC-GTT-CCT 3'
Exon 3 Reverse	5' GGA-ACC-AGT-CCT-GTA-TCT 3'
Sequence Primers	sequence
Exon 1A Forward	5' GAT-CGC-GGA-GGG-AAT-GCC 3'
Exon 1A Reverse	5' CCG-CCC-GGC-CTC-CAT-CTC 3'
Exon 1B Forward	5' GCC-GAG-GAG-GAG-ATG-GAG 3'
Exon 1B Reverse	5' TTC-AGA-CCG-TGC-TAT-CGT 3'
Exon 2 Forward	5' CAG-GAC-GGT-CTT-GAT-CTC 3'
Exon 2 Reverse	5' TTA-CCA-CAA-CAA-CCT-TAT-CT 3'
Exon 3 Forward	5' TGT-TCG-TTC-CTT-GTA-CTG 3'
Exon 3 Reverse	5' ACT-CAT-CAG-TAC-CAT-CAA-AA 3'

Statistical analysis

TMA marker expression was correlated to clinicopathological markers using Spearman rank correlation for non-parametric measures. Marker expression was correlated to overall survival (OS) using Kaplan-Meier survival curves followed by log rank analysis to estimate differences in levels of the analyzed variables. Marker independence for prediction of survival was determined by univariable- followed by multivariable Cox regression analysis.

Results

Patients

Comprehensive clinicopathological features of 100 ccRCC patients are depicted in table 1. Median OS was 55 months (IQR 22-93). At the time of final analysis, 25 patients died

32

because of their disease and 41 patients were still alive, having a median survival time of 82 months (IQR 53-100). 17 patients presented metastases at time of nephrectomy, 18 patients developed metastases within follow-up. Of patients with metastasized disease 7 were treated with immunotherapy, 2 with a combination of immunotherapy and metastasectomy and 4 with metastasectomy. 13 patients received adjuvant radiotherapy for their bone metastases.

Sequencing of the VHL gene

Quality of the DNA derived from formalin fixed paraffin embedded tissue was sufficient for sequencing of the *VHL* gene in 37 patients (Table 1). In total, 16 mutations (43%) were identified of which 1 was located in an intron. Mutations were equally distributed along the gene. Most mutations were single or double-basepair deletions (11x) or point mutations (4x), one insertion-deletion was detected. Twelve mutations resulted in frameshifts. The presence or absence of a mutation in the *VHL* gene did not correlate with clinicopathological parameters, survival of the patients or expression of any of the markers under investigation in this study.
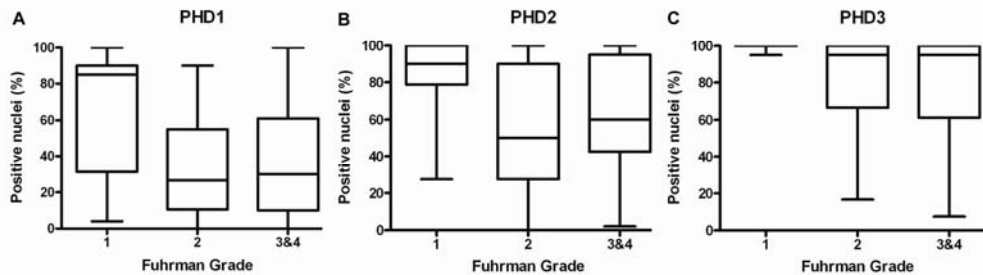
Expression of HIF

Most tumors showed nuclear presence of HIF-1α (94%) and HIF-2α (82%). Median percentages of positive nuclei within a tumor were 27.5% (IQR 6.7-62.5%) for HIF-1α and 2.7% (IQR 0.5-13.5%) for HIF-2α. Expression of HIF-1α and HIF-2α was not associated with any of the clinicopathological parameters considered in this study. HIF-1α was positively correlated with HIF-2α ($p<0.0001$), PHD1 ($p=0.024$), PHD2 ($p<0.0001$), PHD3 ($p=0.004$), FIH ($p<0.0001$) and VHL ($p=0.031$) (Spearman rank correlation). HIF-2α levels were significantly associated with FIH ($p<0.0001$) and PHD2 ($p=0.0155$).

Expression of prolyl hydroxylases

PHD1, 2 and - were localized to the nuclei of RCC cells. PHD1 was detected in on average 39% of all nuclei, PHD2 in 63% and PHD3 in 84%. Although no association between levels of PHD proteins and OS of patients was identified, a significant correlation (PHD1 $p=0.024$, PHD2 $p=0.0067$, PHD3 $p=0.0012$, Kruskal-Wallis) between Fuhrman grade and expression of all three PHD proteins was established (Figure 2). The percentage of nuclei staining positive for PHD 1, 2 and 3 was high in tumors with Fuhrman grade 1.

Figure 2. PHD1, 2 and 3 expression levels by Fuhrman Grade. The percentage of PHD1 **(A)**, PHD2 **(B)** and PHD3 **(C)** positive nuclei is highest in lesions with Fuhrman grade 1. Fuhrman grade 1: 12 patients, Fuhrman grade 2: 45 patients, Fuhrman grade 3&4: 31 patients

Expression of FIH is associated with overall survival

In normal kidney tissue, FIH was primarily localized to the cytoplasm. In ccRCC cells, however, FIH staining was predominantly nuclear. The percentage of RCC nuclei with positive FIH staining ranged widely from 1 to 100%. In addition to the percentage of positive nuclei, the intensity of FIH staining varied between patients (Figure 3). Therefore, both the percentage of positive cells and the intensity of FIH staining (score 1, 2 or 3) were recorded. A low (<15%) percentage of FIH-positive nuclei and a low intensity of FIH staining (score 1) were both significantly correlated with a shorter OS of patients (p=0.001 and p=0.003 log rank) (Figure 4). FIH was positively associated with tumor diameter (p=0.016, Spearman rank) but not with any of the other clinicopathological parameters including stage and grade.

We evaluated the following variables for prognostic value: tumor stage, tumor grade, tumor diameter, presence of metastatic disease, lymph node involvement, presence of necrosis and expression of FIH (Table 3). Of these, stage, grade, diameter, metastatic disease and intensity of FIH showed a statistically significant (p=0.023) correlation with OS in univariable analysis. Inclusion of these factors in a multivariable backwards conditional Cox regression analysis resulted in a model with metastatic disease, stage and FIH intensity as independent predictors for OS (p=0.009) (Table 3).

Figure 3. FIH immunohistochemistry. **(A)** Expression of FIH in normal kidney, FIH is predominantly present in the cytoplasm of tubuli. **(B)** Low expression of FIH in ccRCC. **(C)** High nuclear expression of FIH in ccRCC
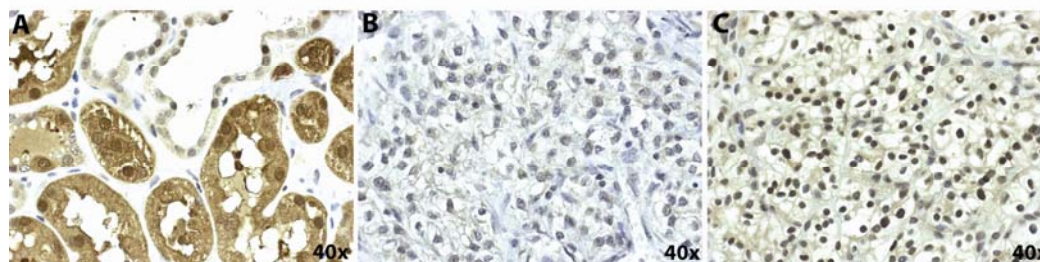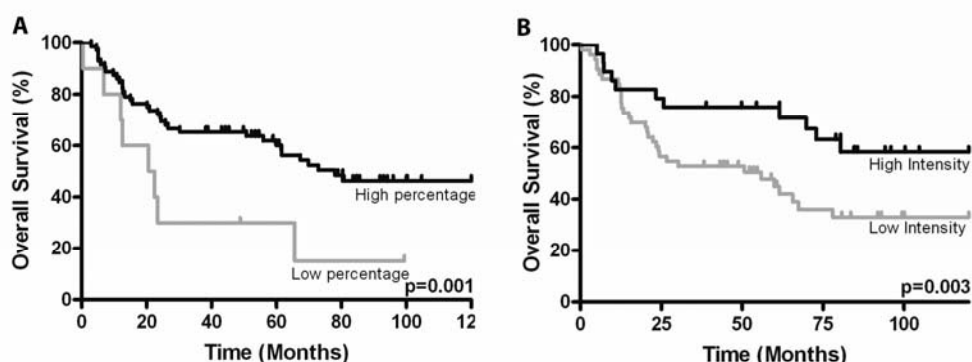
Figure 4. Overall survival. Kaplan Meier curves showing the overall survival of ccRCC patients with low versus high percentages of nuclear FIH **(A)** and low versus high intensity of nuclear FIH staining **(B)**.

Discussion

In this study nuclear FIH expression in the primary tumor was shown to have a significant independent prognostic value for ccRCC patients. FIH inhibits HIF-α in an oxygen-dependent manner. However, FIH remains active unless severe hypoxia occurs.[19] This suggests that FIH may have an important function as one of the final checks on HIF-α transcriptional activity. Although HIF is not the only target for hydroxylation by FIH, it is the most intensively studied and best characterised to date. The presence of FIH has been investigated in various normal and neoplastic human tissues, in which the intensity and subcellular localisation is very heterogeneous. Although in normal human tissues FIH is predominantly cytoplasmic, nuclear expression of FIH can be relatively strong in certain neoplasms.[20] Moreover, FIH has provided variable prognostic values in several tumor types.[16, 21] In pancreatic endocrine tumors (PETs) cytoplasmic FIH levels were significantly higher in more malignant PETs, but were not associated with survival. Nuclear FIH did not correlate with any histopathologic variables in this study.[16] In invasive breast cancer, both cytoplasmic FIH expression and absence of nuclear FIH were independent prognostic factors for a shorter disease-free survival.[21] Our study showed for the first time in ccRCC patients that low expression of nuclear FIH is a significant independent predictor for worse OS. In RCC, FIH can be detected both in the nucleus and cytoplasm, and the specific subcellular lozalisation varies between different RCC patients.[20] This was similar in our study (Figure 3). The mechanism and function of nuclear FIH in RCC, and the reason why low nuclear FIH levels have such strong prognostic

value is currently unknown. The absence of nuclear FIH in more aggressive phenotypes could be explained by increasing gene mutations within these tumors, including FIH gene mutations. This is, however, unlikely since FIH gene mutations have not been found in

RCC.[22] It is therefore possible that FIH is actively retained in the cytoplasm or exported out of the nucleus in tumors associated with worse prognosis.

Table 3. Uni-and multivariable Analysis

Univariable Analysis			
Variable		HR (95%CI)	Significance
Tumor classification			
	T1	1.00	
	T2	1.28 (0.46-3.55)	0.631
	T3	3.13 (1.51-6.48)	0.002
	T4	5.11 (0.64-40.7)	0.123
Fuhrman Nuclear Grade			
	1	1.00	
	2	2.25 (0.77-6.59)	0.138
	3	2.45 (0.79-7.55)	0.120
	4	12.01 (2.11-68.42)	0.005
Tumor Diameter		1.08 (1.01-1.15)	0.026
Distant Metastases		4.09 (2.14-7.83)	0.000
Lymph Node Involvement		1.17 (0.64-2.15)	0.616
Necrosis		1.14 (0.47-2.73)	0.772
FIH (% positive nuclei)		0.99 (0.98-1.02)	0.141
FIH (Intensity)		0.45 (0.23-0.90)	0.023
Multivariable Cox Regression Analysis			
Variable		HR	Significance
Tumor classification			
	T1	1	
	T2	0.43 (0.05-3.58)	0.437
	T3	2.08 (0.82-5.26)	0.121
	T4	7.60 (1.82-31.64	0.005
Distant Metastases		4.45	0.000
FIH (Intensity)		0.40	0.009

Although *VHL* gene mutations are considered an early and important event in the development of ccRCC, studies that investigated *VHL* alterations and survival have provided contradictory results.[13, 23-26] Our data suggests that VHL status is not correlated to common clinical prognostic parameters or survival of ccRCC patients.

Both HIF-1α and HIF-2α, which are central proteins of the HIF pathway, failed to show a correlation to survival and the most important clinicopathological parameters in our study. In ccRCC, both HIF-1α and HIF-2α are important regulators of angiogenesis and cell proliferation.[27-28] HIF-1α, but not HIF-2α, has prognostic value in colorectal cancer, lymph node negative breast carcinoma and ovarian carcinoma.[29-31] In ccRCC HIF-1α did correlate with good prognosis in a study using Western blot, however, immunohistochemical staining of the same population could not confirm this finding.[32-33] Another study reported prognostic value for HIF-1α, but only in metastatic RCC patients.[34] HIF-2α has been related to worse survival in several cancer types.[35-37] In ccRCC, evidence has accumulated revealing the importance of HIF-2α in tumorigenesis.[28, 38-39] However, although HIF-2α has shown to be inversely correlated to TNM and nuclear grade in RCC patients, we and others have shown

no evidence for a correlation of HIF-2α expression with survival.[40] HIF-1α and HIF-2α levels did correlate positively to expression of PHD1, 2 and 3 and FIH. Under hypoxic conditions both HIF-1α and HIF-2α upregulate PHD protein expression. This may serve as a negative feedback to decrease HIF-α activity.[41-42] Since hypoxia is common in RCC and many other solid tumors[43], a correlation between molecules participating in the hypoxia response pathway is not surprising and indicates the intricate interplay between these proteins. Alternatively, FIH may exert its effects on tumor biology in a HIF-independent fashion. In addition to the interaction of FIH with the hypoxia pathway, it was recently discovered that in the presence of oxygen HIF competes with many ankyrin repeat domain-containing proteins (ARDs) for hydroxylation by FIH. Many ARDs have a proposed function in cell proliferation and differentiation. Due to this competition hypoxia or a decreased presence of FIH may lead to accumulation of non-hydroxylated ARDs. Although the exact mechanisms have not yet been elucidated, downstream effects of this accumulation may lead to increased tumor aggressiveness.[44-45]

PHD proteins have been studied in several other tumor types as potential prognostic markers.[16-17] In these studies high nuclear PHD levels were associated with tumor aggressiveness and worse survival. For ccRCC, as far as we know no information was present for PHD expression in relation to patient survival. We show that there is no correlation between PHD1, 2, 3 and RCC patient survival. Surprisingly, in this study high nuclear PHD levels were significantly correlated to a low Fuhrman grade, indicating that in contrast to other tumor types, increased nuclear PHD levels are primarily present in less aggressive (grade 1) ccRCC.

Here we show that FIH is a very promising prognostic marker for ccRCC. However, for its definitive clinical value a prospective clinical trial will be needed. Like most described prognostic markers in literature this study was performed on tissue obtained in the time that immunotherapy was first line therapy for RCC. In the current era of targeted therapy correlation of these prognostic tissue markers to survival is therefore not completely certain, especially when markers have a function in tumor specific immunology. However, since only a minority of our patient population underwent immunotherapy and the here described markers are not known to have a function in the immune system, it is highly unlikely that the prognostic significance will be altered under current treatment standards. Furthermore, prospective clinical trials are needed to determine the additional clinical significance and application of FIH to the currently available prognostic models for non-metastasized disease.

Conclusions

In conclusion, this study shows that nuclear FIH is an important indicator of prognosis in ccRCC patients, with low nuclear FIH expression predicting a poor OS. Unlike previous studies focussing on HIF and its downstream targets, the results presented here highlight the importance of upstream regulatory proteins of the HIF pathway as independent prognostic factors for ccRCC. We anticipate that integration of FIH in established prognostic models could result in a more accurate prediction of survival.

References

1. Parkin DM, Bray F, Ferlay J, Pisani P. Global cancer statistics, 2002. CA Cancer J Clin 2005;55:74-108.

2. Zisman A, Pantuck AJ, Wieder J, et al. Risk group assessment and clinical outcome algorithm to predict the natural history of patients with surgically resected renal cell carcinoma. J Clin Oncol 2002;20:4559-66.

3. Motzer RJ, Hutson TE, Tomczak P, et al. Overall survival and updated results for sunitinib compared with interferon alfa in patients with metastatic renal cell carcinoma. J Clin Oncol 2009;27:3584-90.

4. Zisman A, Pantuck AJ, Dorey F, et al. Improved prognostication of renal cell carcinoma using an integrated staging system. J Clin Oncol 2001;19:1649-57.

5. Frank I, Blute ML, Cheville JC, Lohse CM, Weaver AL, Zincke H. An outcome prediction model for patients with clear cell renal cell carcinoma treated with radical nephrectomy based on tumor stage, size, grade and necrosis: the SSIGN score. J Urol 2002;168:2395-400.

6. Fuhrman SA, Lasky LC, Limas C. Prognostic significance of morphologic parameters in renal cell carcinoma. Am J Surg Pathol 1982;6:655-63.

7. Ficarra V, Novara G, Galfano A, et al. The 'Stage, Size, Grade and Necrosis' score is more accurate than the University of California Los Angeles Integrated Staging System for predicting cancer-specific survival in patients with clear cell renal cell carcinoma. BJU Int 2009;103:165-70.

8. Patard JJ, Kim HL, Lam JS, et al. Use of the University of California Los Angeles integrated staging system to predict survival in renal cell carcinoma: an international multicenter study. J Clin Oncol 2004;22:3316-22.

9. Zigeuner R, Hutterer G, Chromecki T, et al. External Validation of the Mayo Clinic Stage, Size, Grade, and Necrosis (SSIGN) Score for Clear-Cell Renal Cell Carcinoma in a Single European Centre Applying Routine Pathology. Eur Urol;57:102-11.

10. Wolff AC, Hammond ME, Schwartz JN, et al. American Society of Clinical Oncology/College of American Pathologists guideline recommendations for human epidermal growth factor receptor 2 testing in breast cancer. J Clin Oncol 2007;25:118-45.

11. Kaelin WG, Jr. The von Hippel-Lindau tumour suppressor protein: O2 sensing and cancer. Nat Rev Cancer 2008;8:865-73.

12. Schofield CJ, Ratcliffe PJ. Oxygen sensing by HIF hydroxylases. Nat Rev Mol Cell Biol 2004;5:343-54.

13. Kim WY, Kaelin WG. Role of VHL gene mutation in human cancer. J Clin Oncol 2004;22:4991-5004.

14. Bui MH, Seligson D, Han KR, et al. Carbonic anhydrase IX is an independent predictor of survival in advanced renal clear cell carcinoma: implications for prognosis and therapy. Clin Cancer Res 2003;9:802-11.

15. Klatte T, Seligson DB, LaRochelle J, et al. Molecular signatures of localized clear cell renal cell carcinoma to predict disease-free survival after nephrectomy. Cancer Epidemiol Biomarkers Prev 2009;18:894-900.

16. Couvelard A, Deschamps L, Rebours V, et al. Overexpression of the oxygen sensors PHD-1, PHD-2, PHD-3, and FIH Is associated with tumor aggressiveness in pancreatic endocrine tumors. Clin Cancer Res 2008;14:6634-9.

17. Jokilehto T, Rantanen K, Luukkaa M, et al. Overexpression and nuclear translocation of hypoxia-inducible factor prolyl hydroxylase PHD2 in head and neck squamous cell carcinoma is associated with tumor aggressiveness. Clin Cancer Res 2006;12:1080-7.

18. Jans J, van Dijk JH, van Schelven S, et al. Expression and Localization of Hypoxia Proteins in Prostate Cancer: Prognostic Implications After Radical Prostatectomy. Urology 2009.

19. Stolze IP, Tian YM, Appelhoff RJ, et al. Genetic analysis of the role of the asparaginyl hydroxylase factor inhibiting hypoxia-inducible factor (HIF) in regulating HIF transcriptional target genes. J Biol Chem 2004;279:42719-25.

20. Soilleux EJ, Turley H, Tian YM, Pugh CW, Gatter KC, Harris AL. Use of novel monoclonal antibodies to determine the expression and distribution of the hypoxia regulatory factors PHD-1, PHD-2, PHD-3 and FIH in normal and neoplastic human tissues. Histopathology 2005;47:602-10.

21. Tan EY, Campo L, Han C, et al. Cytoplasmic location of factor-inhibiting hypoxia-inducible factor is associated with an enhanced hypoxic response and a shorter survival in invasive breast cancer. Breast Cancer Res 2007;9:R89.

22. Morris MR, Maina E, Morgan NV, et al. Molecular genetic analysis of FIH-1, FH, and SDHB candidate tumour suppressor genes in renal cell carcinoma. J Clin Pathol 2004;57:706-11.

23. Parker AS, Cheville JC, Lohse CM, Igel T, Leibovich BC, Blute ML. Loss of expression of von Hippel-Lindau tumor suppressor protein associated with improved survival in patients with early-stage clear cell renal cell carcinoma. Urology 2005;65:1090-5.

24. Patard JJ, Rioux-Leclercq N, Masson D, et al. Absence of VHL gene alteration and high VEGF expression are associated with tumour aggressiveness and poor survival of renal-cell carcinoma. Br J Cancer 2009;101:1417-24.

25. Schraml P, Hergovich A, Hatz F, et al. Relevance of nuclear and cytoplasmic von hippel lindau protein expression for renal carcinoma progression. Am J Pathol 2003;163:1013-20.

26. Smits KM, Schouten LJ, van Dijk BA, et al. Genetic and epigenetic alterations in the von hippel-lindau gene: the influence on renal cancer prognosis. Clin Cancer Res 2008;14:782-7.

27. Qing G, Simon MC. Hypoxia inducible factor-2alpha: a critical mediator of aggressive tumor phenotypes. Curr Opin Genet Dev 2009;19:60-6.

28. Shinojima T, Oya M, Takayanagi A, Mizuno R, Shimizu N, Murai M. Renal cancer cells lacking hypoxia inducible factor (HIF)-1alpha expression maintain vascular endothelial growth factor expression through HIF-2alpha. Carcinogenesis 2007;28:529-36.

29.	Bos R, van der Groep P, Greijer AE, et al. Levels of hypoxia-inducible factor-1alpha independently predict prognosis in patients with lymph node negative breast carcinoma. Cancer 2003;97:1573-81.

30.	Osada R, Horiuchi A, Kikuchi N, et al. Expression of hypoxia-inducible factor 1alpha, hypoxia-inducible factor 2alpha, and von Hippel-Lindau protein in epithelial ovarian neoplasms and allelic loss of von Hippel-Lindau gene: nuclear expression of hypoxia-inducible factor 1alpha is an independent prognostic factor in ovarian carcinoma. Hum Pathol 2007;38:1310-20.

31.	Rasheed S, Harris AL, Tekkis PP, et al. Hypoxia-inducible factor-1alpha and -2alpha are expressed in most rectal cancers but only hypoxia-inducible factor-1alpha is associated with prognosis. Br J Cancer 2009;100:1666-73.

32.	Lidgren A, Hedberg Y, Grankvist K, Rasmuson T, Bergh A, Ljungberg B. Hypoxia-inducible factor 1alpha expression in renal cell carcinoma analyzed by tissue microarray. Eur Urol 2006;50:1272-7.

33.	Lidgren A, Hedberg Y, Grankvist K, Rasmuson T, Vasko J, Ljungberg B. The expression of hypoxia-inducible factor 1alpha is a favorable independent prognostic factor in renal cell carcinoma. Clin Cancer Res 2005;11:1129-35.

34.	Klatte T, Seligson DB, Riggs SB, et al. Hypoxia-inducible factor 1 alpha in clear cell renal cell carcinoma. Clin Cancer Res 2007;13:7388-93.

35.	Giatromanolaki A, Koukourakis MI, Sivridis E, et al. Relation of hypoxia inducible factor 1 alpha and 2 alpha in operable non-small cell lung cancer to angiogenic/molecular profile of tumours and survival. Br J Cancer 2001;85:881-90.

36.	Griffiths EA, Pritchard SA, McGrath SM, et al. Hypoxia-associated markers in gastric carcinogenesis and HIF-2alpha in gastric and gastro-oesophageal cancer prognosis. Br J Cancer 2008;98:965-73.

37.	Holmquist-Mengelbier L, Fredlund E, Lofstedt T, et al. Recruitment of HIF-1alpha and HIF-2alpha to common target genes is differentially regulated in neuroblastoma: HIF-2alpha promotes an aggressive phenotype. Cancer Cell 2006;10:413-23.

38.	Carroll VA, Ashcroft M. Role of hypoxia-inducible factor (HIF)-1alpha versus HIF-2alpha in the regulation of HIF target genes in response to hypoxia, insulin-like growth factor-I, or loss of von Hippel-Lindau function: implications for targeting the HIF pathway. Cancer Res 2006;66:6264-70.

39.	Kondo K, Kim WY, Lechpammer M, Kaelin WG, Jr. Inhibition of HIF2alpha is sufficient to suppress pVHL-defective tumor growth. PLoS Biol 2003;1:E83.

40.	Sandlund J, Ljungberg B, Wikstrom P, Grankvist K, Lindh G, Rasmuson T. Hypoxia-inducible factor-2alpha mRNA expression in human renal cell carcinoma. Acta Oncol 2009;48:909-14.

41.	Aprelikova O, Chandramouli GV, Wood M, et al. Regulation of HIF prolyl hydroxylases by hypoxia-inducible factors. J Cell Biochem 2004;92:491-501.

42.   Henze AT, Riedel J, Diem T, et al. Prolyl hydroxylases 2 and 3 act in gliomas as protective negative feedback regulators of hypoxia-inducible factors. Cancer Res;70:357-66.

43.   Kim Y, Lin Q, Glazer PM, Yun Z. Hypoxic tumor microenvironment and cancer cell differentiation. Curr Mol Med 2009;9:425-34.

44.   Cockman ME, Webb JD, Ratcliffe PJ. FIH-dependent asparaginyl hydroxylation of ankyrin repeat domain-containing proteins. Ann N Y Acad Sci 2009;1177:9-18.

45.   Meteoglu I, Erdogdu IH, Meydan N, Erkus M, Barutca S. NF-KappaB expression correlates with apoptosis and angiogenesis in clear cell renal cell carcinoma tissues. J Exp Clin Cancer Res 2008;27:53.

Chapter 4

Real-time 3D fluoroscopy guided large core needle biopsy of renal masses: a critical early evaluation according to the IDEAL recommendations

Stephanie G.C. Kroeze[1]
Merel Huisman[2]
Helena M. Verkooijen[2]
Paul J. van Diest[3]
J.L.H. Ruud Bosch[1]
Maurice A.A.J. van den Bosch[2]

[1]Department of Urology, University Medical Center Utrecht, the Netherlands
[2]Department of Radiology, University Medical Center Utrecht, the Netherlands
[3]Department of Pathology, University Medical Center Utrecht, the Netherlands

Abstract

Introduction

3D real-time fluoroscopy cone beam CT is a promising new technique for image guided biopsy of solid tumors. We evaluated technical feasibility, diagnostic accuracy and complications of this technique for guidance of large-core needle biopsy in patients with suspicious renal masses.

Materials and Methods

13 patients with 13 suspicious renal masses underwent large-core needle biopsy under 3D real-time fluoroscopy cone beam CT guidance. Imaging acquisition and subsequent 3D reconstruction was done by a mobile flat-panel detector (FD) C-arm system in order to plan the needle path. Large-core needle biopsies were taken by the interventional radiologist. Technical success, accuracy and safety were evaluated, according to the Innovation, Development, Exploration, Assessment, Long-term study (IDEAL) recommendations.

Results

Median tumor size was 2.6 (range 1.0-14.0) cm. In 10 (77%) patients, the histological diagnosis corresponded to the imaging findings; 5 were malignancies, 5 benign lesions. Technical feasibility was 77% (10/13), in 3 patients biopsy results were inconclusive. The lesion size of these 3 patients was <2.5 cm. One patient developed a minor complication. Median follow-up was 16.0 (range 6.4-19.8) months.

Conclusions

3D real-time fluoroscopy cone beam CT guided biopsy of renal masses is feasible and safe. However, these first results suggest that diagnostic accuracy may be limited in patients with renal masses <2.5 cm.

Introduction

The incidence of renal tumors is rising.[1-2] Most of these tumors are found in the elderly, a group of patients prone for comorbidities and often considered to be surgically high-risk. The standard of care consists of laparoscopic or open (nephron-sparing) surgical resection.[3] Currently, 50-60% of renal tumors are small renal masses, i.e. smaller than 4 cm. Approximately 20% of these small renal masses are benign, which can not always be concluded on preoperative two-phase contrast CT. [4-5]. Availability of a preoperative histological diagnosis would strongly improve clinical management of these patients, which is why the role of role of renal mass biopsy is becoming increasingly important.[6-8]

Currently, renal mass biopsy is performed either under ultrasound, CT or MRI guidance. The choice of modality varies between institutions as each modality has its advantages and shortcomings. Ultrasound guidance, for instance, is readily available and uses no ionizing radiation, but may yield suboptimal results in obese patients. MRI guidance provides excellent soft tissue imaging, but costs are high and available work space for the interventional radiologist is restricted. CT imaging requires ionizing radiation and lacks real-time feedback. While over the years the success rate of renal biopsies of solid masses has increased to up to 90%, remaining limitations include technical failure and indeterminate or inaccurate histological diagnosis, [9] in particular in lesions smaller than 3 cm [10-12]. Also, the diagnostic accuracy of biopsies of small cystic lesions remains a problem since the cancerous tissue is often focally present within the cyst. [10, 13] A new technological development in imaging guided interventions is the C-arm cone beam CT with fluoroscopy overlay. This modality has recently been described in the use of embolization and needle interventions of several organs. [14-16] The advantage of C-arm cone beam CT is the combination of 3D soft tissue imaging and real-time imaging as well as improved accessibility to the intervention site.[17] This system has been developed to allow the interventional radiologist to plan the needle path in order to reduce intra- and interoperator variability, complication rate and technical failure of biopsies. The procedure is performed in the angiography suite which allows for adequate patient monitoring during the procedure. Considering these advantages we postulated that this modality would be a valuable improvement for diagnostic biopsy of renal masses.

Objectively assessing the value of new radiological interventions is challenging. Recently the Innovation, Development, Exploration, Assessment, Long-term study (IDEAL) guidelines were introduced, which propose a five-stage evaluation for the development of complex interventions in order to improve the quality and quantity of research in this field. [18] These steps include innovation (stage 1), development (stage 2a), exploration (stage 2b), assessment (stage 3) and long-term study (stage 4). 3D real-time fluoroscopy cone beam CT

45

guided biopsy has completed the first stage of the IDEAL model and has now arrived at stage 2a; development. In this stage a procedure is performed in a small set of patients to increase experience and to investigate the indications of use. The focus of this stage lies on the description of the procedure, technical modifications and a clear outcome reporting of all cases. In this paper, we evaluate the feasibility, accuracy and complications of real-time 3D fluoroscopy guidance system in combination with needle path planning for biopsy of renal masses in a first series of patients in our institution.

Materials and Methods

Patients

Thirteen patients were included between August 2009 and September 2010. Inclusion criteria were a renal mass suspect for malignancy on CT (solid enhancing mass or Bosniak category ≥ III), visibility of the lesion on non-enhanced CT and accessibility of the lesion. Accessibility of the lesion by XperGuide required a cortical, preferably dorsal, tumor localization. Exclusion criteria were inability to remain immobile in prone position for a prolonged period or inability to follow breath-hold commands. Informed consent was obtained from all patients. Since current international guidelines state that suspicious renal masses require histological examination, ethical approval was waived. All patients underwent renal biopsy according to a standard protocol.

Imaging system and techniques

Image acquisition and subsequent computing was done by means of a mobile flat-panel detector (FD) C-arm system with software applications designed for reconstructing soft-tissue 3D images through fluoroscopy (Allura FD 20, XperCT, XperGuide; Philips Healthcare). The FD system provides high spatial resolution while minimising radiation dose. Calibration is done automatically. The C-arm rotates in a 180-240° angle while generating 312 projections within 7 seconds. Following image acquisition, a 3D data set of the area of interest was computed by the XperCT software system. To construct the optimal needle path by means of the XperGuide program, the interventional radiologist selected a target point within the lesion using the workstation (fig. 1C). Connection of those points resulted in a straight needle path which could be adjusted to preserve important anatomic structures. After generating this needle path the program automatically provided the required angulation and rotation of the C-arm. The C-arm positioning was determined by the software program and the interventional radiologist was able to switch C-arm angles from parallel to perpendicular with respect to the needle tract by means of the user's panel. For positioning the guiding needle and administration of local anaesthetics the parallel C-arm configuration was used.

The needle path was depicted with a safety margin of 1 cm (fig. 1D). After needle insertion the C-arm was configured perpendicular to the needle tract. The planned needle path was visible as an overlay on real-time fluoroscopy (fig. 1E). Once the guiding needle had reached the target point on fluoroscopy, a cone-beam CT was performed in order to establish adequate needle tip position and exclusion of possible complications (fig. 1F).

Procedure

All procedures were performed in the angiography suite by an interventional radiologist experienced in image guided needle interventions. Assistance was provided by a specifically trained medical imaging technician. Before starting the intervention, patients were given a prophylactic intravenous catheter. Patients were placed in prone position (fig. 1A) and constantly monitored (ECG, blood pressure) during the procedure. Patients were instructed to hold their breath at maximal inspiration during initial imaging to avoid motion artefacts. Once the needle path was planned the skin entry point was identified, disinfected and a sterile field was created. Local anesthetic (lidocaine 1%) was administered at the entry site and along the needle tract. A 17 G guiding needle was placed in the calculated angle and fixed with a needle guiding device (fig. 1B) (SeeStar 17G guiding device, Radi Medical Devices). During subsequent needle advancement in accordance with the depicted needle tract, patients were given breath-hold commands for maximal inspirational levels. Large-core needle biopsies were subsequently taken, using an 18 G needle.

Outcome measures

The outcome measures of this study were technical feasibility and safety. Technical feasibility was defined as the situation where the tip of the needle reached the target point adequately and sufficient tissue was obtained for a histological result that was concordant to imaging findings. A specimen with a compact consistency and a minimal length of 1 cm was defined as sufficient for histological analysis. In case of a histopathologically proven diagnosis of malignancy, tumors were surgically removed or patients were referred to a medical oncologist for further treatment. For patients with biopsies that showed a benign lesion (including those that appeared radiologically malignant), follow-up consisted of an ultrasound or CT after 6 months followed by a second biopsy, surgery or watchful waiting if the renal mass remained suspicious. Patients with malignant biopsies undergoing surgical or medical treatment were followed-up with 6 monthly ultrasound or CT as well. Patients were observed for possible complications using the modified Clavien scoring system[19] and discharged the same day when no major complications (Clavien grade>2) occurred.

Results

Thirteen consecutive patients were included (Table 1), 9 males and 4 females. Median age was 74.0 (range 37.9-80.4) years. Median tumor size was 2.6 (range 1.0- 14) cm. Nine lesions were solid, 2 Bosniak III and 2 Bosniak IV. For all patients a needle path was planned according to protocol and in all patients, the biopsy needle could be placed accordingly. Technical modifications of the procedure were therefore not necessary. The median procedural time was 29 (range 20-41) minutes, during which a median number of 2.0 (range 1-4) cores were taken per lesion. Histopathology revealed that 5 lesions were malignant and 5 benign (table 2). The biopsy results of 3 lesions were considered to be inconclusive since imaging showed suspicious lesions, while the biopsies consisted of normal renal parenchyma, insufficient material or just connective tissue. The diameters of these lesions were 1.0, 1.8 and 2.4 cm, respectively. Patients were followed for a median period of 16.0 (range 6.4-19.8) months. During this period the diagnosis of 7 biopsies (5 malignancies and 2 benign lesions) were surgically or clinically confirmed. During follow-up lesion size of the small renal masses in patients that did not undergo surgery remained unchanged on CT. During the intervention, no complications occurred. In the 30 days following the intervention one unexpected grade 2 complication occurred, i.e. femoropopliteal bypass occlusion due to a stop of anticoagulants before the biopsy. All patients were discharged on the day of the procedure.

Table 1: Patient characteristics

Table 1. Patient characteristics

Patient No.	Sex	Age (y)	Size (cm)	Type	Final diagnosis	Concordant
1	F	80.4	2.6	Solid	ccRCC	yes
2	M	76.0	3.0	Bosniak IV	Interstitial nephritis	yes
3	M	56.6	3.3	Solid	Membranoproliferative glomerulonephritis	yes
4	M	37.9	6.0	Solid	Infarction	yes
5	M	64.0	1.0	Solid	Normal kidney parenchyma	no
6	F	46.1	1.2	Bosniak III	Angiomyolipoma	yes
7	F	75.0	6.6	Solid	ccRCC	yes
8	M	74.6	2.4	Solid	Inconclusive (insufficient material)	no
9	M	74.0	1.8	Bosniak IV	Lymphoma	yes
10	M	59.4	1.8	Bosniak III	Connective tissue/fat	no
11	M	79.7	5.5	Solid	Oncocytoma	yes
12	F	75.4	14.0	Solid	Leiomyosarcoma	yes
13	M	65.8	2.6	Solid	ccRCC	yes

Figure 1: Example of the procedural setup. **(A)** The patient is placed in prone position. Image acquisition and computing is performed by means of a mobile flat-panel detector C-arm system with software applications designed for reconstructing soft-tissue 3D images through fluoroscopy (Allura FD 20, XperCT, XperGuide; Philips Healthcare). **(B)** The 17 G guiding needle is placed in the calculated angle and fixed with a needle guiding device (SeeStar 17G guiding device, Radi Medical Devices). **(C)** The renal mass is marked with a dotted line. The target point (white) is selected within the renal mass. **(D)** A needle path is planned by connecting the target point within the renal mass (area within the dotted line) and a selected skin needle entry point on the 3D workstation. The path is inspected with regard to vessel, bone and organ anatomy. **(E)** The 17G guiding needle is advanced under real-time fluoroscopy with overlay of the planned needle path. **(F)** Before renal mass biopsy a cone-beam CT is performed to confirm that the tip of the guiding needle was within the target lesion. The renal mass is marked with a dotted line.
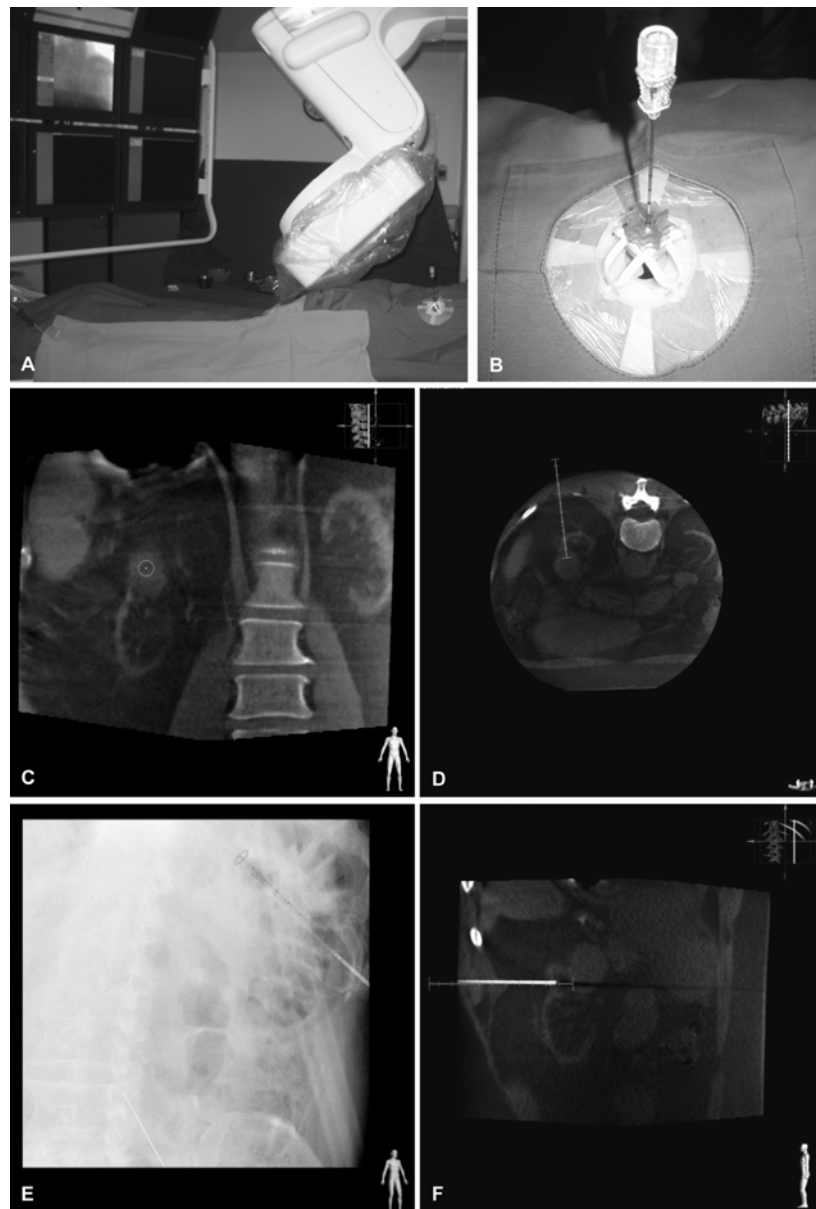
Table 2: Results

	Median (range)	Number
Procedures		
Technical successful procedures		13
Procedure time (min)	29 (20-41)	
Number of cores (n)	2 (1-4)	
Follow-up duration (months)	16.0 (6.4-19.8)	
Complications		
Minor		1
Major		0

Discussion

Large core-needle biopsy of suspicious renal masses plays an increasingly important role in the clinical management of patients with renal masses. The accuracy of renal biopsies with use of conventional imaging (CT- or ultrasound-guided) has increased to up to 90% and minor complications or technical failure occur in less than 5% of biopsies.[10] However, accuracy levels for renal masses less than 3 cm appear to be lower.[10-12] New image guidance techniques are being designed in order to optimize biopsy procedures.[20] The 3D real-time fluoroscopy guidance system has recently been tested for embolization of jugular paragangliomas, and needle interventions of the spine, pelvis and several organs (IDEAL stage 1; innovation and stage 2a; development).[14-16] For renal mass biopsy, potential advantages compared to established techniques (CT- or ultrasound-guidance) consist of allowing the planning of a needle path prior to biopsy and performance in the angiography suite, which provides continuous monitoring of the patient. This is particularly important in this category of patients, due to the high prevalence of comorbidities.[21] Here, we studied the use of the 3D real-time fluoroscopy guidance system for renal mass biopsies, using the IDEAL recommendations (stage 2a; development). We showed that it was feasible to determine a needle track with use of 3D CT, but that the obtained technical feasibility was just 77%. This shows that there might be a need to modify the technique, which is common during stage 2a. The median duration of the procedure was 29 minutes, which is similar to real-time fluoroscopy intervention times described in literature.[14, 22] During the procedures no complications occurred, and only one minor complication occurred after the procedure, indicating that this procedure is safe. While complication were comparable, success rates were lower compared to the presently available studies using the same technique.[14-16] Despite the needle tip being adequately positioned in all cases, 3 out of 13 biopsy results revealed tissue that was considered to be inconclusive; i.e. imaging showed a clear tumor while biopsy contained insufficient material or showed normal renal tissue, or non-renal tissue. These inconclusive biopsy results all occurred in renal masses smaller than 2.5 cm. An explanation for this might be that the kidney is a dynamic target; due to breathing kidneys may displace 2-3 cm in the craniocaudal direction.[23] Although the presented technique includes real-time visualisation of the needle-placement, the planned needle path is based

on static images. This may result in non-target tissue sampling due to lesion motion, especially when target lesions are small in size (<2.5 cm). This has also been described in a series of 3D real-time fluoroscopy guidance system biopsies of which biopsy failure with renal parenchyma was present in 3 out of 10 failures in 145 biopsies of various organs.[14] Anticipation to motion artefacts in the form of breath-hold commands is difficult to achieve in this procedure since patients have to reproduce a certain inspirational level.

All rotation acquisitions were performed unenhanced. As a consequence solid parts may have been difficult to differentiate in cystic masses. However, only one of the four biopsies of cystic lesions resulted in an inconclusive diagnosis. In stage 2 of the IDEAL recommendations the learning curve and the possibility for adoption by other intervention radiologists is also important. In our study, renal mass biopsies were performed by interventional radiologists experienced in image guided needle interventions. No clear learning curve was observed, which may suggest that this technique can be readily adopted by other experienced intervention radiologists. However, although 3D real-time fluoroscopy cone beam CT guided renal biopsy is feasible and safe, it seems that this technique has no advantage to conventional techniques for the very small (<2.5 cm) renal masses. For larger renal masses, this technique is comparable to the conventional techniques in terms of success rate and accuracy.[10] The choice to perform either a 3D real-time fluoroscopy cone beam CT guided renal biopsy or an ultrasound or CT guided biopsy is therefore dependent on the modalities present, the patient and the location of the tumor. 3D real-time fluoroscopy cone beam CT guided renal biopsy might prove its true advantages in static target lesions, such as tumors in the spine or pelvic area.[14-15, 24-25]

Conclusion

In conclusion, 3D real-time fluoroscopy guidance is an important new development in imaging guided interventions and can be used for biopsy of renal masses. However, the diagnostic accuracy for renal masses smaller than 2.5 cm appears to be moderate due to the fact that static images are used for tumor targeting in a moving organ.

References

1. Hollingsworth JM, Miller DC, Daignault S, Hollenbeck BK. Five-year survival after surgical treatment for kidney cancer: a population-based competing risk analysis. Cancer 2007;109:1763-8.
2. Lightfoot N, Conlon M, Kreiger N, et al. Impact of noninvasive imaging on increased incidental detection of renal cell carcinoma. Eur Urol 2000;37:521-7.
3. Heuer R, Gill IS, Guazzoni G, et al. A critical analysis of the actual role of minimally invasive surgery and active surveillance for kidney cancer. Eur Urol;57:223-32.
4. Bosniak MA, Rofsky NM. Problems in the detection and characterization of small renal masses. Radiology 1996;198:638-41.
5. Frank I, Blute ML, Cheville JC, Lohse CM, Weaver AL, Zincke H. Solid renal tumors: an analysis of pathological features related to tumor size. J Urol 2003;170:2217-20.
6. Eshed I, Elias S, Sidi AA. Diagnostic value of CT-guided biopsy of indeterminate renal masses. Clin Radiol 2004;59:262-7.
7. Maturen KE, Nghiem HV, Caoili EM, Higgins EG, Wolf JS, Jr., Wood DP, Jr. Renal mass core biopsy: accuracy and impact on clinical management. AJR Am J Roentgenol 2007;188:563-70.
8. Wood BJ, Khan MA, McGovern F, Harisinghani M, Hahn PF, Mueller PR. Imaging guided biopsy of renal masses: indications, accuracy and impact on clinical management. J Urol 1999;161:1470-4.
9. Laguna MP, Kummerlin I, Rioja J, de la Rosette JJ. Biopsy of a renal mass: where are we now? Curr Opin Urol 2009;19:447-53.
10. Lane BR, Samplaski MK, Herts BR, Zhou M, Novick AC, Campbell SC. Renal mass biopsy--a renaissance? J Urol 2008;179:20-7.
11. Lechevallier E, Andre M, Barriol D, et al. Fine-needle percutaneous biopsy of renal masses with helical CT guidance. Radiology 2000;216:506-10.
12. Wang R, Wolf JS, Jr., Wood DP, Jr., Higgins EJ, Hafez KS. Accuracy of percutaneous core biopsy in management of small renal masses. Urology 2009;73:586-90; discussion 90-1.
13. Volpe A, Mattar K, Finelli A, et al. Contemporary results of percutaneous biopsy of 100 small renal masses: a single center experience. J Urol 2008;180:2333-7.
14. Braak SJ, van Strijen MJ, van Leersum M, van Es HW, van Heesewijk JP. Real-Time 3D fluoroscopy guidance during needle interventions: technique, accuracy, and feasibility. AJR Am J Roentgenol 2010;194:W445-51.
15. Leschka SC, Babic D, El Shikh S, Wossmann C, Schumacher M, Taschner CA. C-arm cone beam computed tomography needle path overlay for image-guided procedures of the spine and pelvis. Neuroradiology 2011, Epublished ahead of print
16. Spelle L, Ruijters D, Babic D, et al. First clinical experience in applying XperGuide   in embolization of jugular paragangliomas by direct intratumoral puncture. Int J Comput Assist Radiol Surg 2009;4:527-33.

17. Wallace MJ, Kuo MD, Glaiberman C, Binkert CA, Orth RC, Soulez G. Three-dimensional C-arm cone-beam CT: applications in the interventional suite. J Vasc Interv Radiol 2009;20:S523-37.

18. McCulloch P, Altman DG, Campbell WB, et al. No surgical innovation without evaluation: the IDEAL recommendations. Lancet 2009;374:1105-12.

19. Clavien PA, Barkun J, de Oliveira ML, et al. The Clavien-Dindo classification of surgical complications: five-year experience. Ann Surg 2009;250:187-96.

20. Beland MD, Mayo-Smith WW, Dupuy DE, Cronan JJ, DeLellis RA. Diagnostic yield of 58 consecutive imaging-guided biopsies of solid renal masses: should we biopsy all that are indeterminate? AJR Am J Roentgenol 2007;188:792-7.

21. Santos Arrontes D, Fernandez Acenero MJ, Garcia Gonzalez JI, Martin MunozM, Paniagua Andres P. Survival analysis of clear cell renal carcinoma according to the Charlson comorbidity index. J Urol 2008;179:857-61.

22. de Mey J, Op de Beeck B, Meysman M, et al. Real time CT-fluoroscopy: diagnostic and therapeutic applications. Eur J Radiol 2000;34:32-40.

23. Kerkhof EM, Raaymakers BW, van Vulpen M, et al. A new concept for non-invasive renal tumour ablation using real-time MRI-guided radiation therapy. BJU Int 2011;107:63-8.

24. Powell MF, DiNobile D, Reddy AS. C-arm fluoroscopic cone beam CT for guidance of minimally invasive spine interventions. Pain Physician 2010;13:51-9.

25. Tam AL, Mohamed A, Pfister M, et al. C-arm cone beam computed tomography needle path overlay for fluoroscopic guided vertebroplasty. Spine (Phila Pa 1976) 2010;35:1095-9.

Chapter 5

Impact of comorbidity on complications following nephrectomy: use of the Clavien Classification of Surgical Complications

Stephanie G.C. Kroeze*

Pauline M.L. Hennus*

J.L.H. Ruud Bosch

Judith J.M. Jans

* Authors contributed equally to the manuscript

Department of Urology, University Medical Center Utrecht, the Netherlands

Abstract

Introduction

To present a single-center experience of open nephrectomy for lesions suspected for RCC, evaluating the association between comorbidity and postoperative complications using a standardized classification system for postoperative complications.

Patients and methods

Clinicopathological data of 198 patients undergoing open radical or partial nephrectomy for lesions suspected of renal cell carcinoma (RCC) were retrospectively analyzed. Comorbidity scored by the Charlson comorbidity index (CCI), body mass index (BMI), age, gender, surgical procedure and surgical history were examined as predictive factors for postoperative complications, which were scored using the modified Clavien Classification of Surgical Complications (CCSC).

Results

The overall complication rate was 34%: 7% grade I, 15% grade II, 5% grade III, 3% grade IV and 4% grade V. Preoperative comorbidities were present in 51% of all patients. There were significantly more major complications (CCSC >2) in patients with major comorbidities (CCI >2) (16% vs. 7%, p=0.018). Patients with high-stage RCC had significantly more severe complications than low-stage RCC (p=0.018). In multivariable analysis, comorbidity (OR 7.55, p=0.004) and tumor stage 3-4 (OR 6.23, p=0.007) were independent predictive factors for major complications.

Conclusions

Major complications occur significantly more often when major comorbidities are present. Comorbidity scores can be used in risk stratification for complications and should be considered during decision-making and counselling of patients before nephrectomy.

Introduction

Surgical resection is the only curative treatment for renal cell carcinoma (RCC). Established surgical treatments for RCC range from radical to nephron-sparing surgery with an open, laparoscopic or robotic approach.[1] In the preoperative assessment of RCC patients various factors are considered important for surgical outcome and prognosis. Besides tumor characteristics (such as stage and grade) these factors include patient physical status and comorbidities.[2-5] With the increasing incidence of RCC in an elderly population, comorbidities and advanced age are important factors that compete with RCC as the primary cause of death.[5-6] This strengthens the importance of preoperative decision-making for those who might benefit from surgical treatment of RCC. Although comorbidity is taken into account when deciding who is fit for surgery, it has not been objectively validated whether comorbidities actually affect complication rates following nephrectomy using a standardized complication grading system.

Although complication rates are often used to compare the success of renal surgical techniques, there is no consensus regarding the methods for reporting postoperative complications. As a consequence, the reported incidence of complications in renal surgery ranges from 2-54%, irrespective of surgical approach.[7-11] This hampers comparison of renal surgical procedures, and complicates an adequate estimation of postoperative morbidity.

Reporting and grading of complications in a structured fashion is only one aspect of the quality of outcome reporting. In 2002, Martin et al. proposed that 10 criteria should be met when reporting complications following surgery, including the use of a grading system to clarify the severity of complications.[12] One system that systematically scores the severity of complications is the Clavien Classification of Surgical Complications (CCSC).[13-14] This system has been developed and validated for complication assessment in general surgery, and can be adjusted to any surgical procedure. In urological practice, the CCSC has been successfully applied to transurethral resection of the prostate, percutaneous nephrolithotomy, laparoscopic radical prostatectomy, laparoscopic live donor nephrectomy, and RCC with vena cava thrombus.[15-19]

To adequately compare renal surgical techniques and assess patient outcome and prognosis, a modification of this system to renal surgery is important. Therefore, this study objectively evaluates the association between comorbidity and postoperative complications following nephrectomy for RCC, by applying the CCSC in grading complications following nephrectomy.

Patients and methods

Patient characteristics

All nephrectomies between January 1999 and December 2008 at the University Medical Center Utrecht were retrospectively retrieved through the hospital surgical registration database. After identifying all these cases, individual patient files were manually checked for in- and exclusion criteria. We included patients undergoing open partial or radical nephrectomy for lesions suspected for RCC. Seventeen patients with von Hippel-Lindau's disease, tuberous sclerosis or Wilms' tumors were excluded. The clinico-pathologic characteristics of the 198 patients are summarized in Table 1.

Table 1. Baseline characteristics of the study population.

Features	Median (interquartile range)	n (%)
Patients (n)		198 (100)
Age (years)	62 (52-71)	
Gender		
Female		69 (35)
Male		129 (65)
Body mass index (kg/m²)	25 (23-28)	
Subtype		
ccRCC		144 (73)
pRCC		26 (13)
RCC NOS		6 (3)
Chromophobe RCC		1 (0.5)
Oncocytoma		6 (3)
Renal collecting duct carcinoma (Bellini)		1 (0.5)
Upper transitional cell carcinoma (UTCC)		4 (2)
Benign		10 (5)
Intent of surgery		
Curative		170 (86)
Cytoreductive		28 (14)
Open nephrectomy		
Radical		158 (80)
Partial		40 (20)
Fuhrman nuclear grade		121 (100)
1		12 (10)
2		68 (56)
3		37 (31)
4		4 (3)
Tumor classification		
pT1		77 (39)
pT2		18 (9)
pT3		83 (42)
pT4		6 (3)
benign/other lesions		14 (7)
Metastasis at time of diagnosis		
Mx/M 0		172 (87)
M 1		26 (13)
Tumor diameter	6.5 (4.0 – 9.5)	
≤ 4 cm		55 (28)
> 4 cm		143 (72)
Charlson Comorbidity Index		
0		96 (49)
1		32 (16)
2		40 (20)
3		8 (4)
4		10 (5)
5		4 (2)
≥ 6		8 (4)
Clavien Classification of Surgical Complications		
No complications		131 (66)
Grade I		14 (7)
Grade II		30 (15)
Grade III a		6 (3)
Grade III b		4 (2)
Grade IV a		4 (2)
Grade IV b		1 (1)
Grade V		8 (4)

ccRCC = clear cell renal cell carcinoma; pRCC = papillary renal cell carcinoma; RCC NOS = renal cell carcinoma not otherwise specified

Patient clinical and pathologic data were obtained by reviewing hospital records and information from the general practitioner, and included age, gender, 2002 tumor-node-metastasis (TNM) classification, Fuhrman grade, primary tumor size, and comorbidities scored according to the Charlson Comorbidity Index (CCI). The CCI was categorized as described by Santos et al.[5] where minor comorbidities are defined as a CCI score ≤ 2 and major comorbidities are defined as a CCI score >2. All operations were performed under general anesthesia by experienced urologists.

Table 2. The modified Clavien Classification of Surgical Complications.

Grade	Definition
0	No complications
I	Any deviation from the normal postoperative course
II	Complications requiring pharmacological treatment
III	Complications requiring surgical, endoscopic or radiological intervention
a	Intervention not under general anesthesia
b	Intervention under general anesthesia
IV	Life-threatening complications requiring ICU management
a	Single organ dysfunction (including dialysis)
b	Multi organ dysfunction
V	Death

Complications

Data were systematically collected according to the Martin criteria.[12] Complications that occurred during the 30-day postoperative period (including information from our outpatient clinic) were retrospectively categorized according to the CCSC[14] (Table 2) by a trained medical researcher, not involved in the primary care of the patients. If a complication was part of the expected postoperative course after nephrectomy (e.g. a temporary expected rise of serum creatinine not leading to dialysis) it was not included in the Clavien score.[20-21] In case of multiple complications in the same patient, all complications were independently rated and the highest grade was used for the statistical analysis.[14, 20] For analysis, both absolute values of the CCSC and values categorized as minor (grade I and II) and major (grade III, IV and V) were used.[22]

Statistical analysis

Association between CCSC and potential risk factors was studied using Chi square analysis and Fisher's exact test. Based on statistical significance ($p<0.05$) in univariable analysis the variables age, pathologic T-stadium and CCI were included in a multivariable logistic regression model to identify independent predictors for major comorbidities. All statistical analyses were performed using SPSS version 15.0 (SPSS Inc., Chicago, IL).

Results

Clinicopathologic characteristics

A total of 198 patients with a renal mass suspicious for RCC treated by open radical or partial nephrectomy during a 10-year period were included. Pathology reports showed RCC in 177 patients, 21 tumors (11%) were benign or of other origin. Table 1 presents the baseline characteristics of the patients. Of the total group, 26 patients (13%) presented with metastases at time of diagnosis.

Table 3. Complications according to the modified Clavien Classification of Surgical Complications.

Grade	N*	Complication	Management
I	15	Flank hematoma (n=2)	Conservative
		Wound infection (n=2)	Bedside drainage
		Chylous ascites (n=1)	Minimal chain fat diet
		Bradycardia (n=1)	Conservative
		Ileus (n=1)	Conservative
		Chronic non-healing wound at site of epidural (n=1)	Conservative
		Neuropraxia lateral cutaneous femoral nerve (n=1)	Conservative
		Radial nerve neuropathy (n=1)	Conservative
		Atrial flutter (n=2)	Conservative
		Benign paroxysmal positional vertigo (BPPV) (n=1)	Conservative
		Leakage from drain wound (n=1)	Conservative
		Neurological disorder undifferentiated (n=1)	Conservative
II	37	Pneumonia (n=16)	Antibiotics
		Urinary tract infection (n=4)	Antibiotics
		Pulmonary embolism (n=2)	Anticoagulants
		Delirium (n=3)	Antipsychotics
		Deep venous thrombosis (n=2)	Anticoagulants
		Prolonged fever (n=3)	Antibiotics
		Anemia (n=3)	Blood transfusion
		Sepsis (n=1)	Antibiotics
		Transient Ischemic Attack (n=2)	Anticoagulants
		Myocardial infarction (n=1)	Anticoagulants
IIIa	5	Retroperitoneal abscess (n=2)	CT-guided drainage
		Ileus (n=2)	Nasogastric tube
		Urinary fistula (n=1)	JJ-stent
IIIb	5	Wound dehiscence (n=4)	Secondary closure
		Retroperitoneal abscess (n=1)	Relaparotomy
IVa	4	Pneumonia, threatening respiratory insufficiency (n=2)	Admission to ICU
		Acute tubular necrosis (n=1)	Admission to ICU
		Cerebrovascular accident (n=1)	Admission to ICU
IVb	1	Necortizing fasciitis, multi organ failure (n=1)	Admission to ICU
V	8	Saddle embolus (n=2)	-
		Necrotizing fasciitis (n=2)	-
		Multi-organ failure leading to death (n=1)	-
		Post-operative bleeding wherefore relaparotomy, multi-organ failure leading to death (n=1)	-
		Ruptured aortic aneurism (n=1)	-
		Cardiac ischemia (n=1)	-

*Because some patients had more than one complication, the number of complications exceeds the number of patients with complications.

Complications following nephrectomy

Retrospective data on complications were available for all 198 patients. A total of 75 complications were recorded in 67 patients during the postoperative period of 30 days (Table 3). The postoperative overall complication rate (67 of 198 patients) was 34%. Minor complications occurred in 22% of patients (7% grade I, 15% grade II). These complications consisted mostly of infections (52% of grade I and II complications), wound healing problems (12%) and neurological disorders (9%). The most common infection in the minor complications group was pneumonia (43% of grade II complications). Interventions were necessary in 5% (3% grade IIIa, 2% grade IIIb) mostly due to wound dehiscence (40%), retroperitoneal abscess (30%) or ileus (20%). Admission to the intensive care occurred in 3% (2% grade IVa, 1% grade IVb), in 2 of these 5 patients due to threatening respiratory insufficiency following pneumonia. There were 8 (4%) fatal complications leading to death (grade V). No relation between the surgeon that performed the procedure and complication rates was observed.

Figure 1. (A) Duration of hospital stay (in days) after nephrectomy in relation to complications. **(B)** Postoperative complications according to the Clavien Classification of Surgical Complications compared with preoperative comorbidity scored by the Charlson Comorbidity Index.
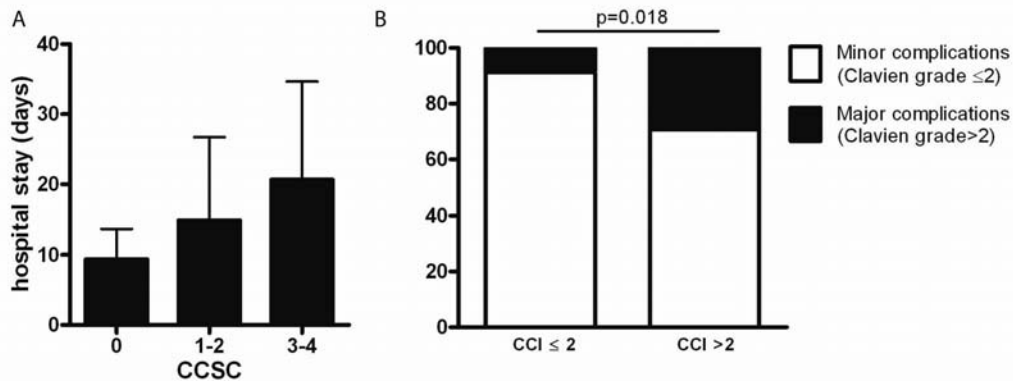
Risk factors for complications following nephrectomy

Preoperative comorbidities were present in 51% of the patients: 36% had minor and 15% had major comorbidities. Preoperative comorbidities were significantly correlated to postoperative complications. Major complications occurred much more frequently (16% vs. 7%, p=0.018) in patients with major comorbidities (Figure 1B), and patients with major comorbidities had an increased risk of intra-operative or postoperative death (14% vs. 3%, p=0.019). Patients with high stage RCC had significantly more complications and severe complications than low stage RCC (p=0.018). Age and year of surgery did not influence complication rates, respectively p=0.33 and p=0.93.

No significant differences in complication rates and severity (p=0.29) were found between a radical versus partial open surgical approach. Furthermore, there was no significant

difference in complication rate between overweight or obese patients and patients with a normal BMI (≤ 25 kg/m^2) (p=0.146). Also, previous abdominal surgical procedures had no significant effect on surgical complications (p=0.18). Of the patients that underwent previous abdominal surgery (36%), 13% underwent minor procedures (e.g. appendectomy, inguinal hernia surgery) and 23% major procedures (e.g. hemicolectomy, cholecystectomy, hysterectomy).

Complication rates had a notable effect on duration of hospital stay (p<0.001). Median hospital stay was 10 (IQR 8-13) days. When no complications occurred, mean hospital stay was 9 days, compared to 16 days for patients with minor complications and 19 days for patients with major complications (Figure 1A).

In the univariable analysis CCI, pathologic T stage and gender were predictors for major complications according to the CCSC (Table 4). In the multivariable analysis both major comorbidities (OR 7.6, p=0.004) and pathologic T3-4 stage (OR 6.2, p=0.007) remained independent predictors for risk of major complications (Table 5).

Table 4. Univariable analysis for prediction of major complications according to the Clavien Classification of Surgical Complications

	p-value
Pathologic T stage	0.018
Age	0.547
Gender	0.024
Charlson Comorbidity Index	0.018
BMI (≤ 25 versus >25 kg/m2)	0.146
Radical versus partial nephrectomy	0.294
Abdominal surgical history	
No abdominal history vs. abdominal surgery	0.180
Minor vs. major abdominal surgery	0.315

Table 5. Multivariable logistic regression analysis* for prediction of major complications according to the Clavien Classification of Surgical Complications

	OR	95% CI	p-value
Charlson Comorbidity Index	7.55	1.91 – 29.8	0.004
T stage			
pT 1	reference	-	-
pT 2	1.35	0.13 – 13.95	0.802
pT 3-4	6.23	1.65 – 23.58	0.007
Gender	x	x	x

OR = odds ratio; CI = confidence interval.
* All significant (p<0.05) univariate variables are included. Operative time and perioperative blood loss are not included because of >10% missing values.

Discussion

In the present study, patients with major comorbidities had more severe postoperative complications. Scoring complications is a generally accepted way of comparing surgical treatment outcome. However, for renal surgery there is no consensus on how postoperative complications should be reported, resulting in a wide range of complication rates. Moreover, the many different renal surgical techniques used, and the ongoing development of new techniques, demand a standardized way of reporting complications to facilitate comparison.[23-24] The Martin criteria can be used as a platform for accurate and comprehensive reporting of surgical complications. Within these criteria the use of an objective grading system for complications is essential. The present study shows that the CCSC is feasible and easily applied for grading complications following renal surgery for suspected RCC. An advantage of the CCSC is that it scores the therapeutic consequences of complications, which are particularly important for patient outcome.

In addition to comorbidity, other factors may influence postoperative complications. With the rising incidence of obesity and increased life expectancy it is important to determine the relationship between these factors and postoperative complications. Studies on obesity as a risk factor for adverse outcomes in surgery show contradictory results, depending on the type of surgery and outcome variables.[25-26] In the present study obesity was not a risk factor for postoperative complications, which is in agreement with Dindo et al.[25] Intra-abdominal adhesions are reported to occur after 50-100% of all abdominal surgical interventions, and can considerably complicate future surgery.[27] However, we found no correlation between previous abdominal surgical procedures and complications. Here, no significant differences in complication rates were found between a radical versus partial open surgical approach, which is in concordance with the observation in literature that the complication rates related to open partial nephrectomy are decreasing over the years.[28]

The 198 nephrectomies reported here had a relatively high complication rate of 34%. However, most of these complications were minor (66%; grade I or II). In most studies, minor complications are regularly omitted. Scoring grade I and II complications is important because they have consequences for the patients. For example, in the present study these minor complications prolonged mean hospital stay by 7 days and thus could delay the initiation of subsequent medical treatment strategies for metastatic disease. Moreover, minimally-invasive surgical techniques may result in relatively more minor than major complications. Therefore, for optimal comparison of both minimally-invasive and invasive surgery, all complications that have therapeutic consequences should be scored.

In the present study, a limitation of retrospective grading of complications over a 10-year period is the possible incompleteness of reported complications. In particular grade I

complications might have been underreported because of their relatively small therapeutic consequences. However, a bias concerning underreporting of low-grade complications is unlikely, since the majority of the complications were grade I or II. Postoperative complication rates are not the only factor determining surgical success, long-term oncological outcomes should also be considered. Besides this, the CCSC cannot be used to assess long-term effects of renal surgery. Furthermore, the study group is relatively small due to the high density of hospitals performing nephrectomies in the Netherlands. Laparoscopic interventions were excluded to avoid a patient group that is too heterogeneous. It is important to include patients with metastasized disease: in our study, because their general condition and performance status prior to surgery was comparable to that of the non-metastasized patients, these patients were eligible for (cytoreductive) nephrectomy. However, multivariable analysis showed that these patients are at risk of more significant postoperative complications, suggesting that extra care is needed in preoperative decision-making for these patients.

The present study is the first to objectively establish that postoperative complications are more severe in patients with major comorbidities after nephrectomy. Possibilities to prevent these complications should be considered and proactive action taken when possible. For example, preoperative preparation in terms of intensive care availability should be considered for these patients. Minor complications consisted mostly of infections which might be prevented by, e.g., better prophylaxis. It is a greater challenge to prevent major complications since COPD, diabetes mellitus and obesity are all risk factors for the major complications described here.[29-30]

Increasingly, governmental agencies and health insurance companies ask individual urology departments to disclose complication and mortality rates of certain procedures for comparison of quality of care on a regional or national level. There is clear consensus among clinicians that such rates should be adjusted for case-mix to allow fair comparisons. Our study shows that the reporting of complications with the CCSC, stratified for CCI, represents one objective way of dealing with this issue.

Conclusions

In conclusion, major complications occur significantly more often in patients with major comorbidities. This shows that, in addition to long-term survival, comorbidity also has a direct impact on postoperative complications. Comorbidity scores could be used in risk stratification for complications and should be taken into account in the preoperative decision-making process and counselling of patients.

References

1. Ljungberg B, Cowan NC, Hanbury DC, et al. EAU guidelines on renal cell carcinoma: the 2010 update. Eur Urol 2010;58:398-406.

2. Bensalah K, Pantuck AJ, Crepel M, et al. Prognostic variables to predict cancer-related death in incidental renal tumours. BJU Int 2008;102:1376-80.

3. de Cassio Zequi S, de Campos EC, Guimaraes GC, Bachega W, Jr., da Fonseca FP, Lopes A. The use of the American Society of Anesthesiology Classification as a prognostic factor in patients with renal cell carcinoma. Urol Int 2010;84:67-72.

4. Heng DY, Xie W, Regan MM, et al. Prognostic factors for overall survival in patients with metastatic renal cell carcinoma treated with vascular endothelial growth factor-targeted agents: results from a large, multicenter study. J Clin Oncol 2009;27:5794-9.

5. Santos Arrontes D, Fernandez Acenero MJ, Garcia Gonzalez JI, Martin Munoz M, Paniagua Andres P. Survival analysis of clear cell renal carcinoma according to the Charlson comorbidity index. J Urol 2008;179:857-61.

6. Kutikov A, Egleston BL, Wong YN, Uzzo RG. Evaluating overall survival and competing risks of death in patients with localized renal cell carcinoma using a comprehensive nomogram. J Clin Oncol 2010;28:311-7.

7. Corman JM, Penson DF, Hur K, et al. Comparison of complications after radical and partial nephrectomy: results from the National Veterans Administration Surgical Quality Improvement Program. BJU Int 2000;86:782-9.

8. Gill IS, Kavoussi LR, Lane BR, et al. Comparison of 1,800 laparoscopic and open partial nephrectomies for single renal tumors. J Urol 2007;178:41-6.

9. Porpiglia F, Volpe A, Billia M, Renard J, Scarpa RM. Assessment of risk factors for complications of laparoscopic partial nephrectomy. Eur Urol 2008;53:590-6.

10. Simmons MN, Gill IS. Decreased complications of contemporary laparoscopic partial nephrectomy: use of a standardized reporting system. J Urol 2007;177:2067-73; discussion 73.

11. Stephenson AJ, Chetner MP, Rourke K, et al. Guidelines for the surveillance of localized renal cell carcinoma based on the patterns of relapse after nephrectomy. J Urol 2004;172:58-62.

12. Martin RC, 2nd, Brennan MF, Jaques DP. Quality of complication reporting in the surgical literature. Ann Surg 2002;235:803-13.

13. Clavien PA, Barkun J, de Oliveira ML, et al. The Clavien-Dindo classification of surgical complications: five-year experience. Ann Surg 2009;250:187-96.

14. Dindo D, Demartines N, Clavien PA. Classification of surgical complications: a new proposal with evaluation in a cohort of 6336 patients and results of a survey. Ann Surg 2004;240:205-13.

15. Harper JD, Breda A, Leppert JT, Veale JL, Gritsch HA, Schulam PG. Experience with 750 consecutive laparoscopic donor nephrectomies--is it time to use a standardized classification of complications? J Urol 2010;183:1941-6.

16. Mamoulakis C, Efthimiou I, Kazoulis S, Christoulakis I, Sofras F. The modified Clavien classification system: a standardized platform for reporting complications in transurethral resection of the prostate. World J Urol 2011;29:205-10.

17. Rabbani F, Yunis LH, Pinochet R, et al. Comprehensive standardized report of complications of retropubic and laparoscopic radical prostatectomy. Eur Urol 2010;57:371-86.

18. Tefekli A, Ali Karadag M, Tepeler K, et al. Classification of percutaneous nephrolithotomy complications using the modified clavien grading system: looking for a standard. Eur Urol 2008;53:184-90.

19. Zastrow S, Leike S, Oehlschlager S, Grimm MO, Wirth M. Surgery for renal cell cancer extending into the inferior vena cava - evaluation of survival and perioperative complications using a standardized classification system. BJU Int 2011;108:1439-43.

20. Clavien PA, Sanabria JR, Strasberg SM. Proposed classification of complications of surgery with examples of utility in cholecystectomy. Surgery 1992;111:518-26.

21. Malcolm JB, Bagrodia A, Derweesh IH, et al. Comparison of rates and risk factors for developing chronic renal insufficiency, proteinuria and metabolic acidosis after radical or partial nephrectomy. BJU Int 2009;104:476-81.

22. Agarwal PK, Sammon J, Bhandari A, et al. Safety profile of robot-assisted radical prostatectomy: a standardized report of complications in 3317 patients. Eur Urol 2011;59:684-98.

23. de la Rosette JJ, Tsakiris P, Ferrandino MN, Elsakka AM, Rioja J, Preminger GM. Beyond prone position in percutaneous nephrolithotomy: a comprehensive review. Eur Urol 2008;54:1262-9.

24. Donat SM. Standards for surgical complication reporting in urologic oncology: time for a change. Urology 2007;69:221-5.

25. Dindo D, Muller MK, Weber M, Clavien PA. Obesity in general elective surgery. Lancet 2003;361:2032-5.

26. McTiernan A. Obesity and cancer: the risks, science, and potential management strategies. Oncology (Williston Park) 2005;19:871-81; discussion 81-2, 85-6.

27. Bruggmann D, Tchartchian G, Wallwiener M, Munstedt K, Tinneberg HR, Hackethal A. Intra-abdominal adhesions: definition, origin, significance in surgical practice, and treatment options. Dtsch Arztebl Int 2010;107:769-75.

28. Lesage K, Joniau S, Fransis K, Van Poppel H. Comparison between open partial and radical nephrectomy for renal tumours: perioperative outcome and health-related quality of life. Eur Urol 2007;51:614-20.

29. Pavlidis TE, Galatianos IN, Papaziogas BT, et al. Complete dehiscence of the abdominal wound and incriminating factors. Eur J Surg 2001;167:351-4; discussion 5.

30. Turtiainen J, Saimanen E, Partio T, et al. Surgical wound infections after vascular surgery: prospective multicenter observational study. Scand J Surg 2010;99:167-72.

Chapter 6

Introduction to and scope of part 2: Minimally invasive treatment of RCC

Active surveillance

Historically, the gold standard treatment of localized renal cell carcinoma (RCC) of any size was radical nephrectomy. For small renal masses (SRMs), partial nephrectomy has become the gold standard. With the more heterogenous presentation and nature of RCC in recent decades, contemporary management of RCC now includes a broad variety of treatment options which will be described in part two of this thesis. SRMs are most frequently found in patients who are at surgical risk due to advanced age, comorbidities, solitary kidneys or patients who are prone to develop multiple renal tumors as a result of hereditary diseases such as von Hippel-Lindau syndrome.[1] It has been shown that not every patient with a SRM will benefit from surgical resection of the tumor, and that many factors compete with RCC in relation to patient survival and health.[2-4] For example, advanced age competes with SRMs in survival of elderly patients. Patient with a solitary kidney also represent a higher risk group for chronic kidney failure and worse prognosis following nephrectomy.[5] Furthermore, most SRMs grow slowly and rarely metastasize.[6] Therefore, it is better to avoid treatment-induced morbidity in several cases.[4] Active surveillance (AS) as management for SRMs has therefore been introduced as appropriate for select patients for whom the risks of treatment are considered too high,[7-9] and patients who have a shorter life expectancy. In patients eligible for AS, metastatic disease is first excluded by imaging. When possible, a renal mass biopsy is taken to histologically confirm RCC. Hereafter, patients are regularly followed by imaging. Growth rate is used as a prognostic factor,[10] although this needs to be further validated.

Minimally invasive nephron-sparing treatment

An important development in the treatment of SRMs is minimally invasive nephron-sparing treatment. The rationale behind this treatment is that SRMs can be treated while morbidity is reduced and renal function is preserved.[8] For patients with a SRM who are young and surgically fit, partial nephrectomy (PN) has become the standard treatment.[9] It has recently been shown that PN has similar oncological outcomes compared to radical nephrectomy, while long term renal function is better preserved.[11] PN can be performed with open, laparoscopic or robotic surgery. For patients with a SRM for whom surgical resection is considered inappropriate, other minimally invasive treatments are being developed.[8] At present, minimally invasive techniques most commonly applied are cryoablation (CA) and radiofrequency ablation (RFA). RFA provides localized thermal coagulative necrosis by

transmitting an alternating current through a probe inserted directly in the tumour. This causes friction of ions within tumor cells, leading to focal heat (50-100ºC) and cell destruction. Since its first reported use on human renal tissue in 1997, the use of RFA as nephron-sparing treatment for SRMs has steadily expanded.[12] Promising results have been reported, as well as factors requiring improvement. For example, when RFA is performed near large blood vessels the blood flow leads thermal energy away from the target tissue, a phenomenon called the heat-sink effect. As renal tumours are generally highly vascularised, RFA lesions can have unpredictable shapes and remain limited in size due to this effect.[13, 14] Furthermore, 'skipping' can occur, meaning that areas of viable tumour cells are found within the RFA lesion. This is observed when the current flows to areas within the lesion that have a lower impedance, leaving areas with a higher impedance untreated.[15, 16] Because these problems tend to occur with monopolar RFA, new RFA techniques, such as bipolar RFA, have been developed.[17] During bipolar RFA the current flows between two electrodes within one probe instead of travelling through the body to a return plate as in monopolar RFA. The current densities within the lesion become much higher and are more localized, thereby decreasing the chance of skipping.

CA of RCC has been introduced in 1995.[18] It causes tumor destruction by alternated freezing (<20ºC) and thawing of the tumor. An advantage of CA is the possibility to real-time monitor tumor destruction by visualisation of the ice ball formation with ultrasound. A disadvantage is that larger tumors are associated with the risk of fracturing the ice-ball, resulting in bleeding and potential consequent kidney loss. Furthermore, it has been reported that perioperative conversion occurs in approximately 17% of treated cases.[19] Criteria for successful RFA or CA are still not well defined. For CA, success is currently defined as shrinkage of the tumor and lack of contrast uptake in follow-up imaging.[8] Successful RFA is defined as the absence of enhancement on follow-up imaging with or without a negative biopsy of the ablated lesion, which does not increase in size over time.[20] Long term oncological outcomes are slowly becoming evident.[21-23] While recurrences appear to be present more often after thermoablation compared to PN, both techniques are good treatment options for select patients. However, because these therapies are still not 100% efficient other possibilities should also be investigated. Potential new approaches for minimally invasive treatment of SRMs are described in **Chapter 10** and **Chapter 11**.

Targeted therapy vs. Immunotherapy for metastatic RCC

First line therapy for metastatic RCC (mRCC) consists of targeted therapeutics such as tyrosine kinase and mTOR inhibitors.[24] These reverse tumor growth by targeting vascular development and cellular catabolism and anabolism. Although this therapy offers clinical benefit, it does not result in complete and durable responses.[25] Furthermore, resistance

develops in nearly all patients 6-15 months after start of the treatment.[26] This is the reason that even though targeted therapy has prolonged progression free survival in mRCC patients, cancer specific survival has not improved.[25, 27] Before the development of targeted therapy, mRCC patients were treated with immunotherapy. RCC is one of the most immunogenic cancers in humans; therefore, immune based therapy appeared to be a promising treatment strategy.[28, 29] The most commonly used immune therapeutics were interferon alpha (IFN-α) and interleukin-2 (IL-2).[30] These immune therapeutics induced complete remissions in 8-14% of cases and durable remissions in 6-8% of cases.[31-33] However, these therapeutics were also associated with severe morbidity.[34] Therefore, clinicians embraced targeted therapeutics after their introduction. Currently, INF-α and IL-2 are rarely being used, and only in a very select patient population.[30] As targeted therapeutics are unable to cure mRCC patients and improve survival, there is a need to optimize and develop new strategies to effectively treat patients with mRCC and prevent formation of metastases after initial curative treatment. The goal of active immunotherapy is to stimulate the immune system to recognize and eliminate tumor cells. Several immunotherapeutic approaches have been clinically tested for RCC.[35, 36] To date, the best source for immunization is apoptotic or necrotic RCC tissue, as RCC seems to express very few clinically promising tumor-associated antigens.[36] Clinical studies using RCC cells as autologous tumor cell vaccine have provided promising results in several RCC patients.[36-38] This approach aims to induce a polyclonal T cell response against a broad range of tumor-derived epitopes, thereby increasing chances of an effective response. Recently, dendritic cell-based vaccines have become of special interest.[39] Dendritic cells (DCs) are the most powerful antigen-presenting cells (APCs) and have the capacity to effectively stimulate a strong antitumor immune response. Disadvantages of the two described approaches are that they are time consuming, complex and every autologous immunisation has to be developed individually *ex vivo*.[36] An *in situ* activation of the antitumor immune response would therefore be of high clinical relevance. This subject will be further explored in **Chapter 9**.

Incomplete treatment of RCC

As described in **Chapter 8,** recurrence or persistence of the tumor is more often present after both RFA and CA compared to PN.[40] Recurrences reported following initial treatment with RFA are currently 11.7%, for CA this is 4.6%, compared to 2.6% for PN.[40] When comparing rates of local recurrences between different treatment modalities, it is important to consider that dissimilar criteria are being used for the clinical application of a certain technique and to define recurrence. For RFA and CA, recurrence is currently defined as the absence of enhancement on follow-up imaging with or without a negative biopsy of the ablated lesion, which does not increase in size over time.[20] For PN this is defined as tumor growth in the

ipsilateral kidney near the site of previous resection.[40] It is indicated in literature that differences exist among SRMs selected for each treatment with regard to tumor size and patient age.[41] SRMs treated with RFA and CA are significantly smaller and patients are older compared to those treated with PN.[40] In spite of the selection bias, multivariate analysis confirmed that patients treated with RFA or CA are significantly more likely to experience recurrent disease.[40] As a consequence, multiple sessions are often necessary.[42-44] CA is most often performed laparoscopically, while a percutaneous approach is most frequently used for RFA.[45, 46] Published data on the issue whether recurrences are dependent on the approach is contradictory. While some series report similar recurrence rates comparing percutaneous and laparoscopic RFA or CA,[47, 48] others find significantly more recurrences following a percutaneous approach.[49] However, an advantage of a percutaneous approach is that repeat procedures have a lower morbidity potential compared to repeat laparoscopic procedures.[46] Surprisingly, recurrences following PN with positive surgical margins are reported sporadically, and positive margins do not affect survival.[50, 51] The differences in recurrence rates among the various nephron-sparing techniques suggest that next to the approach or the size of the SRM, other factors may play a role in this observation. Literature indicates that thermal ablation affects the microenvironment of tumors.[52-54] This is investigated in **Chapter 8**.

Paradoxical roles of thermal ablation in RCC treatment

Following thermal ablation, both tumor stimulation and tumor inhibiting effects have been described in literature.[55] It appears that a delicate balance exists within the body between tumor tolerance and tumor destruction. Both the immune system and the microenvironment play an important role in this process.[54, 56, 57] **Chapter 8** shows an increase in tumor growth and decrease in apoptosis following thermal ablation. On the other hand, in **Chapter 9** the immune system is stimulated by RFA to induce tumor destruction. Thermal ablation results in tumor death by necrosis, apoptosis and microvascular thrombosis. The ability of thermal ablation to induce an anti-tumor response, instead of stimulating immune suppression, depends on several factors.[58] First of all, the response is affected by the cytokine profile triggered by the ablation. Directly after ablation cytokines are released from the ablated tissue.[59, 60] This may lead to immune activation, or to tolerance (e.g. release of IL-10 or TGF-β), which may depend on tumor type and presence and nature of lymphocytes in the tumor microenvironment.[58] Secondly, the response depends on the availability of antigens that can be processed by antigen presenting cells.[61, 62] Antigens can be locally taken up by (DCs) that move to regional lymph nodes where they activate T cells in the presence of cytokines and inflammatory signals, or they can form immune complexes by binding to serum antibodies that can be taken up by DCs. However, in the case of antigen overloading, immune tolerance

can be induced instead of an anti tumor response.[58] Thirdly, the mechanism of cell death (apoptosis vs. necrosis) is of major importance. Apoptosis and necrosis have a different impact on the immune response. Necrosis is characterized by cellular breakdown and release of intracellular contents (pro-inflammatory cytokines, heat shock proteins, "danger signals").[58] This can lead to increased DC maturation and macrophage activation in combination with a general inflammatory response. Apoptotic cells are taken up by macrophages and DCs, but cause no inflammation or stimulation of an immune response. This type of cell death can induce immune tolerance.[57]

References

1. Hollingsworth JM, Miller DC, Daignault S, Hollenbeck BK. Rising incidence of small renal masses: a need to reassess treatment effect. J Natl Cancer Inst 2006;98:1331-4.

2. Kutikov A, Egleston BL, Wong YN, Uzzo RG. Evaluating overall survival and competing risks of death in patients with localized renal cell carcinoma using a comprehensive nomogram. J Clin Oncol 2010;28:311-7.

3. Santos Arrontes D, Fernandez Acenero MJ, Garcia Gonzalez JI, Martin Munoz M, Paniagua Andres P. Survival analysis of clear cell renal carcinoma according to the Charlson comorbidity index. J Urol 2008;179:857-61.

4. Lane BR, Abouassaly R, Gao T, et al. Active treatment of localized renal tumors may not impact overall survival in patients aged 75 years or older. Cancer 2010;116:3119-26.

5. Huang WC, Levey AS, Serio AM, et al. Chronic kidney disease after nephrectomy in patients with renal cortical tumours: a retrospective cohort study. Lancet Oncol 2006;7:735-40.

6. Volpe A, Cadeddu JA, Cestari A, et al. Contemporary management of small renal masses. Eur Urol 2011;60:501-15.

7. Campbell SC, Novick AC, Belldegrun A, et al. Guideline for management of the clinical T1 renal mass. J Urol 2009;182:1271-9.

8. Heuer R, Gill IS, Guazzoni G, et al. A critical analysis of the actual role of minimally invasive surgery and active surveillance for kidney cancer. Eur Urol 2010;57:223-32.

9. Ljungberg B, Cowan NC, Hanbury DC, et al. EAU guidelines on renal cell carcinoma: the 2010 update. Eur Urol 2010;58:398-406.

10. Jewett MA, Mattar K, Basiuk J, et al. Active surveillance of small renal masses: progression patterns of early stage kidney cancer. Eur Urol 2011;60:39-44.

11. Van Poppel H, Da Pozzo L, Albrecht W, et al. A prospective, randomised EORTC intergroup phase 3 study comparing the oncologic outcome of elective nephron-sparing surgery and radical nephrectomy for low-stage renal cell carcinoma. Eur Urol 2011;59:543-52.

12. Zlotta AR, Wildschutz T, Raviv G, et al. Radiofrequency interstitial tumor ablation (RITA) is a possible new modality for treatment of renal cancer: ex vivo and in vivo experience. J Endourol 1997;11:251-8.

13. Chang I, Mikityansky I, Wray-Cahen D, Pritchard WF, Karanian JW, Wood BJ. Effects of perfusion on radiofrequency ablation in swine kidneys. Radiology 2004;231:500-5.

14. Goldberg SN, Hahn PF, Tanabe KK, et al. Percutaneous radiofrequency tissue ablation: does perfusion-mediated tissue cooling limit coagulation necrosis? J Vasc Interv Radiol 1998;9:101-11.

15. Klingler HC, Marberger M, Mauermann J, Remzi M, Susani M. 'Skipping' is still a problem with radiofrequency ablation of small renal tumours. BJU Int 2007;99:998-1001.

16. Michaels MJ, Rhee HK, Mourtzinos AP, Summerhayes IC, Silverman ML, Libertino JA. Incomplete renal tumor destruction using radio frequency interstitial ablation. J Urol 2002;168:2406-9; discussion 9-10.

17. Nakada SY, Jerde TJ, Warner TF, et al. Bipolar radiofrequency ablation of the kidney: comparison with monopolar radiofrequency ablation. J Endourol 2003;17:927-33.

18. Uchida M, Imaide Y, Sugimoto K, Uehara H, Watanabe H. Percutaneous cryosurgery for renal tumours. Br J Urol 1995;75:132-6; discussion 6-7.

19. Laguna MP, Beemster P, Kumar V, et al. Perioperative morbidity of laparoscopic cryoablation of small renal masses with ultrathin probes: a European multicentre experience. Eur Urol 2009;56:355-61.

20. Leveridge MJ, Mattar K, Kachura J, Jewett MA. Assessing outcomes in probe ablative therapies for small renal masses. J Endourol 2010;24:759-64.

21. Tracy CR, Raman JD, Donnally C, Trimmer CK, Cadeddu JA. Durable oncologic outcomes after radiofrequency ablation: experience from treating 243 small renal masses over 7.5 years. Cancer 2010;116:3135-42.

22. Joniau S, Tsivian M, Gontero P. Radiofrequency ablation for the treatment of small renal masses: safety and oncologic efficacy. Minerva Urol Nefrol 2011;63:227-36.

23. Davol PE, Fulmer BR, Rukstalis DB. Long-term results of cryoablation for renal cancer and complex renal masses. Urology 2006;68:2-6.

24. Bastien L, Culine S, Paule B, Ledbai S, Patard JJ, de la Taille A. Targeted therapies in metastatic renal cancer in 2009. BJU Int 2009;103:1334-42.

25. Coppin C, Kollmannsberger C, Le L, Porzsolt F, Wilt TJ. Targeted therapy for advanced renal cell cancer (RCC): a Cochrane systematic review of published randomised trials. BJU Int 2011.

26. Rini BI, Atkins MB. Resistance to targeted therapy in renal-cell carcinoma. Lancet Oncol 2009;10:992-1000.

27. Sun M, Thuret R, Abdollah F, et al. Age-adjusted incidence, mortality, and survival rates of stage-specific renal cell carcinoma in North America: a trend analysis. Eur Urol 2011;59:135-41.

28. Oliver RT, Nethersell AB, Bottomley JM. Unexplained spontaneous regression and alpha-interferon as treatment for metastatic renal carcinoma. Br J Urol 1989;63:128-31.

29. Verra N, de Jong D, Bex A, et al. Infiltration of activated dendritic cells and T cells in renal cell carcinoma following combined cytokine immunotherapy. Eur Urol 2005;48:527-33.

30. McDermott DF. Immunotherapy of metastatic renal cell carcinoma. Cancer 2009;115:2298-305.

31. Coppin C, Porzsolt F, Awa A, Kumpf J, Coldman A, Wilt T. Immunotherapy for advanced renal cell cancer. Cochrane Database Syst Rev 2005:CD001425.

32. Fisher RI, Coltman CA, Jr., Doroshow JH, et al. Metastatic renal cancer treated with interleukin-2 and lymphokine-activated killer cells. A phase II clinical trial. Ann Intern Med 1988;108:518-23.

33. Rosenberg SA, Lotze MT, Muul LM, et al. A progress report on the treatment of 157 patients with advanced cancer using lymphokine-activated killer cells and interleukin-2 or high-dose interleukin-2 alone. N Engl J Med 1987;316:889-97.

34. Belldegrun A, Webb DE, Austin HA, 3rd, et al. Effects of interleukin-2 on renal function in patients receiving immunotherapy for advanced cancer. Ann Intern Med 1987;106:817-22.

35. Uemura H, De Velasco MA. Tumor vaccines in renal cell carcinoma. World J Urol 2008;26:147-54.

36. Van Poppel H, Joniau S, Van Gool SW. Vaccine therapy in patients with renal cell carcinoma. Eur Urol 2009;55:1333-42.

37. Dudek AZ, Mescher MF, Okazaki I, et al. Autologous large multivalent immunogen vaccine in patients with metastatic melanoma and renal cell carcinoma. Am J Clin Oncol 2008;31:173-81.

38. Jocham D, Richter A, Hoffmann L, et al. Adjuvant autologous renal tumour cell vaccine and risk of tumour progression in patients with renal-cell carcinoma after radical nephrectomy: phase III, randomised controlled trial. Lancet 2004;363:594-9.

39. Berntsen A, Trepiakas R, Wenandy L, et al. Therapeutic dendritic cell vaccination of patients with metastatic renal cell carcinoma: a clinical phase 1/2 trial. J Immunother 2008;31:771-80.

40. Kunkle DA, Egleston BL, Uzzo RG. Excise, ablate or observe: the small renal mass dilemma--a meta-analysis and review. J Urol 2008;179:1227-33; discussion 33-4.

41. Matin SF, Ahrar K, Cadeddu JA, et al. Residual and recurrent disease following renal energy ablative therapy: a multi-institutional study. J Urol 2006;176:1973-7.

42. Kunkle DA, Uzzo RG. Cryoablation or radiofrequency ablation of the small renal mass : a meta-analysis. Cancer 2008;113:2671-80.

43. Gervais DA, McGovern FJ, Arellano RS, McDougal WS, Mueller PR. Radiofrequency ablation of renal cell carcinoma: part 1, Indications, results, and role in patient management over a 6-year period and ablation of 100 tumors. AJR Am J Roentgenol 2005;185:64-71.

44. Zagoria RJ, Traver MA, Werle DM, Perini M, Hayasaka S, Clark PE. Oncologic efficacy of CT-guided percutaneous radiofrequency ablation of renal cell carcinomas. AJR Am J Roentgenol 2007;189:429-36.

45. Park S, Cadeddu JA, Shingleton WB. Oncologic outcomes for ablative therapy of kidney cancer. Curr Urol Rep 2007;8:31-7.

46. Long L, Park S. Differences in patterns of care: reablation and nephrectomy rates after needle ablative therapy for renal masses stratified by medical specialty. J Endourol 2009;23:421-6.

47. Finley DS, Beck S, Box G, et al. Percutaneous and laparoscopic cryoablation of small renal masses. J Urol 2008;180:492-8; discussion 8.

48. Hui GC, Tuncali K, Tatli S, Morrison PR, Silverman SG. Comparison of percutaneous and surgical approaches to renal tumor ablation: metaanalysis of effectiveness and complication rates. J Vasc Interv Radiol 2008;19:1311-20.

49. Strom KH, Derweesh I, Stroup SP, et al. Second prize: Recurrence rates after percutaneous and laparoscopic renal cryoablation of small renal masses: does the approach make a difference? J Endourol 2011;25:371-5.

50. Lopez-Costea MA, Fumado L, Lorente D, Riera L, Miranda EF. Positive margins after nephron-sparing surgery for renal cell carcinoma: long-term follow-up of patients on active surveillance. BJU Int 2010;106:645-8.

51. Bensalah K, Pantuck AJ, Rioux-Leclercq N, et al. Positive surgical margin appears to have negligible impact on survival of renal cell carcinomas treated by nephron-sparing surgery. Eur Urol 2010;57:466-71.

52. Nikfarjam M, Muralidharan V, Christophi C. Altered growth patterns of colorectal liver metastases after thermal ablation. Surgery 2006;139:73-81.

53. von Breitenbuch P, Kohl G, Guba M, Geissler E, Jauch KW, Steinbauer M. Thermoablation of colorectal liver metastases promotes proliferation of residual intrahepatic neoplastic cells. Surgery 2005;138:882-7.

54. Nijkamp MW, van der Bilt JD, de Bruijn MT, et al. Accelerated perinecrotic outgrowth of colorectal liver metastases following radiofrequency ablation is a hypoxia-driven phenomenon. Ann Surg 2009;249:814-23.

55. Sabel MS, Su G, Griffith KA, Chang AE. Rate of freeze alters the immunologic response after cryoablation of breast cancer. Ann Surg Oncol 2010;17:1187-93.

56. de Visser KE, Eichten A, Coussens LM. Paradoxical roles of the immune system during cancer development. Nat Rev Cancer 2006;6:24-37.

57. Viorritto IC, Nikolov NP, Siegel RM. Autoimmunity versus tolerance: can dying cells tip the balance? Clin Immunol 2007;122:125-34.

58. Sabel MS. Cryo-immunology: a review of the literature and proposed mechanisms for stimulatory versus suppressive immune responses. Cryobiology 2009;58:1-11.

59. Schell SR, Wessels FJ, Abouhamze A, Moldawer LL, Copeland EM, 3rd. Pro- and antiinflammatory cytokine production after radiofrequency ablation of unresectable hepatic tumors. J Am Coll Surg 2002;195:774-81.

60. Seifert JK, Stewart GJ, Hewitt PM, Bolton EJ, Junginger T, Morris DL. Interleukin-6 and tumor necrosis factor-alpha levels following hepatic cryotherapy: association with volume and duration of freezing. World J Surg 1999;23:1019-26.

61. Gallucci S, Lolkema M, Matzinger P. Natural adjuvants: endogenous activators of dendritic cells. Nat Med 1999;5:1249-55.

62. Sauter B, Albert ML, Francisco L, Larsson M, Somersan S, Bhardwaj N. Consequences of cell death: exposure to necrotic tumor cells, but not primary tissue cells or apoptotic cells, induces the maturation of immunostimulatory dendritic cells. J Exp Med 2000;191:423-34.

Chapter 7

Incomplete thermal ablation stimulates proliferation of residual renal carcinoma cells in a translational murine model.

British Journal of Urology International, pending revisions

S.G.C. Kroeze[1]
H.H.E. van Melick[2]
M.W. Nijkamp[3]
F.K. Kruse[4]
L.W.J. Kruijssen[1]
P.J. van Diest[5]
J.L.H.R. Bosch[1]
J.J.M. Jans[1]

[1]Department of Urology, University Medical Center Utrecht, Utrecht, the Netherlands
[2]Department of Urology, St. Antonius Hospital, Utrecht-Nieuwegein, the Netherlands
[3]Department of Surgical Oncology, University Medical Center Utrecht, Utrecht, the Netherlands
[4]Department of Medical Oncology, University Medical Center Utrecht, Utrecht, the Netherlands
[5]Department of Pathology, University Medical Center Utrecht, Utrecht, the Netherlands

Abstract

Introduction

To compare the effect of incomplete thermal ablation versus partial nephrectomy (PN) on growth stimulation and cellular survival in renal tumours.

Materials and Methods

Renca renal tumours were transplanted under the renal capsule of mice (4-6 mice/group) after which incomplete radiofrequency ablation (RFA), cryoablation (CA) or PN was performed. At several time points after treatment, presence of cell proliferation, apoptosis, hypoxic areas, inflammatory factors and the heat shock proteins 70 and 90 was evaluated using immunohistochemistry.

Results

Two hours following thermal ablation residual tumour cells showed an increased proliferation. This hyperproliferation was significantly stronger after RFA compared to CA (p<0.05) and not present following PN. Residual cells showed increased apoptosis after 2 hours and decreased apoptosis from 2 days following thermal ablation. Apoptotic cells were significantly less present after 3 days following RFA (p<0.001). Hypoxic areas and HSPs were increasingly present from 2 hours up to 7 days after thermal ablation (p<0.0001). Inflammatory cells infiltrated mainly the necrotic areas following thermal ablation, and their abundance peaked at 1 week after ablation (p<0.05). The increased cell growth was preceded hypoxia and presence of HSPs.

Conclusions

CA and RFA result in an increased proliferation and decreased apoptosis of residual renal tumour cells. This hyperproliferation may be caused by stimulatory factors such as hypoxia, HSPs and inflammatory cells, and could facilitate recurrences of renal tumours after thermal ablation. This underlines the importance to achieve complete tumour destruction.

Introduction

The gold standard of treatment of small renal masses (SRM, <4 cm) is partial nephrectomy (PN).[1] Triggered by the increasing incidence of SRMs and in search of options for patients unfit for open or laparoscopic surgery, minimally-invasive nephron-sparing therapies have been developed. Both radiofrequency ablation (RFA) and cryoablation (CA) induce necrosis and apoptosis of tumour cells. Successful ablation is currently defined as the absence of enhancement on follow-up imaging with or without a negative biopsy of the ablated lesion, which does not increase in size over time.[2] Local recurrences following ablation continue to be a problem, particularly in larger tumours. Optimal temperatures for RFA are between 50-100 ºC and for CA below -20 ºC.[3] The thermal energy is conducted from the tip of a probe to the surrounding tissue. Thermal energy conduction is inversely related to distance; therefore, cells at the edge of the lesion may undergo sub-lethal injury. RFA seems to require more re-ablations to achieve treatment success, although a selection bias may be present.[3]

Thermal ablation influences the local tissue microenvironment. Several studies have demonstrated that residual tumour cells may exhibit a more aggressive phenotype.[4-8] Factors associated with this phenomenon are local expression of cytokines, heat shock proteins (HSPs), hypoxia and influx of inflammatory cells. Hypoxia at areas surrounding the ablated region appears to be an important consequence of thermal ablation,[8] since it leads to activation of signalling pathways that allow tumour cells to undergo adaptive changes promoting survival.[9]

Although one aims for complete ablation, this is not always achieved. Therefore, clarifying the cellular effects of thermal ablation versus PN on residual tumour cells is important and may improve the techniques of CA, RFA and PN to prevent an escape from cell death. The aim of this study was to examine renal tumour cell proliferation, apoptosis, and factors important for cellular survival following CA, RFA and PN, in an orthotopic mouse model for renal cancer.

Materials and Methods

Cell culture

Balb/C renal carcinoma cells (Renca, National Cancer Institute, USA) were maintained at 37°C and 5% CO_2 in Dulbecco's Modified Eagle's Medium (Lonza, the Netherlands) supplemented with 10% FCS, 1% penicillin/streptomycin and 1% glutamine.

Animal experiments

All experiments were conducted in agreement with the Netherlands Experiments on Animals Act and European convention guidelines. Surgical procedures were performed under isoflurane anesthesia. Buprenorfine was used subcutaneously for analgesia prior to, and 24 h post surgery. In 103 male Balb/C mice (age 9-11 weeks, Charles River, the Netherlands), a Renca tumour cube with a diameter of 2 mm was transplanted under the renal capsule [10]. After 1 week incomplete RFA, CA or PN was performed (Figure 1). Access to the left kidney was obtained through a flank incision. For RFA treatment a 19G non-cooled bipolar RFA probe with an active length of 1 cm (CelonPro*Surge micro*, Celon AG, Germany) was inserted in the renal tumour. RFA was performed at 2 W, 120 J (60 sec.), using the CELON Power System (Celon AG, Germany).

CA was performed with a 17G probe with a built-in thermocouple (IceSeed, Galil Medical, Israel). Tumour treatment consisted of 2 cycles of 20 seconds freeze followed by 30 seconds thaw.[11] During CA and RFA the tumour was exteriorized while the abdominal cavity and skin were protected with gauze. For partial nephrectomy the kidney was mobilized, the tumour was partly excised to a level of near complete resection, followed by a 1-minute tamponade for haemostasis. Control mice were sham-operated by inserting a probe in the tumour without performing ablation (Sham), or received no treatment (Ctrl). To enable detection of hypoxia, pimonidazole hydrochloride (Hypoxyprobe-1, 90201, HPI Inc., USA) was injected intravenously at a dose of 60mg/kg 1h before termination. At several time points (2h and 1, 3, 7 and 14 days) after treatment mice were sacrificed and kidneys were harvested.

Figure 1: Schematic drawing of the preclinical mouse renal tumour model. **(A)** Incomplete CA and RFA of renal tumours. **(B)** Incomplete PN of renal tumours.
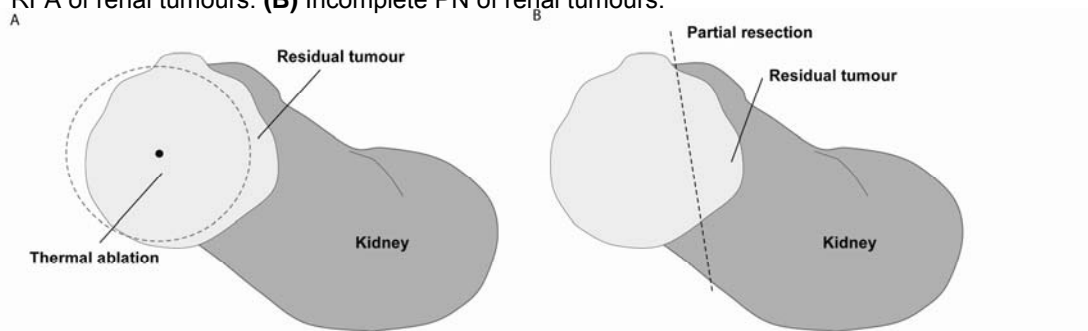
Immunohistochemical analysis

Formalin-fixed paraffin-embedded tissue was cut in 5µm sections. Antigen retrieval was achieved by boiling in citrate buffer (pH 6). Immunohistochemistry was performed to detect proliferation (Ki67 clone SP6, Neomarkers, USA), apoptosis (Casp3 clone C92-605, BD Pharmingen, USA), hypoxia (pimonidazole adducts, Pab2627, HPI Inc, USA), macrophages (F4/80, Serotec, USA), leukocytes (anti-CD45, Abcam, USA) and HSP70 and HSP90 (Santa

Cruz, USA). Brightvision (Immunologic, the Netherlands) was used as secondary antibody, followed by diaminobenzidine/H_2O_2. For Ki67, Casp3, CD45 and F4/80, 5-13 fields at the direct border of the lesion were randomly selected at 20x magnification. Subsequently, positive cells were scored by one observer blinded to treatment using a grid overlay. Hypoxia, HSP70 and HSP90 were analysed using a semi-quantitative method as previously described.[12] Images of all fields directly surrounding the lesion in one representative slide per tumour (6-13 fields per slide) were selected at 10x magnification. The percentage of positive areas in each field was calculated with ImageJ software (National Institute of Health, USA).

Results

CA and RFA stimulate tumour cell proliferation and decrease apoptosis
In untreated tumours the mean proliferation rate was 28.3% ± 6.3 (mean ± SD) (Figure 2). Ablation resulted in a 2-fold higher proliferation rate of cells at the border of the ablated region from 2 hours after thermal ablation (p<0.0001), peaking at 3 days (p<0.0001). Proliferation rates remained high up to 2 weeks following thermal ablation (40.4% ± 1.2 after RFA, 48.2% ± 1.1 after CA, p<0.0001). Importantly, RFA induced significantly more proliferation compared to CA (66.3% ± 1.2 after RFA vs. 57.5% ± 1.2 after CA, p<0.0001). PN showed a slight increase in proliferation at the resection site 1 day following treatment (p=0.003), after which proliferation levels decreased to baseline level. Sham-treatment did not affect proliferation. Apoptotic cells were not abundantly present in untreated tumors (2.4% ± 0.35, mean ± SEM) (Figure 2). Two hours after thermal ablation there was a slight increase of apoptotic cells at the border of the ablated region (p<0.001). However, at 2 days apoptosis at this area was decreasing. After 3 days there was a significant decrease (p<0.01) of apoptotic cells surrounding the RFA treated area. While CA also showed a trend towards decreased presence of apoptotic cells, this difference was not significant. Up to 7 days following thermal ablation there was a plentitude of apoptotic cells within the ablated area (Figure 2D).

Figure 2: (A) Cell proliferation at the border of thermally ablated or partially resected renal tumours (Ki67, mean ± SEM, n=4-6mice/group). Cell proliferation at this region significantly increased from 2 hours following thermal ablation (p<0.0001), with a 2-fold increased proliferation rate at 3 days (p<0.0001). RFA induced significantly more proliferation than CA (p<0.0001). Proliferation rates remained 1.5-fold increased 14 days following treatment. **(B)** Representative images of Ki67 staining at the peak of proliferation rates 3 days following treatment (magnification 20x). Brown nuclear staining indicates proliferation. Scale bar: 204µm. **(C)** Apoptotic cells at the border of thermally ablated or partially resected renal tumours (Casp3, mean ± SEM, n=4-6mice/group). Apoptosis at this region showed a trend of decrease after 24h, only RFA showed a significant decrease of apoptotic cells 3 days following ablation (p<0.001). Within the ablated areas apoptotic cells were frequently present until 7 days following thermal ablation. **(D)** Representative images of Casp3 staining at 3 days following treatment (magnification 20x). Brown nuclear and cytoplasmatic staining indicates apoptosis. Scale bar: 204µm.
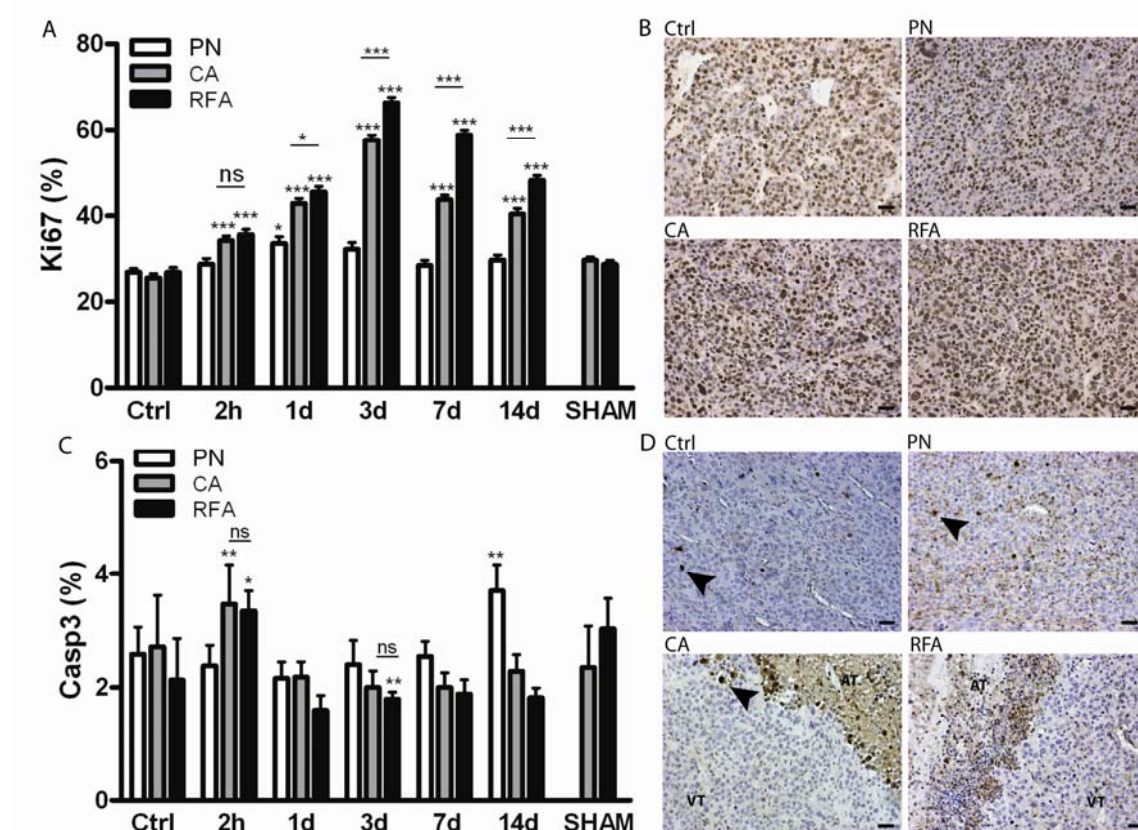
CA and RFA induce tissue hypoxia

In control (untreated) and sham-operated renal tumours, minor hypoxia was observed surrounding necrotic areas throughout the tumour. All thermally ablated tumours invariably revealed profound hypoxia in the viable tumour at the border of the ablated area (Figure 3). This hypoxic region was most pronounced 2h after ablation in both CA and RFA (27.3% ± 1.0 after RFA, 27.8% ± 1.3% after CA), and remained present up to 1 week. CA-treated

tumours showed a more rapid decrease in hypoxia compared to RFA-treated tumours; hypoxia was significantly more present from day 3 in RFA compared to CA (p<0.0001). PN and SHAM treatment did not detectably increase hypoxia at the border of the (resected) tumour.

Figure 3: (A) Hypoxia at the border of thermally ablated and partially resected renal tumours, detected by pimonidazole staining (mean ± SEM, n=4-6mice/group). Hypoxia is significantly increased in both CA and RFA treated tumours 2 h after treatment (<0.0001), and was present up to 7 days. **(B)** Representative images of pimonidazole staining 2 hours following treatment. Intense brown staining indicates hypoxia (magnification 10x). RFA and CA strongly induced hypoxia at the border of the ablated area (VT= viable tissue). PN induced slight hypoxia at the border of the resected area (arrow). Scale bar: 102µm.
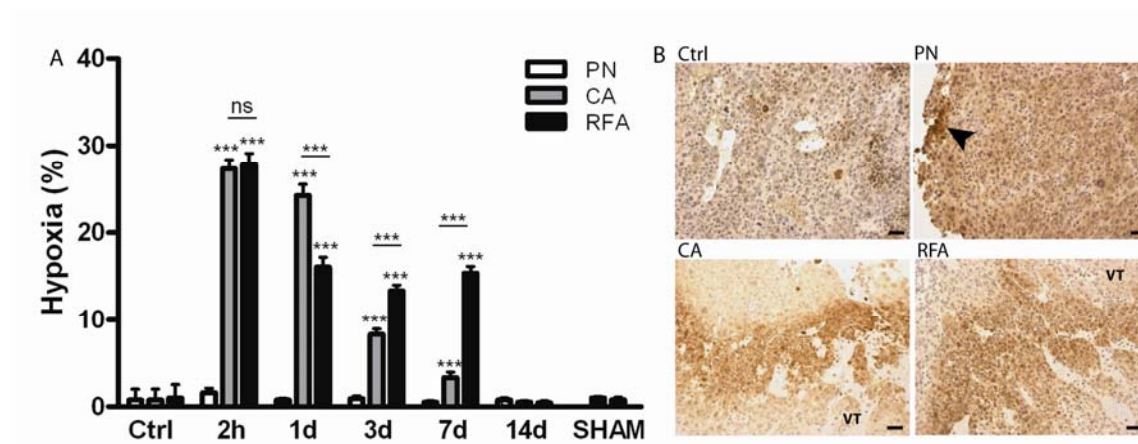
Inflammatory cells following CA and RFA

CA resulted in an increased number of macrophages at the border of ablated tumours after 3 days (24.9% ± 6.8, p=0.014), reaching a maximum after one week (30.2% ± 6.6, p<0.0001) (Figure 4A). Macrophages were less abundant following RFA, and were only significantly increased 14 days following RFA (26.4% ± 7.8, p=0.003). Leukocytes (CD45+ cells) were significantly more present in the tumour tissue surrounding the ablated area 3 days after CA and RFA treatment (10.5% ± 0.7 after CA, 10.5% ± 0.5 after RFA, p<0.05), and peaked after 1 week (12.3% ± 0.9 after CA, 11.1 ± 0.9 after RFA, Figure 4B). After 2 weeks leukocytes had returned to baseline level in the tumour tissue surrounding the ablated area, but not within the ablated area. Within the ablated area leukocytes and macrophages showed an increased influx from day 1 following treatment, which was higher following CA compared to RFA (p<0.05). In both treatments the peak presence of inflammatory cells was found several days later than the observed peak in hyperproliferation. PN and SHAM treatment did not result in a significant influx of macrophages or leukocytes.

Figure 4: (A) Presence of macrophages at the border of the thermally ablated or resected renal tumours (mean ± SEM, n=4-6mice/group). A significant influx of macrophages is observed 3 days following CA (p<0.05) and 14 days following RFA (p<0.05). **(B)** Influx of macrophages inside the ablated area of CA and RFA treated tumours. Macrophages are present 1 day following CA and 3 days following RFA. **(C)** Representative images of F4/80 staining for macrophages at the border of thermally ablated or resected renal tumours 14 days following treatment (magnification 20x). Scale bar: 204µm. **(D)** Presence of leukocytes at the border of the thermally ablated or resected renal tumours (mean ± SEM, n=4-6mice/group). A significant influx of leukocytes is observed from 3 days following CA and RFA (p<0.05). **(E)** Influx of leukocytes inside the ablated area of CA and RFA treated tumours. Leukocyte influx peaks at 7 days following thermal ablation. **(F)** Representative images of CD45-staining for leukocytes at the border of thermally ablated or resected renal tumours 7 days following treatment (magnification 20x). Scale bar: 204µm.
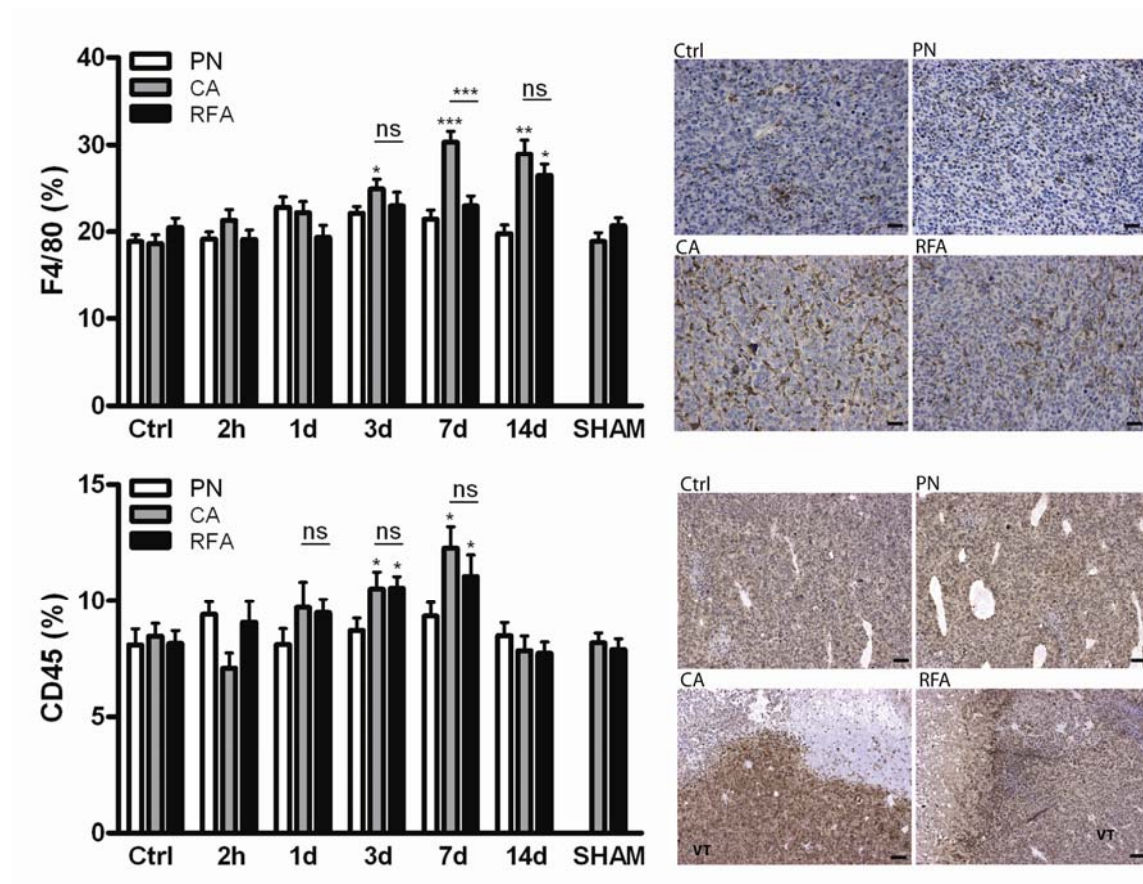

HSPs are increased following RFA, CA and PN

HSP90 was present in untreated tumours, but was only increased at the border of RFA treated tumours, where it showed a marked increase after 2h (4.9% ± 3.7 compared to 0.4% ± 0.9 baseline level, p<0.05) and a peak after 3 days (15.8% ± 8.2, p<0.0001) (Figure 5B). HSP70 was observed in untreated tumours, and was increasingly present in all treatment groups after 2h (p<0.05) (Figure 5A) and a peak after 1 day. RFA resulted in a 3-fold higher

presence of HSP70 compared to CA (6.9% ± 1.3 vs. 2.3% ± 0.7, p<0.001). From day 3 HSP70 could not be observed in the PN treatment group and showed a strong decrease in CA and RFA treated tumours compared to earlier time points. SHAM treatment did not result in a significant difference of HSP70 and HSP90.

Figure 5: (A) Expression of HSP70 at the border of thermally ablated and partially resected renal tumours (mean ± SEM, n=4-6 mice/group). HSP70 is significantly increased in both CA, RFA and PN treated tumours 2h after treatment (p<0.0001). Increased levels of HSP70 remained present up to 7 days for RFA and CA, and 1 day following PN. **(B)** Representative images of HSP70 staining 2 hours following treatment. Intense brown staining indicates increased expression of HSP70 above the baseline levels of HSP70 (lighter brown staining) (magnification 10x). Especially induced a strong HSP70 expression at the border of the ablated area (VT= viable tissue). After PN small areas of increased HSP70 levels were observed at the border of the resected area (arrow). **(C)** Increased expression of HSP90 was only observed at the border of RFA treated tumours, up to 3 days following treatment (p<0.0001). **(D)** Representative images of HSP90 staining 3 days following treatment (magnification 10x). All tumours showed a slight physiological presence of HSP90 (light brown staining). An increased expression in RFA treated tumours is observed as dark brown staining (VT=viable tissue). Scale bar: 102µm.
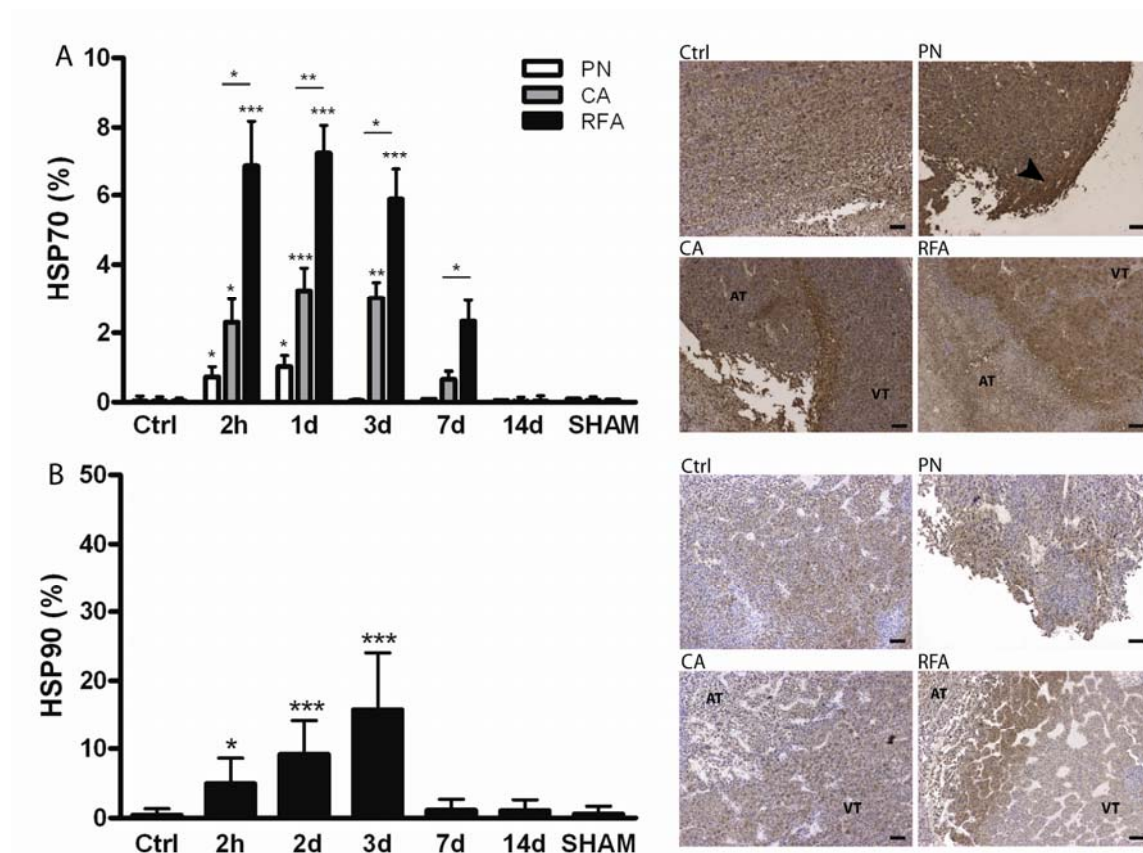
Discussion

The success of CA and RFA depends on several factors, including location of the tumour within the kidney, tumour size, tumour biology and the influence of tumour micro-environment. Local recurrence rates after RFA and CA remain higher than after PN.[13] In this translational study we show that incomplete ablation induces changes that stimulate growth of surviving renal tumour cells. These results are in accordance with various studies of thermal ablation in the liver, demonstrating aggressive local regrowth following treatment.[4-6, 8, 14] The mechanisms stimulating hyperproliferation and apoptosis include hypoxia, immune modulation and regulation of cell survival by HSPs. Therefore, we determined which factors were present at the border of incompletely ablated renal tumours.

We found that both CA and RFA caused profound hypoxia directly adjacent to the ablated area. The presence of hypoxia has been demonstrated in a number of solid tumours and is related to tumour aggressiveness. [15-16] While prolonged periods of hypoxia are damaging to normal cells, cancer cells can undergo adaptive changes that allow growth and survival under the hypoxic conditions. The increased levels of hypoxia induced by thermal ablation are sufficient to provide an additional growth-stimulating microenvironment for the surviving tumour cells. In addition to hypoxia, HSPs showed an early overexpression at the border of the ablated area. HSPs are overexpressed under conditions of cellular stress. It is known that along with heat activation, factors such as inflammation, hypoxia and tissue trauma play a major role. [17] Indeed, RFA resulted in overexpression of both HSP70 and HSP90 at the border of the ablated area 2h following treatment, while CA and PN caused upregulation of HSP70 that was less pronounced. Although some conflicting results on the influence of HSPs on damaged cells are reported, there is strong evidence that HSP overexpression plays an important role in increased cell survival through recovery of damaged cells, cell proliferation and inhibition of apoptosis. Increased expression of HSPs in surviving tumour cells at the border of thermally ablated tumours may lead to the development of more aggressive tumour cells.[17-19]

Another factor that may be involved in hyperproliferation and cell survival is the immune response. The process of inflammation following thermal ablation involves a complex network of chemical signals and cell interactions in response to tissue damage. Surviving tumour cells at the border, as well as dead tumour cells within the ablated area release chemokines that attract inflammatory cells.[20] As described by others, leukocytes were present first upon thermally induced necrosis, followed by infiltration of macrophages.[21] The high baseline level of macrophages in renal tumours can be explained by the observation that often tumour-derived chemical signals stimulate a continuous migration of monocytes into tumour tissue.[20] Macrophages can be differentiated into two types: tumour-supportive

and tumour-suppressive macrophages. Tumour-supportive macrophages and other inflammatory cells provide growth factors and cytokines that stimulate cell proliferation, angiogenesis and metastasis formation. Hypoxia is one of the major stimulators of the tumour-supportive macrophages.[20, 22] The here observed inflammatory cells are, however, unlikely to be the major factor involved in the hyperproliferation of tumour cells in the early phase after thermal ablation, since the influx of macrophages was observed only several days after tumour cell hyperproliferation. However, because 2 weeks after treatment tumour cells were still proliferating 1.5-fold more compared to the control tissue, macrophages could play a stimulatory role in this later phase.

Although it has been described that surgical resection may affect tumourigenesis.[23-25] there was only a slightly increased cell proliferation rate and no significant difference in apoptosis observed after PN in this study. This is in accordance with clinical studies of positive surgical margins after partial nephrectomy that indicate that recurrence rates are only slightly increased in these patients, and do not affect survival.[26-28] This suggests that a growth stimulatory effect on residual tumour cells is limited in RCC and the observed proliferation following CA and RFA can be ascribed to the thermal ablation.

We compared the two most commonly used thermally ablative procedures for SRMs, to PN. With the described cellular effects we do not intend to question thermal ablation as a method. CA and RFA initiate cellular effects that may have secondary consequences: a number of growth stimulatory factors involving hypoxia, HSPs and immune responses may interact with surviving tumour cells. Based on the observation that RFA induces significantly more hyperproliferation, it might be recommended to use RFA for smaller lesions or employ larger safety margins around the tumour, although further clinical testing would be required to examine this. Even though it is technically easier to perform multiple consecutive RFA procedures compared to CA,[29] our results stress the importance of complete ablation. Whenever possible, PN remains the procedure of choice since it induces limited cellular proliferation, it is likely to cause the most complete tumour resection and has the best clinical results. Adjuvant therapies inhibiting hypoxia- or HSP-related responses after thermal ablation may be an appealing strategy to prevent escape of viable cells from lethal injury.[8, 17]

Conclusion

Following incomplete CA and RFA we show an increased proliferation and decreased apoptosis of surviving renal tumour cells. This hyperproliferation may be caused by stimulatory factors such as hypoxia, HSPs and inflammatory cells, and could facilitate recurrences of renal tumours after thermal ablation. This underlines the importance of complete tumour destruction.

References

1. Papworth K, Sandlund J, Grankvist K, Ljungberg B, Rasmuson T. Soluble carbonic anhydrase IX is not an independent prognostic factor in human renal cell carcinoma. Anticancer Res 2010;30:2953-7.

2. Leveridge MJ, Mattar K, Kachura J, Jewett MA. Assessing outcomes in probe ablative therapies for small renal masses. J Endourol 2010;24:759-64.

3. Heuer R, Gill IS, Guazzoni G, et al. A critical analysis of the actual role of minimally invasive surgery and active surveillance for kidney cancer. Eur Urol 2010;57:223-32.

4. Nikfarjam M, Muralidharan V, Christophi C. Altered growth patterns of colorectal liver metastases after thermal ablation. Surgery 2006;139:73-81.

5. Ohno T, Kawano K, Yokoyama H, et al. Microwave coagulation therapy accelerates growth of cancer in rat liver. J Hepatol 2002;36:774-9.

6. von Breitenbuch P, Kohl G, Guba M, Geissler E, Jauch KW, Steinbauer M. Thermoablation of colorectal liver metastases promotes proliferation of residual intrahepatic neoplastic cells. Surgery 2005;138:882-7.

7. Ke S, Ding XM, Kong J, et al. Low temperature of radiofrequency ablation at the target sites can facilitate rapid progression of residual hepatic VX2 carcinoma. J Transl Med 2010;8:73.

8. Nijkamp MW, van der Bilt JD, de Bruijn MT, et al. Accelerated perinecrotic outgrowth of colorectal liver metastases following radiofrequency ablation is a hypoxia-driven phenomenon. Ann Surg 2009;249:814-23.

9. Ruan K, Song G, Ouyang G. Role of hypoxia in the hallmarks of human cancer. J Cell Biochem 2009;107:1053-62.

10. Chang YS, Adnane J, Trail PA, et al. Sorafenib (BAY 43-9006) inhibits tumor growth and vascularization and induces tumor apoptosis and hypoxia in RCC xenograft models. Cancer Chemother Pharmacol 2007;59:561-74.

11. Hedican SP, Wilkinson ER, Lee FT, Jr., Warner TF, Nakada SY. A novel murine model for the study of human renal cryoablation. BJU Int 2007.

12. Raleigh JA, Chou SC, Calkins-Adams DP, Ballenger CA, Novotny DB, Varia MA. A clinical study of hypoxia and metallothionein protein expression in squamous cell carcinomas. Clin Cancer Res 2000;6:855-62.

13. Kunkle DA, Egleston BL, Uzzo RG. Excise, ablate or observe: the small renal mass dilemma--a meta-analysis and review. J Urol 2008;179:1227-33; discussion 33-4.

14. Yang WL, Nair DG, Makizumi R, et al. Heat shock protein 70 is induced in mouse human colon tumor xenografts after sublethal radiofrequency ablation. Ann Surg Oncol 2004;11:399-406.

15. Seeber LM, Horree N, van der Groep P, van der Wall E, Verheijen RH, van Diest PJ. Necrosis related HIF-1alpha expression predicts prognosis in patients with endometrioid endometrial carcinoma. BMC Cancer 2010;10:307.

16.   Theodoropoulos VE, Lazaris A, Sofras F, et al. Hypoxia-inducible factor 1 alpha expression correlates with angiogenesis and unfavorable prognosis in bladder cancer. Eur Urol 2004;46:200-8.

17.   Richardson PG, Mitsiades CS, Laubach JP, Lonial S, Chanan-Khan AA, Anderson KC. Inhibition of heat shock protein 90 (HSP90) as a therapeutic strategy for the treatment of myeloma and other cancers. Br J Haematol 2011;152:367-79.

18.   Bhardwaj N, Dormer J, Ahmad F, et al. Heat Shock Protein 70 Expression Following Hepatic Radiofrequency Ablation is Affected by Adjacent Vasculature. J Surg Res 2010.

19.   Kim EK, Park JD, Shim SY, et al. Effect of chronic hypoxia on proliferation, apoptosis, and HSP70 expression in mouse bronchiolar epithelial cells. Physiol Res 2006;55:405-11.

20.   Coffelt SB, Hughes R, Lewis CE. Tumor-associated macrophages: effectors of angiogenesis and tumor progression. Biochim Biophys Acta 2009;1796:11-8.

21.   Ono M. Molecular links between tumor angiogenesis and inflammation: inflammatory stimuli of macrophages and cancer cells as targets for therapeutic strategy. Cancer Sci 2008;99:1501-6.

22.   Bedke J, Hemmerlein B, Perske C, Gross A, Heuser M. Tumor-associated macrophages in clear cell renal cell carcinoma express both gastrin-releasing peptide and its receptor: a possible modulatory role of immune effectors cells. World J Urol 2010;28:335-41.

23.   Hofer SO, Molema G, Hermens RA, Wanebo HJ, Reichner JS, Hoekstra HJ. The effect of surgical wounding on tumour development. Eur J Surg Oncol 1999;25:231-43.

24.   Mizutani J, Hiraoka T, Yamashita R, Miyauchi Y. Promotion of hepatic metastases by liver resection in the rat. Br J Cancer 1992;65:794-7.

25.   Stuelten CH, Barbul A, Busch JI, et al. Acute wounds accelerate tumorigenesis by a T cell-dependent mechanism. Cancer Res 2008;68:7278-82.

26.   Lam JS, Bergman J, Breda A, Schulam PG. Importance of surgical margins in the management of renal cell carcinoma. Nat Clin Pract Urol 2008;5:308-17.

27.   Permpongkosol S, Colombo JR, Jr., Gill IS, Kavoussi LR. Positive surgical parenchymal margin after laparoscopic partial nephrectomy for renal cell carcinoma: oncological outcomes. J Urol 2006;176:2401-4.

28.   Yossepowitch O, Thompson RH, Leibovich BC, et al. Positive surgical margins at partial nephrectomy: predictors and oncological outcomes. J Urol 2008;179:2158-63.

29.   Kunkle DA, Uzzo RG. Cryoablation or radiofrequency ablation of the small renal mass : a meta-analysis. Cancer 2008;113:2671-80.

Chapter 8

Radiofrequency ablation combined with Interleukin-2 induces an anti-tumor immune response to renal cell carcinoma in a murine model.

Stephanie G.C. Kroeze[1]
Laura G.M. Daenen[2]
Maarten W. Nijkamp[3]
Jeanine M. L. Roodhart[2]
Gijsbert C. de Gast[4]
J.L.H. Ruud Bosch[1]
Judith J.M. Jans[1]

[1]Department of Urology, University Medical Center Utrecht, the Netherlands
[2]Department of Medical Oncology, University Medical Center Utrecht, the Netherlands
[3]Department of Surgical Oncology, University Medical Center Utrecht, the Netherlands
[4]Department of Medical Oncology and Immunotherapy, Dutch Cancer Institute, Amsterdam, the Netherlands

Abstract

Introduction

Immune-based therapies have gained renewed interest in the search for treatment strategies for metastasized renal cell carcinoma (RCC). This study aimed to determine whether RFA, when combined with Interleukin-2 (IL-2), induces a tumor-specific immune response and could serve as an *in situ* vaccine against RCC.

Materials and Methods

Mice with orthotopic renal tumors were treated with RFA combined with IL-2, RFA only, IL-2 only or received no treatment (control). Immunohistochemistry was performed to determine which cells were present in the tumor after treatment. *In vitro* tumor-specific cytotoxicity assays were performed with CD8+ T and NK cells derived from spleens of treated mice. To study whether treatment could prevent formation of metastases or affect growth of established metastases, lung metastases were induced i.v. before or after treatment, and subsequently quantified.

Results

The number of NK, CD4+ and CD8+ T cells was significantly increased in tumor tissue of RFA/IL-2 treated mice ($p<0.0001$). Both NK and CD8+ T cells showed a strong anti-tumor activity *in vitro* following RFA/IL-2 treatment. The formation of lung metastases was significantly prevented in mice treated with RFA/IL-2 ($p<0.0001$). In addition, lung metastases were significantly smaller in RFA/IL-2 treated mice ($p=0.025$ compared to IL-2).

Conclusions

RFA of the primary tumor combined with IL-2 induces a systemic anti-tumor immune response to renal cell carcinoma, which is much stronger than IL-2 monotherapy. This effect appears to be mediated by both NK and CD8+ T cells, and can play an important role in the development of new immunotherapeutic treatment strategies for RCC.

Introduction

With a worldwide incidence of approximately 200,000 new cases and a mortality of 102,000 patients each year, kidney cancer is one of the most lethal genitourinary malignancies. [1] The most common form of kidney cancer is renal cell carcinoma (RCC). Of all RCC patients, approximately 15% will present with synchronous metastases, and a further 20% will develop metastases after initial curative treatment of a single primary tumor. Metastasized RCC is associated with a very poor 5-year survival of 12%. [2] First line therapy for metastatic disease consists of targeted therapy, which is frequently combined with cytoreductive nephrectomy. [3] Since this therapy does not induce durable complete remissions, the search for improved therapies continues. [4]

RCC tumor immunotherapy has recently received renewed attention following the identification of several immunogenic tumor antigens that are recognized by autologous T cells. [5] Developments in RCC immunotherapy currently focus on dendritic cell (DC) and autologous tumor cell-based vaccines. [5] Both approaches have been clinically tested in the metastatic and adjuvant setting of RCC, however, so far the results of autologous tumor cell vaccines are modest. [6-7] Although the efficacy of DC-based vaccines is more promising, [8] production of these vaccines is generally complicated. An alternative approach to RCC immunotherapy is therefore desirable.

Recent experimental and clinical studies have demonstrated that the *in situ* presence of radiofrequency ablation (RFA)-induced tumor debris creates a systemic anti-tumor immune response in several tumor types that results in recognition and subsequent destruction of distant tumor cells. [9-10] Metastatic regression following RFA has been reported. [11-12] However, although the immune response generated by RFA is tumor-specific, it is weak. [13] We postulate that an additional immune activation stimulus is required for an efficient induction of immunity following RFA. To test this hypothesis, we combined RFA with the immunostimulatory agent Interleukin-2 (IL-2). IL-2 increases the cytolytic activity of activated cytotoxic T-cells and natural killer (NK) cells [14] and is successful in a small subset of patients with metastasized RCC. [15]

We determined whether RFA of the primary renal tumor combined with IL-2 can induce an anti-tumor immune response strong enough to prevent metastasis formation or decrease growth of established lung metastases. This combinatory approach of tumor destruction and immune stimulation might create an *in situ* environment resembling immunotherapy vaccination *ex vivo*, and could be important in the development of a relatively simple new treatment strategy for metastasized or high-risk RCC.

Materials and Methods

Cell culture

Balb/C renal carcinoma cells (Renca, National Cancer Institute, USA) were maintained at 37°C and 5% CO_2 in Dulbecco's Modified Eagle's Medium (DMEM, Lonza, the Netherlands) supplemented with 10% Fetal Calf Serum, 1% Penicillin/Streptomycin and 1% glutamine.

Animal study design

All experimental protocols were conducted in agreement with the Netherlands Experiments on Animals Act and the European convention guidelines. In 126 male Balb/C mice (age 9-11 weeks, Charles River, the Netherlands), a Renca tumor cube with a diameter of 2 mm was transplanted under the renal capsule. The effect of RFA combined with IL-2 on lung metastases was assessed in 4 separate experiments (Figure 1). All experiments consisted of 4 treatment arms; RFA combined with IL-2, RFA only, IL-2 only or no treatment (control). In mice that underwent RFA or RFA/IL-2 treatment, RFA was performed 1 week after tumor induction. A single 19G non-cooled bipolar RFA electrode with an active length of 1 cm (CelonPro*Surge micro,* Celon AG, Germany) was inserted in the tumor. RFA was performed using the CELON Power System (Celon AG, Germany) at 2 Watts, creating a total energy outlet of 110 Joules. IL-2 treatment (Proleukin[®], Novartis, Switzerland), consisting of i.p. injections of 10^5 IU 2 times a day for 5 days, was started 2 days after RFA, when the amount of IL-2 receptors is high on activated CD8+ T cells.[16]

Immunohistochemical analysis of inflammatory cells

The presence of inflammatory cells in the primary tumor was assessed using immunohistochemistry. For this experiment (Figure 1A), tumor bearing mice (5mice/group, n=20) were treated with RFA/IL-2, RFA only, IL-2 only or received no treatment (control). Three weeks following the initiation of treatment mice were sacrificed and immunohistochemical stainings were performed. Renal tumor tissue was snap frozen or formalin fixed and paraffin embedded. Cryosections were stained for presence of CD8+ T cells (BD Biosciences, USA), CD4+ T cells (BD Biosciences, USA) and regulatory T cells (Tregs) (FoxP3, eBioscience, USA). Paraffin sections were stained for presence of NK cells (Ly-49G2, eBioscience, USA). Brightvision (Immunologic, the Netherlands) was used as secondary antibody, all reactions were developed using diaminobenzidine/H_2O_2. For quantification, the average number of positive cells per field (5-36 images per tumor) was blindly scored using ImageJ software (National Institute of Health). An H&E slide was prepared of lungs of mice, and the average diameter of lung metastases was measured using ImageJ software (National Institute of Health).

Figure 1: Time schedules of the performed experiments. The time is represented in days. As an example, the schedules of RFA and IL-2 treated mice are shown. In all 4 experiments, other arms consisted of mice that were treated with RFA-only, IL-2 only or remained untreated (control). **(A)** n=20, 5 mice/group, **(B)** n=24, 6 mice/group, **(C)** n=41, RFA/IL-2 treatment (n=8), IL-2 treatment (n=12), RFA treatment (n=8), control (untreated) (n=13). **(D)** n=41, RFA/IL-2 treatment (n=8), IL-2 treatment (n=12), RFA treatment (n=8), control (untreated) (n=13).
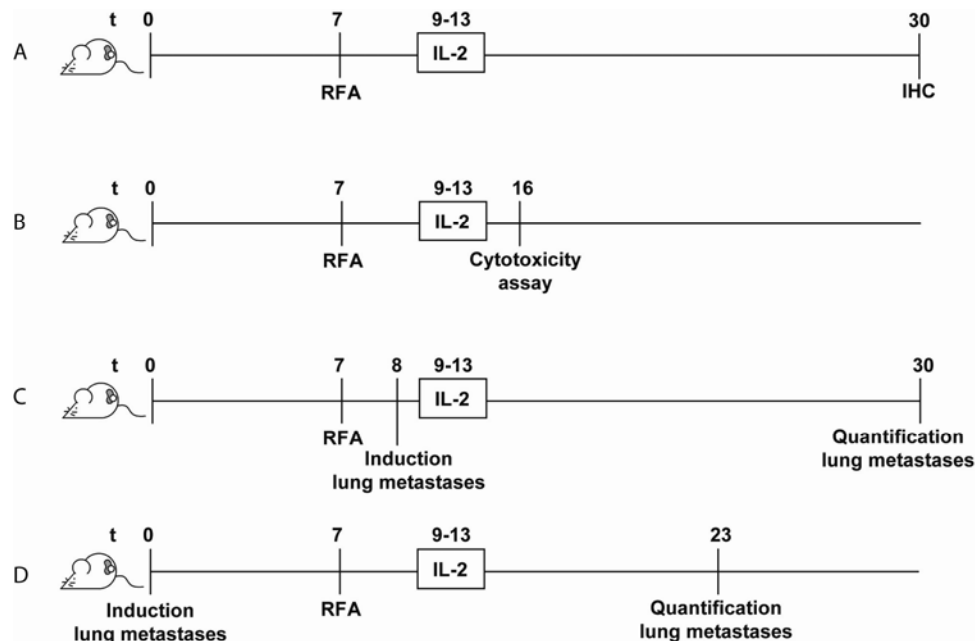
Cytotoxicity assay

To assess whether tumor-specific cytotoxicity was present, tumor bearing mice (6mice/group, n=24) received the combination treatment of RFA/IL-2, IL-2 only, RFA only or no treatment (control) (Figure 1B). Nine days following the start of IL-2 therapy mice were sacrificed, spleens were removed and a single cell suspension was prepared as previously described. [17] Briefly, spleens were mashed in a sterile petri dish containing MACS buffer (Miltenyi Biotec, the Netherlands) and passed through a 70µm cell strainer. Red blood cell lysis was performed with NH_4Cl lysis buffer. Splenocytes were counted using a 3-part differential analyzer (Cell-Dyn 1800, Abbott, the Netherlands), and incubated with antibodies to CD49b (DX5) (NK cells) and CD8 (CD8+ T cells), followed by Goat anti-Rat IgG microbeads (Miltenyi Biotec). Cells were magnetically separated with MS columns (Miltenyi Biolitec, Germany). NK cells were tested for purity by flow cytometry (FACScalibur, BD Biosciences, USA) using CD49b-PE (eBioscience, USA) as positive and CD3-FITC (BD Biosciences, USA) as negative control. CD8+ T cells were tested for purity using CD8+-PE and CD3-FITC as positive controls. Viability was tested using propidium iodide (Sigma Aldrich, the Netherlands). Renca cells were labeled with PKH-26 (Sigma Aldrich, the

Netherlands) and plated in round-bottom 96-well plates (Corning, USA). Freshly isolated CD8+ T or NK cells from mouse spleens were co-incubated with effector:target ratios of 1, 5, 10 and 20. After 3 hours, cells were labeled with antibodies for apoptosis (AnnexinV-FITC, IQ Products, the Netherlands) and cell death (ToPro-3, Molecular Probes, the Netherlands), and FACS analyzed. [18]

Analysis of prevention or regression of lung metastases

To examine whether RFA/IL-2 treatment could prevent the formation of lung metastases, 41 tumor bearing mice received a treatment of RFA/IL-2 (n=8), IL-2 only (n=12), RFA-only (n=8) or no treatment (n=13, control) (Figure 1C). Lung metastases were induced by injecting 10^5 Renca cells through the tail vein 1 day following RFA treatment. [19] To examine whether RFA/IL-2 treatment had an effect on existing lung metastases, lung metastases were similarly induced in 41 tumor bearing mice (Figure 1D). After 1 week, mice received a treatment of RFA/IL-2 (n=8), IL-2 only (n=12), RFA-only (n=8) or no treatment (n=13, control). In both experiments, 3 weeks after induction of lung metastases mice were sacrificed and the number of macroscopic metastases was counted. If the metastases were too numerous to count a cut-off value of 100 metastases was used. [19]

Statistical Analysis

Differences between groups were analyzed with the Student's t-test or one-way ANOVA for parametric measures, followed by a Bonferroni correction. Analysis was performed using the SPSS package version 16.0 for Windows (SPSS, Inc., Chicago, IL).

Results

Increased presence of NK and CD8+ T cells in renal tumors of RFA/IL-2 treated mice.

All mice in all experiments survived treatment. If RFA induces an immunologic response directed towards tumor cells, local infiltration of cytolytic effector cells in the primary tumor may occur. To test this, immunohistochemistry was performed on treated tumors and controls. In control renal tumors inflammatory cells were sparsely present (Figure 2). In RFA and RFA/IL-2 treated mice, influx of inflammatory cells was mostly observed in and around the ablated area. A significant increase in CD8+ T cells was observed 3 weeks following RFA/IL-2 (p<0.0001) compared to IL-2 alone. An influx of NK cells was observed only in the RFA/IL-2 treatment group, 3 weeks following therapy. The number of Tregs decreased upon RFA treatment (p=0.003). CD4+ T cells were increasingly present in renal tumors of RFA/IL-2 treated mice (p=0.001) compared to IL-2. Since both T helper cells and Tregs express

CD4, and no increase in Tregs could be observed, this population most likely consists of T helper cells.

Figure 2: Quantification of the immunohistochemical stainings (mean ± SEM) on the primary tumor 3 weeks following treatment (n=5/group), 5-36 images per tumor were analyzed at a magnification of 10x for CD8+, CD4+ and NK cells, and 20x for FoxP3+ cells. **=p<0.001, ***=p<0.0001.
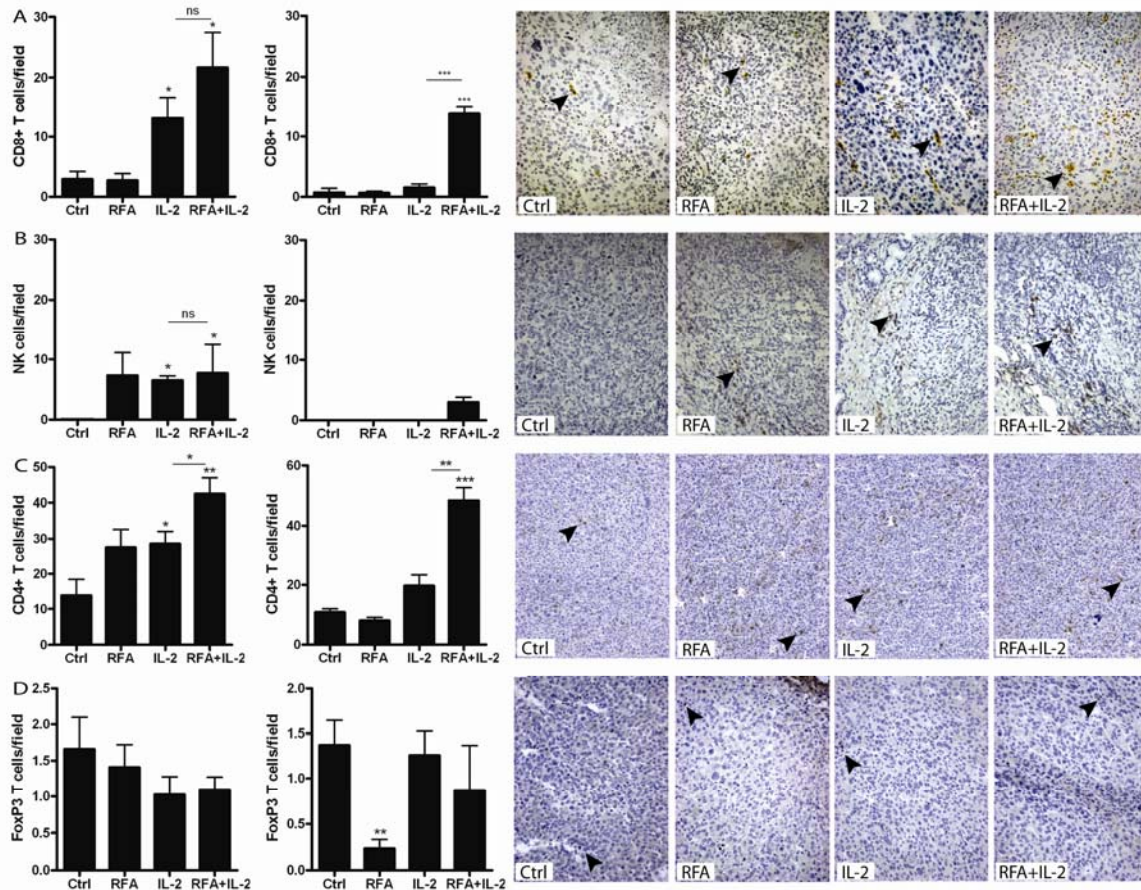
Tumor-specific immune response to Renca is both CD8+ T cell and NK cell mediated.

Two types of cytolytic effector cells (CD8+ T cells and NK cells) showed an increased presence in the remaining primary tumor after RFA/IL-2 treated mice. To determine whether NK and CD8+ T cells are responsible for an anti-tumor immune response, their potential to directly induce tumor cell death was examined *in vitr*o, after isolation from the spleen. Spleens of all treated mice showed an increase in the number of white blood cells compared to the controls (Figure 3A). CD8+ T cell mediated tumor cell death was 4-fold higher in mice treated with RFA/IL-2 (p<0.0001, Figure 3B), and 2-fold higher compared to IL-2 treatment (p<0.05). NK-induced cell death occurred primarily with NK cells isolated from mice treated with RFA/IL-2 (p<0.0001), and to a lesser extent with NK cells from mice treated with IL-2 (p<0.05) (Figure 3C). RFA alone did not influence the cytotoxic activity of NK and CD8+ T cells *in vitro*.

Figure 3: (A) Graph showing the amount (cells/L) of white blood cells (WBC), and their subdivision into lymphocytes (Ly), monocytes (MNC), and granulocytes (GRA) found in the spleen (n=6/group) (mean ± SD). **(B)** Graph displaying the FACS results of the cytoxicity assay of CD8+ T cells derived from spleens of mice (n=6/group) (mean ± SEM). The ratio of treatment-induced apoptosis (AnnexinV-FITC, FL-1) and cell-death (ToPro-3, FL-4) of Renca cells compared to the control (no T cells added) is shown at different effector (CD8+ T cell):target (Renca) ratios (0:1, 1:1, 5:1, 10:1 and 20:1). **(C)** Graph displaying the FACS results of the cytoxicity assay of NK cells derived from spleens of mice (n=6/group) (mean ± SEM). The ratio of treatment-induced apoptosis (AnnexinV-FITC, FL-1) and cell-death (ToPro-3, FL-4) of Renca cells compared to the control (no NK cells added) is shown at different effector (NK cell):target (Renca) ratios (0:1, 1:1, 5:1, 10:1 and 20:1). *=p<0.05, **=p<0.001, ***=p<0.0001.
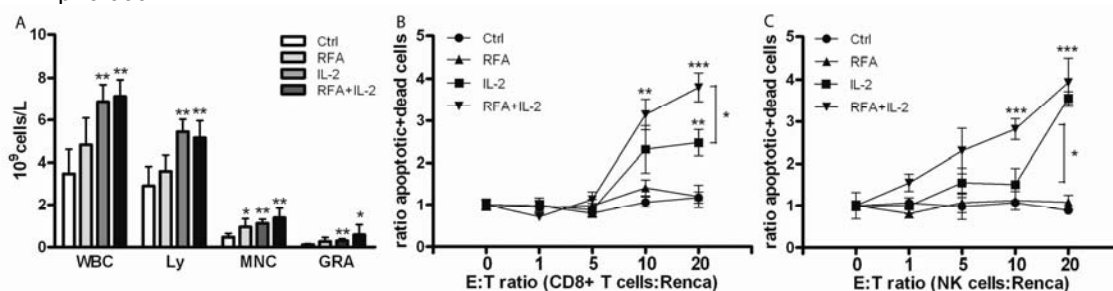

Combination therapy of RFA and IL-2 prevents lung metastases formation.

Because NK and CD8+ T cells derived from RFA/IL-2 treated mice were able to induce renal tumor cell-death *in vitro*, we hypothesized that the combination therapy of RFA/IL-2 would also kill tumor cells *in vivo* and thereby prevent formation of lung metastases. To assess the effect of this combinatorial treatment, lung metastases were induced in tumor bearing mice after RFA of the primary tumor (Figure 1C). Treatment with RFA/IL-2 resulted in a significant decrease and size of lung metastases formation (p<0.0001) (Figure 4A, B, E). The effect of RFA/IL-2 was significantly better compared to treatment with IL-2 (p<0.05). RFA did not affect lung metastases formation.

To study whether RFA/IL-2 could cause regression of established lung metastases, lung metastases were induced in tumor bearing mice one week before treatment (Figure 1D). Treatment with RFA/IL-2 and IL-2 induced regression of lung metastases (p<0.0001) however, there was no significant difference in the number of metastases between these two groups (Figure 4C). Interestingly, the size of the metastatic lesions was significantly smaller in RFA/IL-2 treated mice (p=0.025) compared to IL-2 in both experiments (Figure 4D).

Figure 4: (A) Number of macroscopic lung metastases measured 3 weeks following i.v. injection of 10^5 Renca cells directly after RFA treatment (mean ± SD) (n=8-13 mice/group). **(B)** Graph showing the average diameter of lung metastases (mean ± SEM) 3 weeks following i.v. injection of 10^5 Renca cells after RFA treatment (n=8-13 mice/group), measured on an H&E slide of lungs (magnification 1x). **(C)** Number of macroscopic lung metastases measured 3 weeks following i.v. injection of 10^5 Renca cells, 1 week before RFA treatment (mean ± SD). **(D)** Graph showing the average diameter of lung metastases (mean ± SEM) 3 weeks following i.v. injection of 10^5 Renca cells, 1 week before RFA treatment (n=10 mice/group), measured on an H&E slide of lungs (magnification 1x). **(E)** H&E stainings of lungs (1x) showing the prevention of metastasis formation in RFA/IL-2 treated mice. *=$p<0.05$, **=$p<0.001$, ***=$p<0.0001$
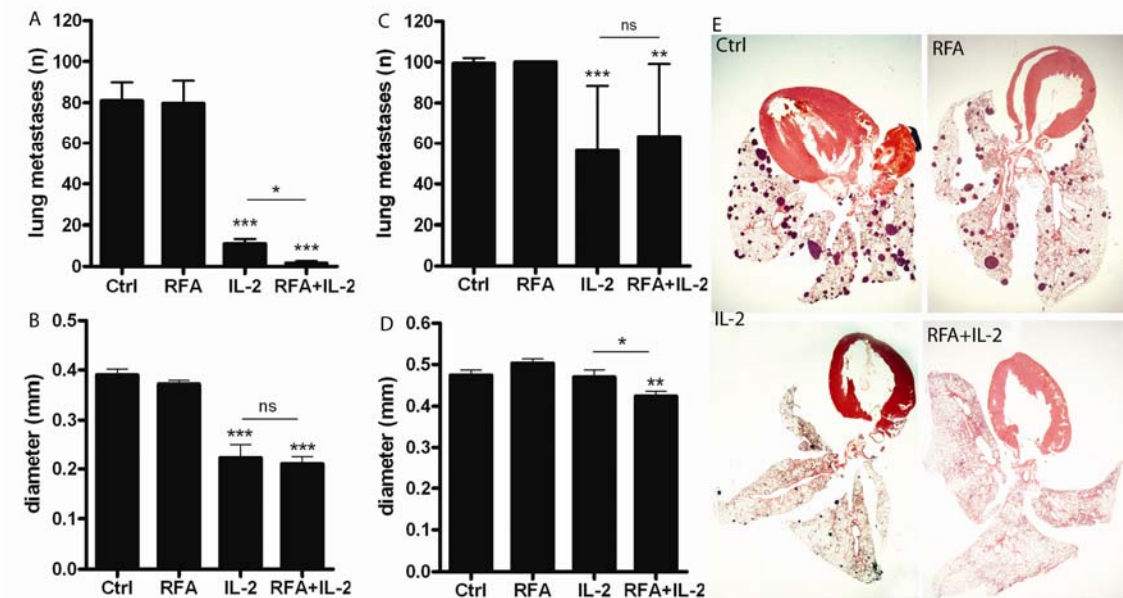

Discussion

In this translational study we show that RFA of the primary tumor significantly enhances the IL-2 induced anti-tumor immune response to renal cell carcinoma. This combination therapy stimulated a tumor-specific cytotoxic activity of CD8+ T cells and NK cells against renal cell carcinoma. Although RFA alone can induce an immune response to ablated tumor tissue, [13, 20] this response has shown to be insufficient to protect for recurrences and metastasis formation in clinical studies. [13, 21-22] Our data showing the immune effects of RFA alone are consistent with these findings, and imply that RFA requires an additional immune stimulation (e.g. IL-2) to ensure an efficient immune response.

A balance between tumor tolerance and anti-tumor immune activation exists within the human body. Usually, the immune system tolerates the progression of RCC, since its cells lack antigens recognized by the body as 'non-self'. Immature dendritic cells (DCs) could take up and process tumor antigens. In the absence of strong activating signals (e.g. pro-

inflammatory cytokines, heat shock proteins) during this process, DCs do not mature and activate T cells but induce tolerance. [23] In RCC Tregs are frequently present. [24] The presence of Tregs within the tumor is thought to promote tolerance. [25] Here we showed that the necrosis and apoptosis induced by RFA can help to tip the balance towards activation of a systemic anti-tumor immune response. The necrosis and apoptosis are thought to be acting as an activation factor to DCs (Figure 5). "Danger" signals and cytokines released following RFA can induce a further activation and maturation of DCs. [22, 26] Following the activation of tumor-specific CD8+ T cells by these DCs, IL-2 promotes the clonal expansion and anti-tumor cytotoxic activity of CD8+ T cells along with NK cells. [14] This is in concordance with our observation that RFA alone could not induce an immune-response strong enough to affect distant tumor cells, but the combination with IL-2 resulted in a prevention of lung metastasis outgrowth. This effect was much stronger compared to IL-2 as monotherapy. Furthermore, the size of established lung metastases was decreased, and NK and CD8+ T cells were shown to induce tumor-specific cell death *in vitro*. Moreover, the here described decrease of Tregs following RFA could have further helped in shifting the tumor tolerance to anti-tumor immunity. [27]

Figure 5: Schematic drawing showing the hypothesis on the anti-tumor immune response to renal cell carcinoma, which is activated by a combination treatment of RFA of the primary tumor and systemically administered IL-2.
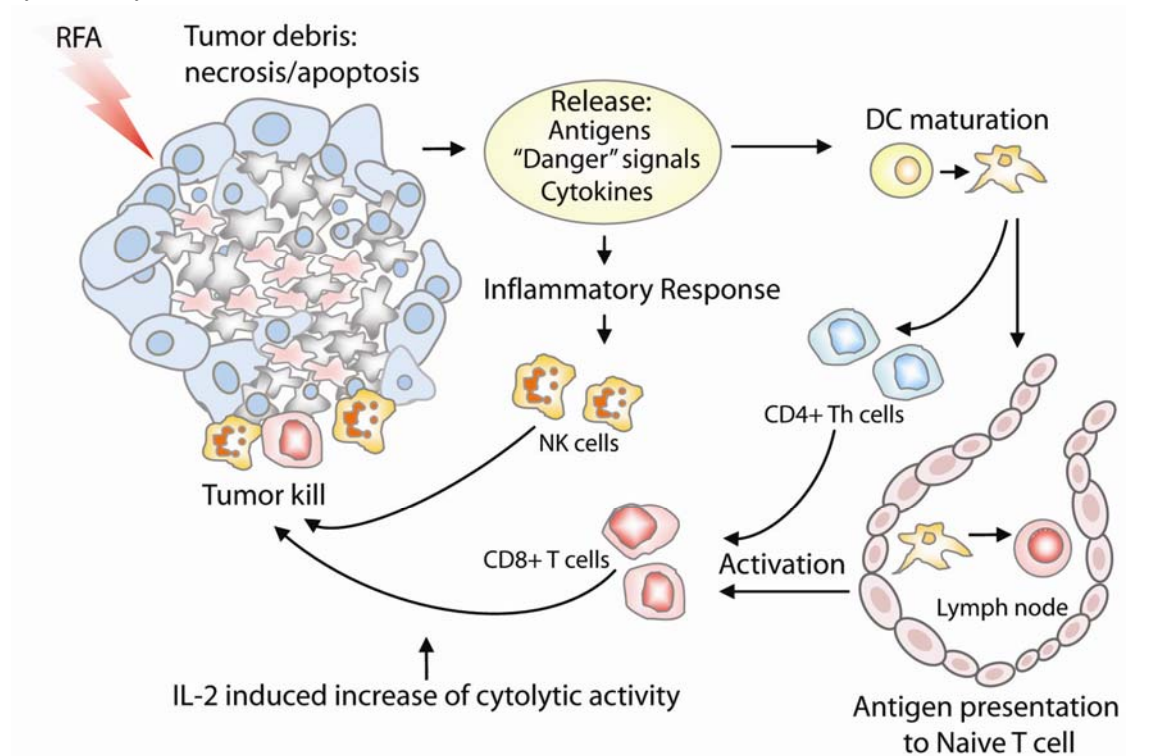
Most anti-tumor vaccines that have been successful in animal models so far were tested in a model for tumor prevention. In the majority of clinical trials hereafter, these vaccines were tested in patients with advanced disease and higher tumor burden, which has resulted in lower success rates than expected (reviewed by [28]). This raises the important issue of the timing of initiation of immunotherapy. It has been shown that a large tumor burden can induce systemic immunosuppression. Moreover, a large primary tumor can attract and tolerate the treatment-activated tumor-specific immune cells. [29] Here, the anti-tumor immune response that has been initiated by RFA/IL-2 could strongly prevent the formation of lung metastases. An important aspect of this study is that the effect on a higher tumor burden with established metastases was also examined. We showed that RFA/IL-2 was able to decrease established disease, although no complete remission of lung metastases was observed under the current conditions. This might mean that the tumor burden was already too high at the time of treatment.

Advantages of using RFA as an *in situ* vaccine include debulking of the primary renal tumor to lower the tumor burden in a safe and minimally invasive way. RFA can disrupt local mechanisms that help the renal tumor to evade the immune system, and the tumor debris that remains inside the body can express unique tumor antigens that are specific for that individual tumor. This vaccination method allows for a potential circumvention of the complex procedures of current anti-tumor vaccines. [5]

This study primarily aimed to establish a proof of principle of the possibilities of RFA combined with an immunomodulatory agent as an *in situ* vaccine against RCC. Due to the promising results on metastasis formation, this preclinical study forms a basis for further studies in this direction. For example, it would be interesting to determine the role of DCs in this process. Furthermore, it could be examined whether the observed effect would also be present in the variety of human RCCs. RFA combined with an immune stimulant could be a potential treatment option for patients with (oligo)metastatic disease, or in the adjuvant setting for high-risk non-metastatic patients. However, while we showed benefits from the combination of RFA with IL-2, IL-2 remains a toxic treatment for which only a select group of patients is eligible. The anti-tumor effect of RFA might be effectively enhanced with other immunostimulatory agents that have less toxic side effects. Of note, current first-line therapy tyrosine kinase inhibitors also appear to have an immunological effect on renal tumors. [30] Furthermore, local stimulation of DCs together with ablation of the primary tumor might also be attractive option. [9]

Based on the literature, it appears that only immunotherapy has the potential to cure metastasized RCC patients. Here we show a new strategy in the development of immunotherapy of RCC. A combination of RFA and IL-2 suits the development of novel treatment strategies for RCC within the modern approach of personalized medicine.

Conclusions

In conclusion, this study provides initial evidence that in addition to the local control of tumor growth, RFA can generate the appropriate conditions for activating a specific anti-tumor immune response in renal tumors, once combined with IL-2 treatment. This effect appears to be mediated by both NK and CD8+ T cells. These findings can play an important role in the development of new multimodal treatment strategies for high-risk or metastatic RCC patients.

References

1. Parkin DM, Bray F, Ferlay J, Pisani P. Global cancer statistics, 2002. CA Cancer J Clin 2005;55:74-108.

2. Sun M, Thuret R, Abdollah F, et al. Age-adjusted incidence, mortality, and survival rates of stage-specific renal cell carcinoma in North America: a trend analysis. Eur Urol 2011;59:135-41.

3. Bex A, Jonasch E, Kirkali Z, et al. Integrating surgery with targeted therapies for renal cell carcinoma: current evidence and ongoing trials. Eur Urol 2010;58:819-28.

4. Rini BI, Atkins MB. Resistance to targeted therapy in renal-cell carcinoma. Lancet Oncol 2009;10:992-1000.

5. Van Poppel H, Joniau S, Van Gool SW. Vaccine therapy in patients with renal cell carcinoma. Eur Urol 2009;55:1333-42.

6. Dudek AZ, Mescher MF, Okazaki I, et al. Autologous large multivalent immunogen vaccine in patients with metastatic melanoma and renal cell carcinoma. Am J Clin Oncol 2008;31:173-81.

7. Jocham D, Richter A, Hoffmann L, et al. Adjuvant autologous renal tumour cell vaccine and risk of tumour progression in patients with renal-cell carcinoma after radical nephrectomy: phase III, randomised controlled trial. Lancet 2004;363:594-9.

8. Zhou J, Weng D, Zhou F, et al. Patient-derived renal cell carcinoma cells fused with allogeneic dendritic cells elicit anti-tumor activity: in vitro results and clinical responses. Cancer Immunol Immunother 2009;58:1587-97.

9. den Brok MH, Sutmuller RP, Nierkens S, et al. Efficient loading of dendritic cells following cryo and radiofrequency ablation in combination with immune modulation induces anti-tumour immunity. Br J Cancer 2006;95:896-905.

10. Gravante G, Sconocchia G, Ong SL, Dennison AR, Lloyd DM. Immunoregulatory effects of liver ablation therapies for the treatment of primary and metastatic liver malignancies. Liver Int 2009;29:18-24.

11. Kim H, Park BK, Kim CK. Spontaneous regression of pulmonary and adrenal metastases following percutaneous radiofrequency ablation of a recurrent renal cell carcinoma. Korean J Radiol 2008;9:470-2.

12. Sanchez-Ortiz RF, Tannir N, Ahrar K, Wood CG. Spontaneous regression of pulmonary metastases from renal cell carcinoma after radio frequency ablation of primary tumor: an in situ tumor vaccine? J Urol 2003;170:178-9.

13. den Brok MH, Sutmuller RP, van der Voort R, et al. In situ tumor ablation creates an antigen source for the generation of antitumor immunity. Cancer Res 2004;64:4024-9.

14. Lotze MT, Grimm EA, Mazumder A, Strausser JL, Rosenberg SA. Lysis of fresh and cultured autologous tumor by human lymphocytes cultured in T-cell growth factor. Cancer Res 1981;41:4420-5.

15. Rosenberg SA, Yang JC, White DE, Steinberg SM. Durability of complete responses in patients with metastatic cancer treated with high-dose interleukin-2: identification of the antigens mediating response. Ann Surg 1998;228:307-19.

16. Smith KA. Interleukin-2: inception, impact, and implications. Science 1988;240:1169-76.

17. Kuhtreiber WM, Kodama S, Burger DE, Dale EA, Faustman DL. Methods to characterize lymphoid apoptosis in a murine model of autoreactivity. J Immunol Methods 2005;306:137-50.

18. Fischer K, Mackensen A. The flow cytometric PKH-26 assay for the determination of T-cell mediated cytotoxic activity. Methods 2003;31:135-42.

19. Schwartz MJ, Liu H, Hwang DH, Kawamoto H, Scherr DS. Antitumor effects of an imidazoquinoline in renal cell carcinoma. Urology 2009;73:1156-62.

20. Wissniowski TT, Hansler J, Neureiter D, et al. Activation of tumor-specific T lymphocytes by radio-frequency ablation of the VX2 hepatoma in rabbits. Cancer Res 2003;63:6496-500.

21. Kunkle DA, Egleston BL, Uzzo RG. Excise, ablate or observe: the small renal mass dilemma-- a meta-analysis and review. J Urol 2008;179:1227-33; discussion 33-4.

22. Zerbini A, Pilli M, Penna A, et al. Radiofrequency thermal ablation of hepatocellular carcinoma liver nodules can activate and enhance tumor-specific T-cell responses. Cancer Res 2006;66:1139-46.

23. Banchereau J, Steinman RM. Dendritic cells and the control of immunity. Nature 1998;392:245-52.

24. Desar IM, Jacobs JH, Hulsbergen-vandeKaa CA, et al. Sorafenib reduces the percentage of tumour infiltrating regulatory T cells in renal cell carcinoma patients. Int J Cancer 2011;129:507-12.

25. Kobayashi N, Hiraoka N, Yamagami W, et al. FOXP3+ regulatory T cells affect the development and progression of hepatocarcinogenesis. Clin Cancer Res 2007;13:902-11.

26. Fagnoni FF, Zerbini A, Pelosi G, Missale G. Combination of radiofrequency ablation and immunotherapy. Front Biosci 2008;13:369-81.

27. Todorova VK, Klimberg VS, Hennings L, Kieber-Emmons T, Pashov A. Immunomodulatory effects of radiofrequency ablation in a breast cancer model. Immunol Invest 2010;39:74-92.

28. Finn OJ. Cancer vaccines: between the idea and the reality. Nat Rev Immunol 2003;3:630-41.

29. Fishman M, Seigne J. Immunotherapy of metastatic renal cell cancer. Cancer Control 2002;9:293-304.

30. Ozao-Choy J, Ma G, Kao J, et al. The novel role of tyrosine kinase inhibitor in the reversal of immune suppression and modulation of tumor microenvironment for immune-based cancer therapies. Cancer Res 2009;69:2514-22.

Chapter 9

Intratumoral administration of holmium-166 acetylacetonate microspheres: multimodality imaging and antitumor efficacy in renal cancer.

Public Library of Science ONE, under review

Wouter Bult[1,2]*

Stephanie G. C. Kroeze[3]*

Mattijs Elschot[1]

Peter R. Seevinck[4]

Freek J. Beekman[5,6]

Hugo W.A.M. de Jong[1]

Donald R.A. Uges[2]

Jos G. Kosterink[2]

Peter R. Luijten [1]

Wim E. Hennink[7]

Alfred D van het Schip[1]

J. L. H. Ruud Bosch[3]

J. Frank W. Nijsen[1#]

Judith J. M. Jans[3#]

*,# Both authors contributed equally

[1]Department of Radiology and Nuclear Medicine, Imaging Division, University Medical Center Utrecht, Heidelberglaan 100, 3584 CX Utrecht, the Netherlands

[2]Department of Hospital and Clinical Pharmacy, University Medical Center Groningen, PO Box 30001, 9700 RB Groningen, the Netherlands

[3]Laboratory of Experimental Oncology, University Medical Center Utrecht, Heidelberglaan 100, 3584 CX Utrecht, the Netherlands

[4]Image Sciences Institute, University Medical Center Utrecht, Heidelberglaan 100, 3584 CX Utrecht, the Netherlands

[5]Milabs, Heidelberglaan 100, 3584 CX Utrecht, the Netherlands

[6]Faculty of Applied Sciences, Section Radiation Detection & Medical imaging, Delft University of Technology, Mekelweg 15, 2629 JB Delft, The Netherlands

[7]Department of Pharmaceutics, Utrecht Institute for Pharmaceutical Sciences, Utrecht University, P.O. Box 80082, 3508 TB Utrecht, The Netherlands

Abstract

Introduction

The increasing incidence of small renal tumors in an aging population with comorbidities has stimulated the development of minimally invasive treatments. This study aimed to assess the efficacy and multimodality imaging properties of intratumoral administration of holmium-166 acetylacetonate microspheres (^{166}HoAcAcMS). This new technique locally ablates renal tumors through high-energy beta particles, while the gamma rays allow for nuclear imaging and the paramagnetism of holmium allows for MRI.

Methods

^{166}HoAcAcMS were administered intratumorally in orthotopic renal tumors (Balb/C mice). Post administration CT, SPECT and MRI was performed. At several time points (2 h, 1, 2, 3, 7 and 14 days) after MS administration, tumors were measured and histologically analyzed. Holmium accumulation in organs was measured using inductively coupled plasma mass spectrometry.

Results

^{166}HoAcAcMS were successfully administered to tumor bearing mice. A striking near-complete tumour-control was observed in ^{166}HoAcAcMS treated mice (0.10 ± 0.01cm^3 vs. 4.15 ± 0.3cm^3 for control tumors). Focal necrosis and inflammation was present from 24h following treatment. Renal parenchyma outside the radiated region showed no histological alterations. Post administration CT, MRI and SPECT imaging revealed clear depots of ^{166}HoAcAcMS in the kidney.

Conclusions

Intratumorally administered ^{166}HoAcAcMS has a great potential as new local treatment of renal tumors for surgically unfit patients. In addition to a strong cancer control, it provides powerful multimodality imaging opportunities.

Introduction

Kidney cancer accounts for approximately 3% of all cancers. With a world-wide incidence of 208,000 new cases and a mortality of 102,000 patients each year, it is one of the most lethal genitourinary malignancies.[1] In recent years a dramatic increase of incidentally detected small renal tumors has occurred, mainly due to more widespread use of non-invasive imaging techniques. These tumors are frequently found in patients who are at surgical risk due to factors such as advanced age and comorbidities.[2] It has been shown that not every patient will benefit from surgical resection of the tumor and that it is better to avoid surgically-induced morbidity in several cases.[3-5] The recommended treatment for small renal tumors is nephron-sparing surgery,[6] but for patients for whom surgical resection is considered inappropriate, minimally invasive techniques are also being developed.[7, 8] Although historically external beam radiotherapy (EBRT) has not been effective for treatment of renal tumors due to breathing-related movement of the kidneys and radiosensitivity of adjacent tissue, new radiation methods may provide a successful alternative.[9] An important new development to circumvent the radiosensitivity issues of healthy tissue around the tumor is the selective local administration of radioactive sources to the tumor.[10, 11] An example of this selective local administration is transcatheter radioembolization with yttrium-90 (^{90}Y) resin microspheres (MS), which has shown promising results in treatment of unresectable hepatic metastases.[12-14] Possibly, intratumoral injection might be more effective than intra-arterial injection.[15] In this paper, a novel local ablation technique is presented using small (10 - 15 μm) holmium-166 acetylacetonate microspheres (^{166}HoAcAcMS) with a high holmium load .[16] ^{166}Ho emits both high-energy beta particles ($E_{\beta max}$ 1.77 and 1.85 MeV, maximum tissue penetration 8 mm, mean tissue penetration 2.5 mm) and gamma rays (0.081 MeV) that allow for nuclear imaging and has a half-life of 26.8 h.[17] Moreover, non-radioactive holmium-165 can be visualized by CT and MRI, due to its high mass attenuation coefficient and its paramagnetic properties, respectively.[18] These imaging opportunities offer many advantages such as visualizing the distribution of holmium microspheres inter- and post-treatment for direct therapy evaluation and follow-up. This study provides a proof of principle for intratumoral administration of ^{166}HoAcAcMS as novel treatment strategy for kidney cancer in patients not eligible for surgery, and demonstrates the elegant *in vivo* multimodality imaging necessary for treatment guidance and monitoring.

Materials and Methods

Cell culture

Balb/C renal carcinoma cells (Renca, National Cancer Institute, USA) were maintained at 37°C and 5% CO_2 in Dulbecco's Modified Eagle's Medium (Lonza, the Netherlands) supplemented with 10% fetal bovine serum (Lonza, the Netherlands), 1% penicillin/streptomycin and 1% glutamine. To prepare for *in vivo* transplantation, cells were trypsinized, washed and kept on ice until transplantation.

Ethics Statement

All experimental protocols were conducted in agreement with the Netherlands Experiments on Animals Act and the European convention guidelines, and accepted by the Animal Experiments Committee Utrecht, the Netherlands (2009.III.01.003).

Animal experiments

Male Balb/C mice (Charles River, the Netherlands) aged 9-11 weeks were used for experiments. All surgical procedures were performed under isoflurane anesthesia (IsoFlo, Abbott Animal Health, the Netherlands). To provide analgesia each mouse received 3 µg buprenorfine subcutaneously (Buprecare, AST Pharma, the Netherlands) prior to, and 24 h post surgery.

Orthotopic kidney tumor model

In 60 mice, the left kidney was exposed through a flank incision and a Renca tumor cube of 2 mm diameter was transplanted under the renal capsule. Renal tumors were allowed to grow for 1 week, while wellbeing of mice was followed by measuring body weight and scoring physical appearance.

Holmium acetylacetonate MS

HoAcAcMS were prepared as described by Bult et al.[16] Sixty mg HoAcAcMS was transferred to a high-density poly-ethylene vial (Posthumus Plastics, the Netherlands), and neutron irradiated in a nuclear reactor (Reactor Institute Delft, the Netherlands) to render the MS radioactive. To assess the MS integrity after neutron irradiation particle size was determined using a coulter counter (Multisizer 3, Beckman Coulter, the Netherlands), performing light microscopy and electron microscopy (Phenom, Phenom B.V., the Netherlands). The size of the HoAcAcMS used range from 10-15 µm. With this size the stability of the MS is good[19] and diffusion throughout the tissue is not to be expected.

Administration of microspheres

Radioactive [166]HoAcAcMS (600 MBq) were suspended in 1.2 ml of an aqueous poloxamer F68 solution (Pluronic® solution, 2% w/v), and 50 µl was taken up in 29 G insulin syringes (Becton Dickinson Ultra Fine, the Netherlands). The activity was measured using a dose calibrator (VDC-404, Veenstra Instruments, the Netherlands). Prior to administration, the syringes were placed in an acrylic glass cylinder to limit the dose on the hands. The syringe was agitated vigorously to obtain a homogenous suspension and 10 µl of the [166]HoAcAcMS (approximately 5 MBq or 500 µg MS) suspension was administered intratumorally via an open approach (n=4-5/group). After administration the syringes were measured in a dose calibrator to calculate the dose administered to the tumors. Control mice (n=3-7/group) received intratumoral administration of 0.9 % NaCl. At 2 hours, 1, 2, 3, 7 and 14 days after the administration of MS mice were sacrificed by cervical dislocation.

Imaging

Immediately following administration of [166]HoAcAcMS, anesthetized mice were placed in a small animal CT (U-CT, MILabs, the Netherlands). Images were acquired at a tube voltage of 45 kV, a tube current of 350 mAs and a voxel size of 83 µm (isotropic). Two mice were underwent multimodality imaging. Single photon emission tomography imaging (SPECT) was performed on a U-SPECT system (MILabs, the Netherlands) with a general purpose mouse collimator (75 focussing 0.6 mm diameter pinholes) to assess the [166]HoAcAcMS distribution on a sub-half-millimeter resolution.[20] Images were reconstructed using previously described methods,[21] and compensated for distance dependent sensitivity and blurring of the projection of the pinholes during reconstruction through point source based system calibration.[22] Each mouse was positioned in the same bed in both the CT and SPECT images, making image registration straightforward. From the SPECT images, the dose distribution could be calculated as described by the MIRD S-voxel method.[23] The MCNPX 2.5.0 Monte Carlo Code[24] was used to estimate the [166]Ho dose convolution kernel. For each voxel in a 15.375^3 mm^3 cube of tissue material ($\rho = 1.06$ g cm^{-1}) the absorbed dose was calculated as a result of the [166]Ho source uniformly distributed in the center voxel of the cube. The voxel size chosen was 375 µm (isotropic), equal to the voxel size of the reconstructed SPECT images. Dose maps were calculated by convolution of the SPECT images with a simulated [166]Ho dose kernel. MRI was performed on a 4.7 T horizontal bore small animal scanner (Agilent, UK). Images were acquired using a multi-slice gradient echo MR sequence with an echo time of 3.0 msec and repetition time of 242 msec, a field of view (FOV) of 64x32 mm^2, a scan matrix of 256x128 with 38 slices resulting in a voxel size of 0.25x0.25x0.5 mm^3, eight signal averages and a 25 flip angle.

Histopathologic analysis

Tumor-bearing and contralateral kidney, liver, spleen and heart/lung were weighed and radioactivity was measured in a dose calibrator. Tumor size was measured using digital callipers and tumor volumes were calculated using the equation V= (A x 0.5) x B^2 (A = largest diameter, B = smallest diameter). Tumor-bearing kidneys were processed and embedded in paraffin. A haematoxylin and eosin (HE) section of each kidney was evaluated for glomerular, tubular and vascular changes and inflammation of the irradiated tumor and surrounding renal parenchyma, as previously described.[25, 26]

Inductively coupled plasma mass spectrometry

Inductively coupled plasma mass spectrometry (ICP MS) was performed to determine the holmium content in the organs used for histopathologic analysis after NaCl or [166]HoAcAcMS treatment. Paraffin was removed from embedded tissue by gentle heating. The organs were digested in 1 mL *aqua regia* (concentrated nitric, perchloric, and sulphuric acid in a ratio 4:1:1) under heating. After destruction, all samples were passed through cotton gauze to remove the insoluble paraffin residue. The samples were diluted in 2% nitric acid, and measured on a Varian 820 MS (Varian, the Netherlands).

Results

Microsphere administration

MS had a smooth surface, both before and after neutron irradiation. The size distribution was not affected by neutron irradiation, and the specific activity of the [166]HoAcAcMS was 10 MBq mg^{-1} at the time of delivery. [166]HoAcAcMS were successfully administered to 24 Renca tumor-bearing Balb/C mice. As a control, 36 (n=3-7 mice per time point) tumor-bearing animals received 10 µl of saline. The mean tumor diameter at the time of treatment was 5.6 mm ± 1.6 mm. The average administered dose was 2.7 MBq ± 1.2 MBq (corresponding to 270 ± 120 µg [166]HoAcAcMS).

Efficacy

Neither discomfort nor aberrant behaviour was observed in these mice. The bodyweight of mice in the [166]HoAcAcMS (22.2 ± 1.8 g) and saline group (22.1 ± 1.2 g) remained constant throughout the experiment. The efficacy of [166]HoAcAcMS after intratumoral injection is depicted in Figure 1A. The tumor volume in the saline control group increased from 0.12 ± 0.03 cm^3 (day 3 after treatment) to 4.15 ± 0.3 cm^3 two weeks post injection. Importantly, the tumor volume in the [166]HoAcAcMS group remained constant from 0.14 ± 0.01 cm^3 at three days post injection to 0.10 ± 0.01 cm^3 after two weeks. ICP MS analysis showed that 72.9% (33.1 – 83.6) (median (IQR)) of the total holmium measured was detected in the tumors of

mice that received [166]HoAcAcMS. In 15 mice in the holmium group 16.9% (IQR 2.6 – 52.5) holmium was found in the lungs, most likely due to the inadvertent delivery of [166]HoAcAcMS in a blood vessel in or around the tumor.[27]

Figure 1: (A) Tumor volume at different time points after treatment. The solid line represents the tumor volume of the [166]HoAcAcMS group. The dashed line represents the tumor volume of the saline control group. **(B)** HE staining of kidney and tumor tissue 2 weeks after [166]HoAcAcMS treatment (n indicates normal kidney, t indicates tumor.) **(C)** HE staining (20x) of renal parenchyma outside the radiated region 2 weeks following [166]HoAcAcMS administration, showing no glomerular, tubular or vascular alterations. **(D)** HE staining (20x) of irradiated tumor 1 day following [166]HoAcAcMS administration. HoAcAcMS are present as focal intratumoral deposits (arrows). At the site of injection, tumor necrosis and cell death is visible. **(E)** HE staining of irradiated tumor (20x) 2 days following [166]HoAcAcMS administration. Inflammatory cells are present at the radiated area. **(F)** HE staining of irradiated tumor (20x) 1 week after [166]HoAcAcMS administration. Grade 3 radiation damage [25] is only visible in renal parenchyma directly surrounding the tumor.
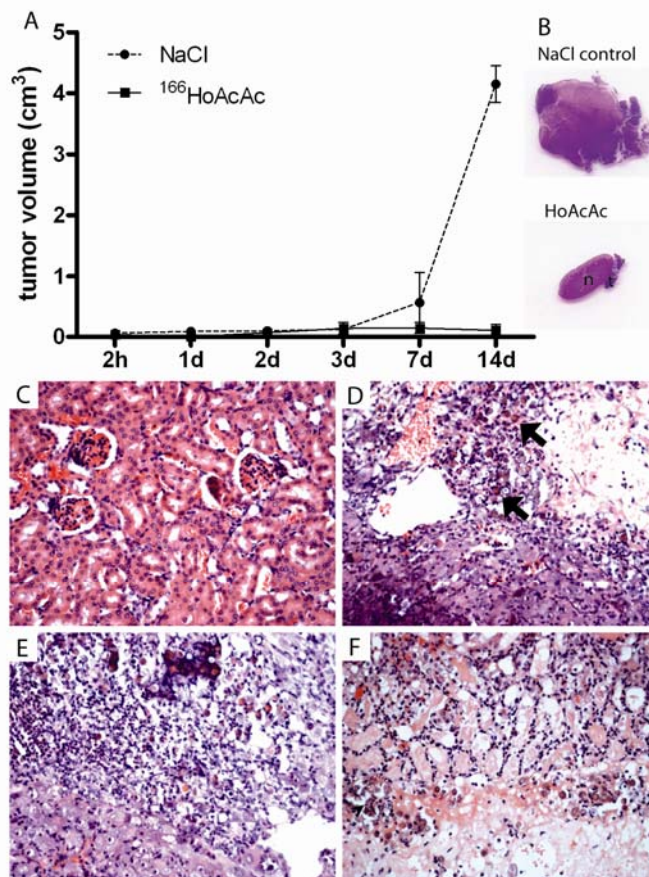

Histology

[166]HoAcAcMS were present as focal intratumoral deposits (Figure 1D). Tumor necrosis was visible at the site of injection from 24 h following [166]HoAcAcMS administration (Figure 1D), inflammatory cells were visible within 48 h (Figure 1E). Grade 3 radiation damage[25] was only visible in renal parenchyma directly surrounding the tumor 2 weeks after treatment (Figure

1F). In all cases, renal parenchyma outside the radiated region showed no glomerular, tubular or vascular alterations (Figure 1A).

Imaging

The powerful multimodality imaging characteristics of holmium were demonstrated with CT, SPECT and MRI in mice that were terminated immediately following intratumoral administration of [166]HoAcAcMS (Figure 2A to D). CT imaging revealed deposits of [166]HoAcAcMS (approximately 300 μg, corresponding to 2.7 MBq [166]Ho) in the kidney area. Substantial accumulation of particles was seen at the site of injection (Figure 2B). [166]HoAcAcMS were clearly visualized using SPECT imaging and the SPECT images served as a template for the construction of a dose map (Figure 2E). The dose map shows a selective deposition of therapeutic beta particles at the site of injection, leading to a local tumor absorbed dose in excess of 2200 Gy. The average tumor dose was calculated using the equation as postulated by Vente et al.: Dose (Gy) = (Dosage administered (MBq) x 15.87 mJ MBq^{-1})/tumor weight (g).[28] The calculated average tumor dose in this study was 323 Gy. The radiation dose to the healthy tissue was below 23 Gy in the largest part of the kidney and surrounding organs (Figure 2F). For a more detailed anatomical depiction of the soft tissue, MR images were acquired. On T_2* weighted MRI scans, holmium causes a rapid signal decay due to the paramagnetic nature of this element. Consequently, holmium appears as blackening on T_2* weighted images. As can be seen in Figure 3, holmium is clearly visible as a dark spot in the upper side of the kidney, where it was administered in the tumor. By combining the sensitivity and high quantitative accuracy of SPECT imaging[29-31] with the soft tissue imaging of MRI, the [166]HoAcAcMS therapy can accurately be evaluated to ensure complete tumor ablation.

Figure 2: An example of the multimodality imaging characteristics of intratumorally administered [166]HoAcAcMS. Images are acquired immediately following administration of the MS. (A) A schematic representation of the mouse anatomy (I: Lungs; II: Liver; III: Stomach; IV: Kidney; *: Artefact caused by holmium on MRI image 3C) (B) CT image, depicting the HoAcAcMS in the kidney area as a white area (arrow). (C) MR image showing the soft tissue detail of this imaging modality and the deposition of HoAcAcMS as a dark spot. (D) SPECT image, showing a selective visualisation of radioactive MS in the kidney area. (E) Fused SPECT and CT image. (F) MRI image fused with the dose map, showing the absorbed dose distribution in the kidney area.
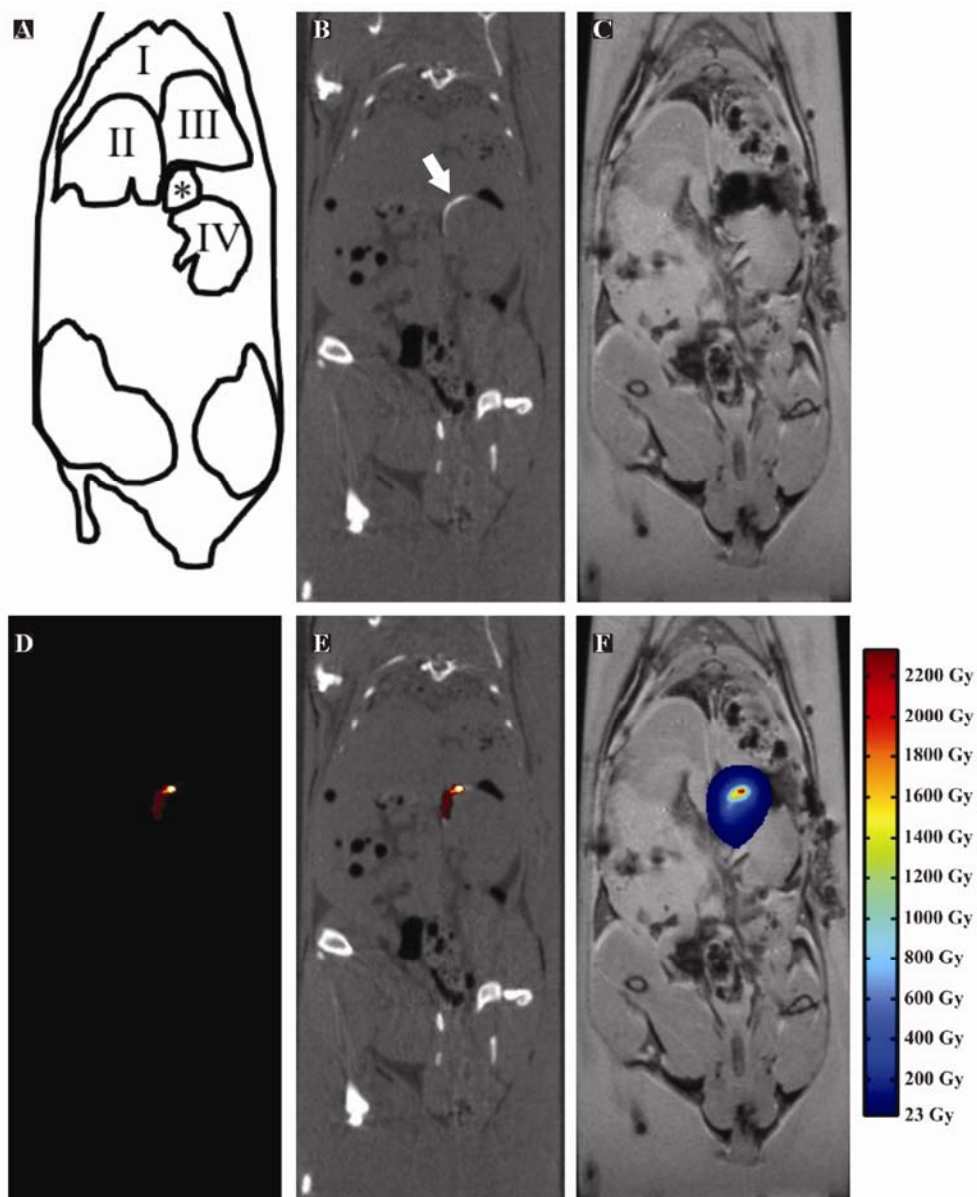
Discussion

The feasibility and efficacy of [166]HoAcAcMS as a minimally invasive treatment was assessed in a mouse model for kidney cancer. Importantly, the intratumoral administration of 2.7 MBq [166]HoAcAcMS arrested tumor growth, which was apparent one week post-administration when approximately 95% of the ionizing radiation dose has been delivered. Assuming all beta energy is deposited in the tumor, the calculated average tumor absorbed dose was 323 Gy, with local doses as high as 2200 Gy. The average tumor absorbed dose is approximately 4-5 fold higher than the 60-80 Gy absorbed dose used in EBRT as a value sufficient for complete tumor kill. Despite the high calculated absorbed dose, the localized nature of the radiation dose considerably reduces unwanted damage of surrounding tissues. The radiation dose to the healthy tissue was below 23 Gy in the largest part of the kidney and surrounding organs. 23 Gy is the maximum tolerance dose for uniform kidney irradiation.[32] Given the maximum penetration depth of the emitted beta particles (8 mm), the radiation dose to healthy parenchyma is expected to be negligible when translating to the clinical situation.

In addition to efficacy, the multimodality imaging characteristics of [166]HoAcAcMS were investigated. Deposits of approximately 2.7 MBq or 270 micrograms of [166]HoAcAcMS were clearly visible on SPECT, or CT and MRI. [166]HoAcAcMS can therefore be regarded as a true multimodality imaging agent. The specificity of SPECT was superior to that of both CT and MRI. In this study CT imaging was used to determine the distribution of [166]HoAcAcMS, since the low amounts of activity administered result in a long acquisition time with SPECT (6 minutes for CT versus 45 minutes SPECT). However, in patients faster SPECT image acquisition will be possible, as the amount of activity will be 20- to 100-fold higher. Furthermore, by combining the sensitivity and high quantitative accuracy of SPECT imaging [29-31] with the soft tissue imaging of MRI, the [166]HoAcAcMS therapy could accurately be evaluated to ensure complete tumor ablation during the procedure.

The use of radioactive microspheres in the treatment of an experimental tumor model was successful, and results are very promising. Although the orthotopic mouse model resembles the human situation in many aspects, a number of points need to be addressed before intratumoral administration of [166]HoAcAcMS could be routinely applied in humans. First of all, toxicity studies should be performed in humans. Radioactive holmium poly(L-lactic acid) particles of 20-50 μm for intra-arterial application have been evaluated for biodistribution, efficacy and toxicity in rats, rabbits and pigs, and have shown their stability and safety,[28, 33] a phase-I study of patients with liver metastases has recently been initiated.[34] Similar toxicity experiments will need to be performed for the [166]HoAcAcMS described here prior to initiating a clinical trial.

Tumors in study ranged from 4 to 8 mm at the time of treatment, which is similar to the penetration range of the beta particles in tissue. It is expected that for nephron-sparing treatment of tumors smaller than 4 cm, 4 to 8 injections with ^{166}HoAcAcMS are required for an effective eradication. This is comparable to conventional minimally invasive ablative treatments that often need multiple probes to achieve complete tumor kill.[35] The advantage of radionuclide therapy compared to thermal ablative minimally invasive techniques is the prolonged delivery of energy to the tumor tissue, due to the half life. Using multiple deposits of ^{166}HoAcAcMS, an accurate delivery of the dose can be given independent of shape and size of the tumor. As observed, an average tumor dose of 323 Gy was obtained with one deposit. When positioning the deposits within 1 cm apart it is expected that the complete tumor kill can be achieved. However, more research is warranted to further investigate the relationship between deposit localisation and tumor kill in larger tumors.

A technical problem we encountered was the delivery of approximately 50% of the intended dose (5 MBq), possibly due to adsorption of radioactive MS onto the syringe wall and dosage errors due to the small injected volume. When treating patients, the administered volume is higher, resulting in a smaller difference between aimed and actual administered dose. Furthermore, varying concentrations of holmium were found in the lungs of several mice. Tumor vascularity as well as particle size is an important factor for the fate of the radioactivity.[36] Although the presence of holmium in the lungs is likely due to the inadvertent vascular delivery of the MS during the intratumoral injections[27] and with a size of 12.5 µmm diffusion within the tissue is less likely, a future study should be performed to examine these 2 factors specifically. Lung uptake was not observed when administering ^{166}HoAcAcMS percutaneously under ultrasound guidance in feline liver tumors.[37] Ultrasound guidance not only helps to distinguish healthy tissue from tumorous tissue, it also visualises tumor vasculature. Unfortunately, percutaneous ultrasound guided administration was not feasible in this model. Nevertheless, in patients the procedure can be performed percutaneously under CT or ultrasound guidance. An illustration of a CT guided approach is shown in Figure 3. A new method that could be used is the multiplanar Global Positioning System-like technology.[38] A minimally invasive approach would make intratumoral administration of ^{166}HoAcAcMS suitable for treatment of patients for whom surgical resection is considered inappropriate.

Conclusions

The present study demonstrates that intratumoral administration of ^{166}HoAcAcMS is a promising novel minimally invasive treatment of kidney cancer. Tumor growth was arrested and no signs of radiation damage outside the treatment zone were observed. Importantly, multimodality imaging including CT, SPECT and MRI of small amounts of ^{166}HoAcAcMS was

feasible. This will lead to an improved therapy evaluation and follow-up and provides a fundamental advantage over current therapies.

Figure 3. Schematic drawing showing the percutaneous approach to [166]HoAcAcMS administration. The [166]HoAcAcMS are administered intratumorally by a shielded syringe under real-time CT guidance.
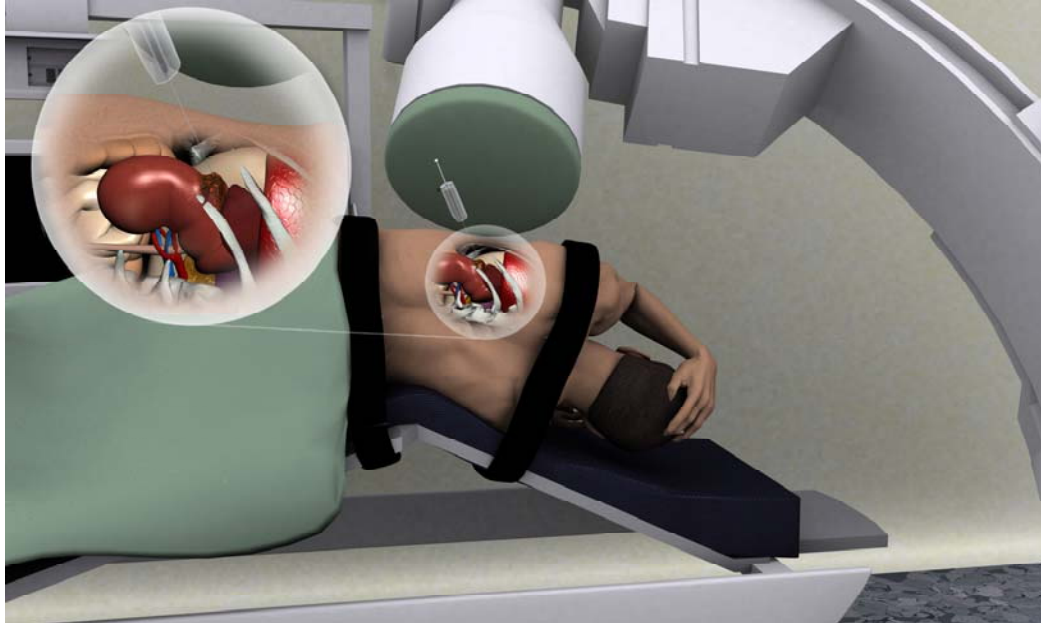
References

1.   Parkin DM, Bray F, Ferlay J, Pisani P. Global cancer statistics, 2002. CA Cancer J Clin 2005;55:74-108.

2.   Hollingsworth JM, Miller DC, Daignault S, Hollenbeck BK. Rising incidence of small renal masses: a need to reassess treatment effect. J Natl Cancer Inst 2006;98:1331-4.

3.   Kutikov A, Egleston BL, Wong YN, Uzzo RG. Evaluating overall survival and competing risks of death in patients with localized renal cell carcinoma using a comprehensive nomogram. J Clin Oncol 2010;28:311-7.

4.   Santos Arrontes D, Fernandez Acenero MJ, Garcia Gonzalez JI, Martin Munoz M, Paniagua Andres P. Survival analysis of clear cell renal carcinoma according to the Charlson comorbidity index. J Urol 2008;179:857-61.

5.   Lane BR, Abouassaly R, Gao T, et al. Active treatment of localized renal tumors may not impact overall survival in patients aged 75 years or older. Cancer 2010;116:3119-26.

6.   Ljungberg B, Cowan NC, Hanbury DC, et al. EAU guidelines on renal cell carcinoma: the 2010 update. Eur Urol 2010;58:398-406.

7.   Heuer R, Gill IS, Guazzoni G, et al. A critical analysis of the actual role of minimally invasive surgery and active surveillance for kidney cancer. Eur Urol 2010;57:223-32.

8.   Muto G, Castelli E, Migliari R, D'Urso L, Coppola P, Collura D. Laparoscopic Microwave Ablation and Enucleation of Small Renal Masses: Preliminary Experience. Eur Urol 2011.

9.   Kerkhof EM, Raaymakers BW, van Vulpen M, et al. A new concept for non-invasive renal tumour ablation using real-time MRI-guided radiation therapy. BJU Int 2011;107:63-8.

10.   MacKie S, de Silva S, Aslan P, et al. Super selective radio embolization of the porcine kidney with 90yttrium resin microspheres: a feasibility, safety and dose ranging study. J Urol 2011;185:285-90.

11.   Gao W, Liu L, Liu ZY, Wang Y, Jiang B, Liu XN. Intratumoral injection of 32P-chromic phosphate in the treatment of implanted pancreatic carcinoma. Cancer Biother Radiopharm 2010;25:215-24.

12.   Coldwell D, Sangro B, Salem R, Wasan H, Kennedy A. Radioembolization in the Treatment of Unresectable Liver Tumors: Experience Across a Range of Primary Cancers. Am J Clin Oncol 2010.

13.   Smits ML, Nijsen JF, van den Bosch MA, et al. Holmium-166 radioembolization for the treatment of patients with liver metastases: design of the phase I HEPAR trial. J Exp Clin Cancer Res 2010;29:70.

14.   Vente MA, Wondergem M, van der Tweel I, et al. Yttrium-90 microsphere radioembolization for the treatment of liver malignancies: a structured meta-analysis. Eur Radiol 2009;19:951-9.

15.   Lin WY, Tsai SC, Hsieh JF, Wang SJ. Effects of 90Y-microspheres on liver tumors: comparison of intratumoral injection method and intra-arterial injection method. J Nucl Med 2000;41:1892-7.

16. Bult W, Seevinck PR, Krijger GC, et al. Microspheres with ultrahigh holmium content for radioablation of malignancies. Pharm Res 2009;26:1371-8.

17. Nijsen JF, Zonnenberg BA, Woittiez JR, et al. Holmium-166 poly lactic acid microspheres applicable for intra-arterial radionuclide therapy of hepatic malignancies: effects of preparation and neutron activation techniques. Eur J Nucl Med 1999;26:699-704.

18. Seevinck PR, Seppenwoolde JH, de Wit TC, et al. Factors affecting the sensitivity and detection limits of MRI, CT, and SPECT for multimodal diagnostic and therapeutic agents. Anticancer Agents Med Chem 2007;7:317-34.

19. Bult W, de Leeuw H, Steinebach OM, et al. Radioactive Holmium Acetylacetonate Microspheres for Interstitial Microbrachytherapy: An In Vitro and In Vivo Stability Study. Pharm Res 2011.

20. van der Have F, Vastenhouw B, Ramakers RM, et al. U-SPECT-II: An Ultra-High-Resolution Device for Molecular Small-Animal Imaging. J Nucl Med 2009;50:599-605.

21. Branderhorst W, Vastenhouw B, Beekman FJ. Pixel-based subsets for rapid multi-pinhole SPECT reconstruction. Phys Med Biol 2010;55:2023-34.

22. van der Have F, Vastenhouw B, Rentmeester M, Beekman FJ. System calibration and statistical image reconstruction for ultra-high resolution stationary pinhole SPECT. IEEE Trans Med Imaging 2008;27:960-71.

23. Bolch WE, Bouchet LG, Robertson JS, et al. MIRD pamphlet No. 17: the dosimetry of nonuniform activity distributions--radionuclide S values at the voxel level. Medical Internal Radiation Dose Committee. J Nucl Med 1999;40:11S-36S.

24. Hendricks JSM, G.W.; Waters, L.S.; Roberts, T.L.; Egdorf, H.W.; Finch, J.P.; Trellue, H.R.; Pitcher, E.J.; Mayo, D.R.; Swinhoe, M.T.; Tobin, S.J.; Durkee, J.W. MCNP Extention, Version 2.5.0. Los Alamos: Los Alamos National Laboratory Report; 2005. Report No.: LA-UR-05-2675.

25. Forrer F, Rolleman E, Bijster M, et al. From outside to inside? Dose-dependent renal tubular damage after high-dose peptide receptor radionuclide therapy in rats measured with in vivo (99m)Tc-DMSA-SPECT and molecular imaging. Cancer Biother Radiopharm 2007;22:40-9.

26. Madrazo A, Suzuki Y, Churg J. Radiation nephritis: acute changes following high dose of radiation. Am J Pathol 1969;54:507-27.

27. Tian JH, Xu BX, Zhang JM, Dong BW, Liang P, Wang XD. Ultrasound-guided internal radiotherapy using yttrium-90-glass microspheres for liver malignancies. J Nucl Med 1996;37:958-63.

28. Vente MA, Nijsen JF, de Wit TC, et al. Clinical effects of transcatheter hepatic arterial embolization with holmium-166 poly(L-lactic acid) microspheres in healthy pigs. Eur J Nucl Med Mol Imaging 2008;35:1259-71.

29. D'Asseler Y. Advances in SPECT imaging with respect to radionuclide therapy. Q J Nucl Med Mol Imaging 2009;53:343-7.

30. de Wit TC, Xiao J, Nijsen JF, et al. Hybrid scatter correction applied to quantitative holmium-166 SPECT. Phys Med Biol 2006;51:4773-87.

31. Vanhove C, Defrise M, Bossuyt A, Lahoutte T. Improved quantification in single-pinhole and multiple-pinhole SPECT using micro-CT information. Eur J Nucl Med Mol Imaging 2009;36:1049-63.

32. O'Donoghue J. Relevance of external beam dose-response relationships to kidney toxicity associated with radionuclide therapy. Cancer Biother Radiopharm 2004;19:378-87.

33. Zielhuis SW, Nijsen JF, Seppenwoolde JH, et al. Long-term toxicity of holmium-loaded poly(L-lactic acid) microspheres in rats. Biomaterials 2007;28:4591-9.

34. Smits ML, Nijsen JF, van den Bosch MA, et al. Holmium-166 radioembolization for the treatment of patients with liver metastases: design of the phase I HEPAR trial. J Exp Clin Cancer Res;29:70.

35. Gervais DA, McGovern FJ, Arellano RS, McDougal WS, Mueller PR. Radiofrequency ablation of renal cell carcinoma: part 1, Indications, results, and role in patient management over a 6-year period and ablation of 100 tumors. AJR Am J Roentgenol 2005;185:64-71.

36. Luboldt W, Pinkert J, Matzky C, Wunderlich G, Kotzerke J. Radiopharmaceutical tracking of particles injected into tumors: a model to study clearance kinetics. Curr Drug Deliv 2009;6:255-60.

37. Bult W, Vente MAD, Vandermeulen E, Gielen I, et al. Interstitial microbrachytherapy using holmium-166 acetylacetonate microspheres: a pilot study in feline liver cancer patients. Brachytherapy, in press.

38. Hung AJ, Ma Y, Zehnder P, Nakamoto M, Gill IS, Ukimura O. Percutaneous radiofrequency ablation of virtual tumours in canine kidney using Global Positioning System-like technology. BJU Int 2011.

Chapter 10

Photodynamic therapy as novel nephron-sparing treatment option for small renal masses

Stephanie.G.C. Kroeze[1,4]

Matthijs C.M. Grimbergen[2]

Holger Rehmann[3]

J.L.H.Ruud Bosch[1]

Judith J.M. Jans[1,4]

1 Department of Urology, University Medical Center Utrecht, the Netherlands

2 Department of Medical Physics & Instrumentation, St Antonius Hospital, Nieuwegein, the Netherlands

3 Department of Physiological Chemistry and Centre of Biomedical Genetics, University Medical Center Utrecht, the Netherlands

4 Laboratory of Experimental Oncology, University Medical Center Utrecht, the Netherlands

Abstract

Introduction

Photodynamic therapy (PDT) has great potential as nephron-sparing therapy for small renal masses. Using meso-tetra-hydroxyphenyl-chlorin (mTHPC), a photosensitizer that targets both vasculature and tissue, we aimed to determine whether renal tumors can be ablated using mTHPC-mediated PDT in a translational renal carcinoma mouse model.

Materials and Methods

mTHPC was administered i.v. in kidney tumor-bearing mice (tumor diameter 7 mm). At several drug-light intervals (DLIs) a cylindrical laser fiber was placed intratumorally for interstitial illumination (wavelength 652nm). mTHPC biodistribution up to 48 h following administration and tumor destruction following mTHPC-mediated PDT was determined. *In vitro* mTHPC uptake and PDT-induced cytotoxicity was studied in human endothelial, renal and renal cell carcinoma (RCC) cell lines.

Results

Ablated regions with a maximum diameter of 9.3 mm and complete loss of cell viablity were observed at a DLI of 4 h, when mTHPC levels were elevated in both blood and tissue. Viable renal tissue remained detectable outside the illuminated area. mTHPC uptake and sensitivity to PDT was increased in endothelial cells compared to RCC and renal cells.

Conclusion

mTHPC-mediated PDT is a nephron sparing therapy. The extent of renal tumor destruction is adequate for clinical translation. Localization of mTHPC in both tumor vasculature and tissue produces a strong combinatorial effect. Our findings justify further pre-clinical studies into the applicability of PDT for RCC, before PDT can become a valuable addition to current minimally invasive treatments of small renal masses.

Introduction

The increasing incidence of small renal masses has stimulated the development of nephron-sparing surgical techniques. In addition to radiofrequency ablation and cryoablation, other modalities such as high-intensity focused ultrasound or microwave thermotherapy are investigated.[1] A therapy that recently has gained ground for treatment of urological solid malignancies is photodynamic therapy (PDT).

PDT employs a photosensitizer that is activated by a specific wavelength of light, in the presence of oxygen, to induce tumor necrosis and apoptosis.[2] PDT targets both tumor vasculature and tumor cells, and is followed by an immune response (fig. 1). The preference of vascular versus cellular targeting depends upon the characteristics of the photosensitizer and the time between administration and illumination (drug-light interval, DLI). Short DLIs target tumor vasculature due to photosensitizer accumulation within blood vessels, whereas a long DLI predominantly induces direct tumor cell destruction due to an increased uptake of photosensitizers in the tumor tissue.[3]

Clinical experience with PDT in the field of urology was initially obtained in superficial bladder cancer using porfimer sodium, providing modest results.[4] Recently, next generation photosensitizers have emerged that are more potent, capable of deeper tissue penetration by activation at higher wavelengths and cause less cutaneous phototoxicity.[5] Together with advances in the development of cylindrical laser probes that directly deliver light into the target area, PDT has great potential as focal therapy for solid urological tumors.[6] Phase I studies using new generation photosensitizers have shown promising results in localized prostate cancer[7] and larger cohort studies with longer follow-up are underway.[8] One of the most potent new generation photosensitizers is meso-tetra-hydroxyphenyl-chlorin (mTHPC, Foscan®). mTHPC is activated at an excitation wavelength (652nm) adequate for deep tissue penetration.[9] It has been approved for palliative treatment of head and neck cancer in Europe and has undergone clinical trials for prostate cancer.[10] While most new photosensitizers are grouped into either being predominantly vascular targeted or tissue targeted, the optimal tumoricidal effect of mTHPC-based PDT involves targeting of both.[11-13]

For renal cell carcinoma (RCC) experience with PDT so far is limited. Small renal tumors would be ideal targets for PDT as they are highly vascularised and have a clear delineation on several imaging modalities. Moreover, experience in approaching renal tumors in a minimally invasive way and percutaneously applicable cylindrical lasers are present. Only two preclinical studies have been published, using a tissue targeting photosensitizer (THOPP-MPEG) in mice[14] and a vascular targeting photosensitizer (WST-09) in pigs.[15] Since targeting of both tumor vasculature and tumor cells simultaneously enhances the tumoricidal effect of PDT[16], mTHPC-mediated PDT may be an promising nephron-sparing treatment of

119

small renal masses. To determine whether this is true, we evaluated the efficacy of mTHPC-mediated PDT in a renal carcinoma mouse model. Furthermore, the relative sensitivity of RCC cells compared to endothelial cells and normal kidney cells was investigated.

Figure 1: Schematic action mechanisms of photodynamic therapy. Localized illumination with a wavelength of 652 nm excites the photosensitizer, which results in the formation of reactive oxygen species (ROS) in the presence of oxygen. This induces direct tumor cell destruction and vascular damage, followed by an inflammatory response.
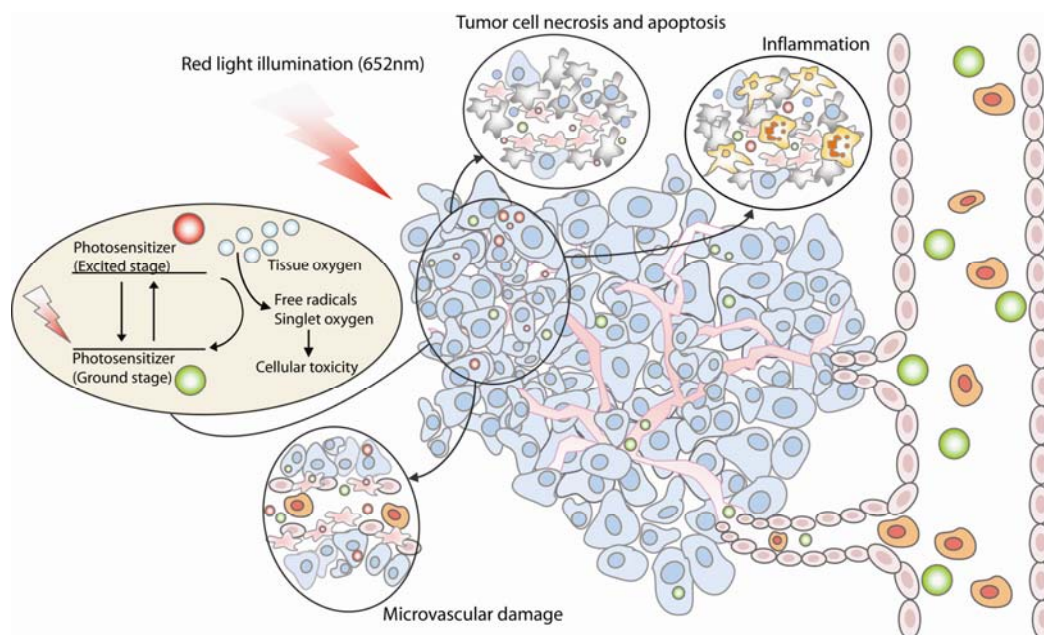
Materials and Methods

Photosensitizer

mTHPC (4 mg/mL) (Biolitec Pharma Ltd, Dublin, Ireland) was dissolved in ethanol, polyethylene glycol 400 and water (1:1:2, vol/vol/vol) at a concentration of 50 µg/ml.

Cell culture

The human renal cell carcinoma cell lines RCC10, A498, 786-0, human renal cell line HK2 and the Balb/C murine renal carcinoma cell line SIRCC1.15 (kindly provided by the National Cancer Institute, Frederick, USA) were maintained at 37°C and 5% CO_2 in Dulbecco's Modified Eagle's Medium (DMEM, Lonza, Breda, the Netherlands) supplemented with 10% Fetal Calf Serum (FCS), 50,000 IU penicillin-G/50,000 µg streptomycin and 2mM glutamine. The human endothelial cell (HMEC) line was cultured in enriched Endothelial Cell Growth Medium-2 (Lonza, Breda, the Netherlands). All *in vitro* experiments were performed in triplicate and repeated.

Induction of renal tumors and administration of PDT

Experimental protocols were approved by the local experimental Animal Welfare Committee and comply with national and European regulations for animal experimentation. Animals were housed under standard laboratory conditions. Male Balb/C mice (Charles River, Maastricht, the Netherlands) 5-7 weeks of age were used (n=4-7/group). All surgical procedures were performed under general anesthesia (Isoflurane USP 1.5-4.0%, oxygen 0.5%) and analgesia (100 µl buprenorphine 0.03 mg/ml s.c. prior to and following surgery). The left kidney was exposed through a flank incision. Renal tumors were established by injecting 1.10^5 SIRCC1.15 cells in 50 µL of phosphate buffered saline and Matrigel^{TM} (BD Biosciences, Breda, the Netherlands, 1:1 vol/vol) into the subcapsular space of the left kidney. PDT was performed when tumors reached a diameter of approximately 7 mm. Mice received 0.3 mg/kg mTHPC intravenously, after which they were housed in the dark for the total duration of the experiment to prevent skin phototoxicity. At several time points following administration of mTHPC (5 min, 4 h, 24 h and 48 h) renal tumors in separate study groups were interstitially illuminated. To this end, a cylindrical PDT fiber with an effective diffuser length of 1 cm (cylindrical diffuser CD 404-10H, Biolitec) was inserted in the center of the renal tumor by use of a 14 G i.v. catheter (Insyte i.v. catheter, BD Medical, Breda, the Netherlands) through a flank incision. Illumination with wavelength of 652 nm was performed at 15 W/cm^2 to a light dose of 30 J/cm^2, while the rest of the mouse was shielded from light.

mTHPC biodistribution

At 5 min, 20 min, 2 h, 4 h, 24 h and 48 h after mTHPC administration, blood and tissues were harvested (n=3-7 mice/group). Methanol:dimethylsulfoxide (DMSO) was added to the plasma (4:1 vol/vol) prior to spectrophotometric analysis. Tissue samples (50 mg) were minced using a scalpel and incubated for 24 h at 37°C in 2% collagenase, 2% DNAse and 5% pronase, before being homogenized using an Ultra-Turrax T25 homogenizer (Janke&Kunkel, Staufen, Germany) and methanol:DMSO (4:1 vol/vol) was added. Plasma and tissue samples were centrifuged for 25 min at 14,000 rpm at 4°C. mTHPC concentrations in the supernatant were measured using a fluorescence spectrophotometer (Cary Eclipse, Agilent Technologies, Amstelveen, The Netherlands) with an excitation wavelength of 410 nm and emission measured between 550 nm and 700 nm.

Histopathologic analysis

7 days following PDT tumor-bearing kidneys were harvested and bisected along the long axis. Paraffin embedded tissue was cut in 5 µm sections and processed for H&E staining. Frozen tissue was mounted in TissueTec®, directly cut in 8 µm sections at the cutting surface

of each bisected kidney, and processed for nicotinamide adenine dinucleotide (NADH) diaphorase staining, which allows for a reliable assessment of tumor-kill.[17] Slides were analysed by an observer blinded to treatment status. The maximum diameter of the necrotic region was determined by photographing the H&E section from the central region of the lesion directly at the cutting surface of each bisected kidney, at magnifications of 0.8-1x using a light microscope with attached camera (Stemi 2000-C, Carl Zeiss, Sliedrecht, the Netherlands). The diameter was calculated using ImageJ software (National Institute of Health) by measuring the number of pixels representing the largest diameter of the ablated area and converting this number into mm.

mTHPC uptake and cytotoxicity of mTHPC-mediated PDT

To determine the uptake of mTHPC in various human cell lines, 300,000 cells were incubated for 24 h with 0.05 µg/mL mTHPC in a 24-wells plate. Hereafter, cells were harvested and single-cell suspensions were analyzed by FACS (FL3) (BD FACScalibur, BD Pharmingen, Breda, the Netherlands). To study the cytotoxicity of mTHPC-mediated PDT, cells were plated in a black 96-wells plate (ViewPlate-96, Perkin Elmer, Groningen, The Netherlands) at 80% confluence and allowed to adhere for 24 hours. After washing with PBS cells were incubated with medium containing 2% FCS and 0 (light-only control), 0.01, 0.05 and 0.1 µg/mL mTHPC. An additional control received neither mTHPC nor illumination. Cells were washed with PBS and each well was illuminated with a light dose of 1.0 J/cm^2 using a microlens optical fibre (Rare Earth Medicine Inc, West Yarmouth, USA) to provide a flat surface illumination with a fluence rate range of 0.56-3.28 W/cm^2 at an emission wavelength of 652 nm. The fiber output was measured using a LM150 head and fieldmaster power meter (Coherent, Auburn, USA). Twenty four hours after illumination cell survival was assessed using a 3-(4,5-dimethylthiazol-2-yl)-2,5-diphenyl tetrazolium bromide (MTT) assay as described previously.[18] The absorbance at 572 nm, indicative of cellular activity, was measured with a microplate reader (Cary Eclipse Microplate reader, Agilent Technologies, Amstelveen, the Netherlands).
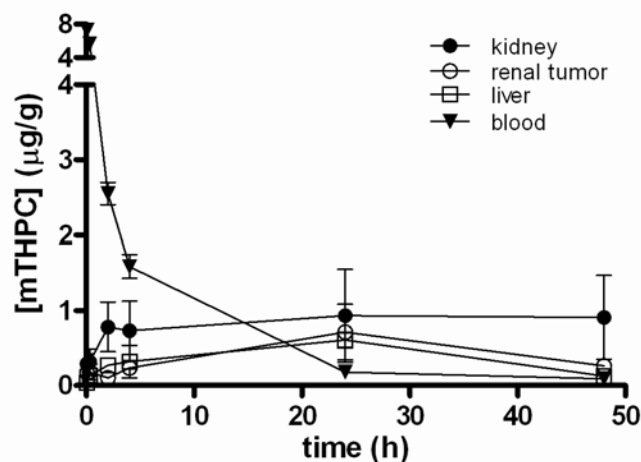
Statistical Analysis

Results were analyzed using ANOVA and Students' T test for parametric measures with the SPSS package version 15.0 for Windows (SPSS, Inc., Chicago, IL).

Results

mTHPC biodistribution

To determine the biodistribution of mTHPC over time, spectrophotometric analysis was performed. Blood mTHPC levels were high shortly following i.v. injection but decreased rapidly (fig. 2). After 4 hours levels had dropped to approximately a quarter. Simultaneously, mTHPC levels slowly increased in tumor tissue with maximal levels reached at 24 hours after administration. No selective accumulation in tumor tissue over normal renal tissue was observed.

Figure 2: Biodistribution of mTHPC in tumor-bearing mice (n=3-7/group) over time. Mice received an i.v. injection of 0.3 mg/kg mTHPC. 5 min. and 2, 4, 24 and 48 h later plasma, kidney, renal tumor and liver samples were harvested and processed for spectrophotometric analysis. Data is presented as the mean concentration of mTHPC (µg/mg) ± the standard deviation.

mTHPC-mediated PDT in the mouse model

To determine the anti-tumor effect of mTHPC-mediated PDT, tumor tissue was subjected to immunohistochemical analysis. The necrotic area was largest at a DLI of 4 h, with an average diameter of 7.9±1 mm (fig. 3A,B). The maximum diameter reached was 9.3 mm at the DLI of 4 h. At this time point tumor destruction within the illuminated region was complete, as determined using NADH staining (figure 3C). Both blood and tumor mTHPC levels were elevated at 4 h. Whenever only blood mTHPC levels (DLI: 5 min) or tissue mTHPC levels (DLI: 48 h) were high, clusters of viable tumor cells remained visible within the illuminated region (figure 3C) and the necrotic area was smaller. In all mice viable healthy renal tissue was present outside the illuminated tumor region, in line with the local nature of the treatment (figure 3B). No cell death was observed in mice that received mTHPC without illumination or illumination without mTHPC.

Figure 3: (A) Diameter of the necrotic surface area of renal tumors (n=4-7/group) 7 days after mTHPC-mediated PDT. The diameter was measured with ImageJ software using H&E stainings of renal tumors. Data is presented as the mean ± the standard deviation. *p<0.001 for drug-light intervals (DLIs) of 4 and 24 h compared to DLIs of 5 min. and 48 h. No cell death was observed in mice that received illumination without mTHPC (=ctrl). **(B)** H&E staining (0.8x) of renal tumor 1 week following PDT, showing a necrotic area (left) of the tumor and part of renal tissue. An area of viable renal tissue is visible on the right. **(C)** H&E and NADH staining (20x) of renal tumors 1 week following PDT showing viable cells, indicated by blue staining on NADH, within the ablated areas of DLI of 5 min and 48 h. Complete loss of viability, indicated by lack of staining, is present at DLIs of 4 h and 24 h. Inflammatory cells are present in all ablated regions.
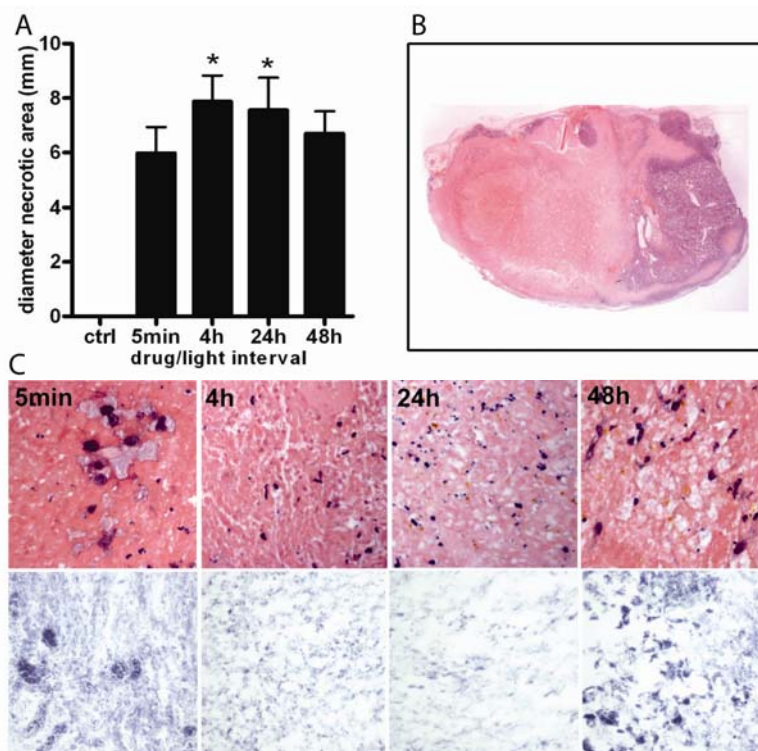

mTHPC uptake versus mTHPC-mediated PDT cytotoxicity in vitro

In vitro experiments were performed to determine whether mTHPC uptake and sensitivity to mTHPC-mediated PDT differ among RCC cell lines, endothelial cells and renal cells. 24 hours following *in vitro* administration, mTHPC concentration was significantly higher in endothelial cells than in all other cell types (p=0.0004) (fig. 4A). mTHPC uptake between different RCC cell lines varied. Importantly, mTHPC levels of renal parenchyma cells remained within the range of the RCC cells.

Endothelial cells were highly sensitive to mTHPC-mediated PDT. At all mTHPC concentrations used markedly more endothelial cells died than any other cell line (p<0.05 for 0.01 and 0.05 mg/mL at a fluence of 1.0 J/cm^2). For RCC cell lines there was a discrepancy between mTHPC uptake and sensitivity to PDT. While uptake levels varied between RCC cell lines and were sometimes higher than renal parenchyma cells, RCC cells were equally

or less sensitive to PDT than either renal or endothelial cells (fig 4B). However, when increasing mTHPC doses were administered, cell death did occur in all RCC cell lines. The dose at which >50% of all cells, including RCC cell lines, were killed was as low as 0.05 µg/mL at a light dose of 1.0 J/cm^2. In all control cell lines that did not receive mTHPC no FACS signal was visible.

Figure 4: (A) *In vitro* cellular concentration of mTHPC after a 24 h incubation with 0.05 µg/mL mTHPC. Data is presented as the mean fluoroscence intensity (3 samples/group) ± the standard deviation. **p=0.0004 for HMEC compared to all other cell lines studied here. **(B)** *In vitro* cytotoxicity of mTHPC-mediated PDT at a fluence of 1.0 J/cm^2 after a 24 h incubation of 0 (light-only control), 0.01, 0.05 and 0.10 µg/mL mTHPC. The control group (ctrl) consists of cells receiving neither mTHPC nor illumination. Data is presented as the mean percentage of surviving cells after 24 h (3 samples/group) ± the standard deviation. At all mTHPC concentrations endothelial cells showed more sensitivity to mTHPC-mediated PDT than renal and RCC cell lines (p<0.05 for 0.01 and 0.05 mg/mL). The dose at which >50% of all cells, including RCC cell lines, were killed was 0.05 µg/mL at a light dose of 1.0 J/cm^2.
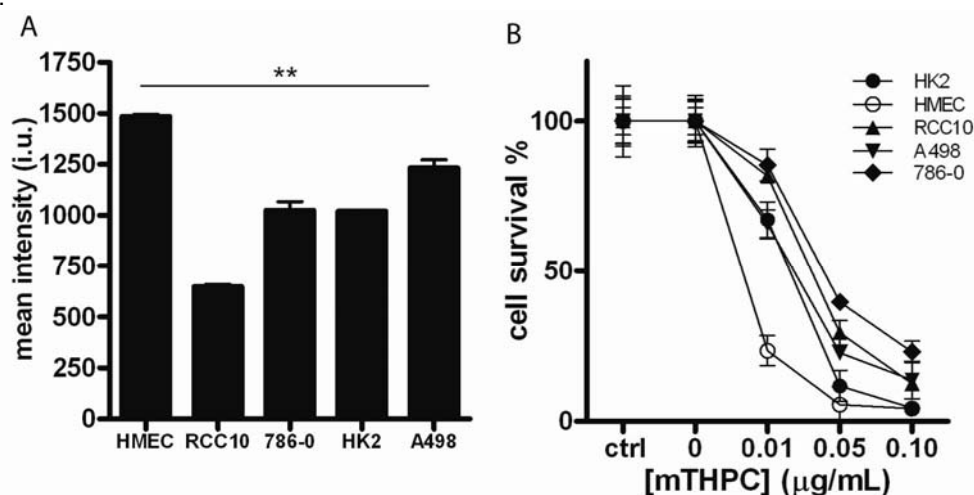
Discussion

This preclinical study was performed to evaluate the applicability of mTHPC-mediated PDT for nephron-sparing treatment of small renal masses. We determined whether mTHPC-mediated PDT induces renal tumor destruction and investigated sensitivity of human RCC and endothelial cells to mTHPC-mediated PDT. Here we showed that focal mTHPC-mediated PDT leads to renal tumor destruction. No cell viability was observed within the illuminated region at a DLI of 4 hours, while viable renal tissue remained visible outside this area. This is important for the further development of PDT as a nephron-sparing clinical treatment.

Conform to literature, the efficacy was optimal when both blood and tissue mTHPC concentrations were highest, suggesting that mTHPC-mediated PDT has both vascular and tissue targeted effects.[13, 16] The combination of vascular and tissue damage could be advantageous for treatment of small renal masses. Clear cell renal tumors are generally highly vascularised and would profit especially from mTHPC-mediated PDT. While papillary and chromophobe cell carcinoma are more frequently hypovascular[19], they could also be potential candidates because of the tissue-targeted effect of mTHPC. Research in PDT previously focussed on selective accumulation of photosensitizers in tumors, which can be observed in various tumor types at longer DLIs (>48 h). More recently, studies have shown that a high level of photosensitizer specifically in the tumor alone does not necessarily correlate with effective PDT.[13, 16, 20] The selective distribution of a photosensitizer between blood and tissues over time, which varies between different DLIs, may be more important for efficacy. We did not find tumor selective uptake or sensitivity to PDT of renal tumors. Instead, we observed an optimal antitumor effect at a short DLI when mTHPC levels were high both in blood and tumor. Further evidence that cellular uptake by tumor tissue is not the only factor determining PDT efficacy stems from our *in vitro* experiments. These showed that especially endothelial cells were sensitive to PDT compared to RCC cell lines and renal cells. Furthermore, there was a discrepancy between mTHPC uptake and sensitivity to mTHPC-mediated PDT in the RCC and renal cell lines. This may imply that RCC cells are intrinsically less sensitive to PDT than renal parenchyma or endothelial cells and that the PDT-induced tumor destruction is for a large part caused by vascular damage. The increased affinity of mTHPC for endothelial cells has also been described by others.[11, 13, 21] This observation is important for the clinical translation of mTHPC-mediated PDT of renal tumors. Since renal tumors often have a large vascular network and are highly perfused, mTHPC-mediated PDT for renal tumors might have to be performed at a notably shorter DLI compared to the currently existing treatment schemes for less perfused tumors.[22] For less perfused renal tumors the DLI might have to be longer. A DLI of 5 minutes was not as effective as 4 hours, suggesting that circulating mTHPC is not the primary target (unlike e.g. WST09). The DLI needs to be long enough for mTHPC to enter endothelial cells lining the blood vessels before a maximum PDT response is initiated.

For the translation to treatment of human renal tumors several aspects should be further investigated. An important drawback of photodynamic therapy is the skin photosensitivity. mTHPC has a photosensitivity period following administration.[23] While patients initially have to stay indoors the first 24 hours, most people will be completely back to their normal routine around day 20. Decreasing the dose and improving the preferential uptake (either by concentrating on systemic carrier platforms or on selective vascular application of mTHPC) could shorten this period.[24-26] Another consideration is the lesion size. In previous preclinical

studies in which either a vascular- or tissue based photosensitizer was administered to renal (tumor) tissue a maximum ablated region of respectively 10-14 mm and 3-4 mm was obtained.[14-15] Here an ablated region with a maximum diameter of 9.3 mm and absence of viable tissue within this region could be obtained. The mouse model used is the only reliable renal cell carcinoma model present. Orthotopic tumor models are preferred as the tumor host environment is important in determining the tumor response to PDT.[27-28] However, for a clinical translation to treatment of tumors up to 4 cm a porcine model study would be more favourable in terms of kidney size. The fact that no tumorspecificity to mTHPC-mediated PDT was observed in our study means that the calculation of the size of the illuminated area is of most importance to prevent positive margins. If a single fiber is not sufficient to achieve complete tumor kill, a grid as used for brachytherapy, with simultaneous intratumoral placement of multiple fibers, would enable treatment of larger renal tumors with PDT.[29] Furthermore, since uptake levels varied between RCC cell lines and it is also known from biliary tract carcinomas that uptake differs between phenotypes,[30] it is valuable to obtain further insight in variability in uptake between renal tumors.

Conclusions

In conclusion, we show that mTHPC-mediated PDT holds potential as a minimally invasive treatment option for small renal masses. Further pre-clinical studies are necessary before mTHPC-mediated PDT can become a valuable addition to current minimally invasive modalities in the treatment of small renal masses.

References

1. Autorino R, Haber GP, White MA, Stein RJ, Kaouk JH. New developments in renal focal therapy. J Endourol 2010;24:665-72.

2. Juarranz A, Jaen P, Sanz-Rodriguez F, Cuevas J, Gonzalez S. Photodynamic therapy of cancer. Basic principles and applications. Clin Transl Oncol 2008;10:148-54.

3. Chen B, Pogue BW, Hoopes PJ, Hasan T. Vascular and cellular targeting for photodynamic therapy. Crit Rev Eukaryot Gene Expr 2006;16:279-305.

4. Manyak MJ, Ogan K. Photodynamic therapy for refractory superficial bladder cancer: long-term clinical outcomes of single treatment using intravesical diffusion medium. J Endourol 2003;17:633-9.

5. O'Connor AE, Gallagher WM, Byrne AT. Porphyrin and nonporphyrin photosensitizers in oncology: preclinical and clinical advances in   photodynamic therapy. Photochem Photobiol 2009;85:1053-74.

6. Pinthus JH, Bogaards A, Weersink R, Wilson BC, Trachtenberg J. Photodynamic therapy for urological malignancies: past to current approaches. J Urol 2006;175:1201-7.

7. Arumainayagam N, Moore CM, Ahmed HU, Emberton M. Photodynamic therapy for focal ablation of the prostate. World J Urol 2010;28:571-6.

8. Lindner U, Trachtenberg J, Lawrentschuk N. Focal therapy in prostate cancer: modalities, findings and future considerations. Nat Rev Urol 2010;7:562-71.

9. Triesscheijn M, Baas P, Schellens JH, Stewart FA. Photodynamic therapy in oncology. Oncologist 2006;11:1034-44.

10. Moore CM, Nathan TR, Lees WR, et al. Photodynamic therapy using meso tetra hydroxy phenyl chlorin (mTHPC) in early prostate cancer. Lasers Surg   Med 2006;38:356-63.

11. Cramers P, Ruevekamp M, Oppelaar H, Dalesio O, Baas P, Stewart FA. Foscan uptake and tissue distribution in relation to photodynamic efficacy. Br J Cancer 2003;88:283-90.

12. Mitra S, Maugain E, Bolotine L, Guillemin F, Foster TH. Temporally and spatially heterogeneous distribution of mTHPC in a murine tumor observed by two-color confocal fluorescence imaging and spectroscopy in a whole-mount model. Photochem Photobiol 2005;81:1123-30.

13. Triesscheijn M, Ruevekamp M, Aalders M, Baas P, Stewart FA. Outcome of mTHPC mediated photodynamic therapy is primarily determined by the vascular response. Photochem Photobiol 2005;81:1161-7.

14. Pomer S, Grashev G, Sinn H, Kalble T, Staehler G. Laser-induced fluorescence diagnosis and photodynamic therapy of human renal cell carcinoma. Urol Int 1995;55:197-201.

15. Matin SF, Tinkey PT, Borne AT, Stephens LC, Sherz A, Swanson DA. A pilot trial of vascular targeted photodynamic therapy for renal tissue. J Urol 2008;180:338-42.

16. Chen B, Pogue BW, Hoopes PJ, Hasan T. Combining vascular and cellular targeting regimens enhances the efficacy of photodynamic therapy. Int J Radiat Oncol Biol Phys 2005;61:1216-26.

17. Marcovich R, Aldana JP, Morgenstern N, Jacobson AI, Smith AD, Lee BR. Optimal lesion assessment following acute radio frequency ablation of porcine kidney: cellular viability or histopathology? J Urol 2003;170:1370-4.

18. Berlanda J, Kiesslich T, Oberdanner CB, Obermair FJ, Krammer B, Plaetzer K. Characterization of apoptosis induced by photodynamic treatment with hypericin in A431 human epidermoid carcinoma cells. J Environ Pathol Toxicol Oncol 2006;25:173-88.

19. Onishi T, Oishi Y, Goto H, Yanada S, Abe K. Histological features of hypovascular or avascular renal cell carcinoma: the experience at four university hospitals. Int J Clin Oncol 2002;7:159-64.

20. Garrier J, Bressenot A, Grafe S, et al. Compartmental targeting for mTHPC-based photodynamic treatment in vivo: Correlation of efficiency, pharmacokinetics, and regional distribution of apoptosis. Int J Radiat Oncol Biol Phys 2010;78:563-71.

21. Ris HB, Li Q, Krueger T, et al. Photosensitizing effects of m-tetrahydroxyphenylchlorin on human tumor xenografts: correlation with sensitizer uptake, tumor doubling time and tumor histology. Int J Cancer 1998;76:872-4.

22. Tan IB, Dolivet G, Ceruse P, Poorten VV, Roest G, Rauschning W. Temoporfin-mediated photodynamic therapy in patients with advanced, incurable head and neck cancer: A multicenter study. Head Neck 2010.

23. Wagnieres G, Hadjur C, Grosjean P, et al. Clinical evaluation of the cutaneous phototoxicity of 5,10,15,20-tetra(m-hydroxyphenyl)chlorin. Photochem Photobiol 1998;68:382-7.

24. Betz CS, Rauschning W, Stranadko EP, et al. Optimization of treatment parameters for Foscan-PDT of basal cell carcinomas. Lasers Surg Med 2008;40:300-11.

25. Chen K, Wacker M, Hackbarth S, Ludwig C, Langer K, Roder B. Photophysical evaluation of mTHPC-loaded HSA nanoparticles as novel PDT deliverysystems. J Photochem Photobiol B 2010.

26. Gravier J, Schneider R, Frochot C, et al. Improvement of meta- tetra(hydroxyphenyl)chlorin-like photosensitizer selectivity with folate-based targeted delivery. synthesis and in vivo delivery studies. J Med Chem 2008;51:3867-77.

27. Fidler IJ, Kim SJ, Langley RR. The role of the organ microenvironment in the biology and therapy of cancer metastasis. J Cell Biochem 2007;101:927-36.

28. Chen B, Pogue BW, Zhou X, et al. Effect of tumor host microenvironment on photodynamic therapy in a rat prostate tumor model. Clin Cancer Res 2005;11:720-7.

29. Trachtenberg J, Bogaards A, Weersink RA, et al. Vascular targeted photodynamic therapy with palladium-bacteriopheophorbide photosensitizer for recurrent prostate cancer following definitive radiation therapy: assessment of safety and treatment response. J Urol 2007;178:1974-9; discussion 9.

30. Kiesslich T, Neureiter D, Alinger B, et al. Uptake and phototoxicity of meso-tetrahydroxyphenyl chlorine are highly variable in human biliary tract cancer cell lines and correlate with markers of differentiation and proliferation. Photochem Photobiol Sci 2010;9:734-43.

Chapter 11: Key findings and future perspectives

In recent years there has been a shift to a higher incidence of small renal masses (SRM, <4cm) compared to more advanced tumors. These SRMs currently account for 48-66% of all diagnosed Renal Cell Carcinomas (RCCs).[1] Conversely, the incidence of more advances stages of RCC has slightly declined.[2] Overall, 20% of RCC patients will present with synchronous metastases, and a further 25% with metachronous metastases within 5 years after treatment with curative intent.[2-3] The likelihood of metastatic development for patients with SRMs is much lower compared to RCCs of more advanced stages, as 4.2-7.0% presents with synchronous metastases and only 1-8.4% will be diagnosed with metastases within 10 years of follow-up.[4-6] Despite the low frequency of metastatic progression, there are certain specific challenges concerning treatment for SRMs.

When a SRM is detected upon imaging, current challenges involve distinguishing malignant from benign tumors and determining the appropriate treatment of patients with malignant masses. Of all SRMs approximately 80% is malignant and 20% benign.[7] Because there are no specific features on imaging that can conclusively classify a SRM as malignant or benign[8-9], it is most likely that preoperative renal mass biopsy (RMB) will play an increasingly significant role in the near future. RMB can be performed under CT, MRI or ultrasound guidance and has a diagnostic accuracy of over 90%.[10] Complications of RMB are limited and there is a negligible risk of tumor seeding of the needle track. The current challenge is dealing with the higher false negative rates for RMB of SRMs compared to larger renal tumors.[11] Especially masses smaller than 3 cm are difficult to biopsy due to the movement of the kidney during breathing.[12-13] In **Chapter 4** we therefore studied the use of real-time 3D fluoroscopy guided large core RMB. The advantage of this technique is the combination of 3D soft tissue imaging and real-time imaging as well as improved accessibility of the intervention site. Our key finding was that -despite the expected advantages- the diagnostic accuracy was limited for tumors smaller than 2.5 cm. An explanation for this might be that although the presented technique included real-time visualisation of the needle-placement, the planned needle path is based on static images. When the kidney moves during breathing, the planned needle path may therefore not reach the tumor at the time of biopsy. Anticipation to motion artefacts in the form of general anaesthesia may help, however it would compromise the minimally invasive nature of the procedure.

Next to distinguishing benign from malignant lesions, preoperative RMB will be important in the future for two other reasons. One is that minimally invasive procedures such as radiofrequency ablation (RFA) and cryoablation (CA) are increasingly used as treatment for SRMs in patients who are not eligible for surgery.[14] Because the tumor remains in situ, RMB

is necessary to preoperatively determine the histology by RMB. The second reason is that many diagnostic and prognostic tissue markers are being discovered. With these markers we are able to determine the prognosis of the patient and possibly the response to medical treatment. This means that following RMB clinical management decisions can be made, which will give RMB an important clinical value in the future. However, before RMB will have gained a definite place in the diagnostic management of SRMs, the diagnostic accurary of SRMs should be further improved.

Chapter 2 reviews all diagnostic tissue markers that are differentially expressed between the RCC subtypes clear cell RCC (ccRCC) and/or papillary RCC (pRCC), and may be of diagnostic use. In addition, markers with prognostic value for ccRCC and/or pRCC were described and their clinical values were discussed. Key findings were that so far 5 validated diagnostic markers (AMACR, CK7, CK8, CK19, p53) are present that differentiate between ccRCC and pRCC. Few independent prognostic markers have been identified for pRCC in single studies, compared to an abundance of biomarkers identified for ccRCC. In **Chapter 3** we highlight the prognostic value of one specific tissue marker for ccRCC. This marker (Factor Inhibiting HIF (FIH)) plays an important role in the cellular response to hypoxia. We showed that low expression of FIH correlates to a worse survival. FIH could therefore be of clinical value in determining the prognosis of ccRCC patients following surgical resection of the primary tumor. Despite the existence of many promising markers for ccRCC, their exact role in clinical decision making still needs to be determined. One future direction of prognostic tissue markers is to integrate several markers in existing prognostic nomograms.[15] Prognostic nomograms consist of information that can be easily obtained, such as patient characteristics and histology reports. However, they provide limited information to the biological characteristics (eg. aggressiveness) of the tumor.[16] The addition of prognostic tissue markers could be of high clinical value. Alternatively, several markers can be combined in multimarker models.[17]

Current challenges of clinical use of tissue markers are multiple. For one, despite the large number of prognostic markers, it is not known which ones are of highest clinical value. Next to this, many marker studies have been performed when immunotherapy was the first line of treatment for metastatic RCC. The correlation with survival and tissue marker expression is therefore currently not certain, since treatment now consists of targeted therapy with tyrosine kinase inhibitors. This is also a major flaw for developed diagnostic markers. For the future value of prognostic and diagnostic markers, multicenter prospective studies are therefore needed to determine which tissue markers have the best prognostic value, and a prognostic model with these markers needs to be developed.

Following the discovery of a SRM, a clinical management plan has to be made. SRMs are most frequently found in patients who are at surgical risk due to advanced age, comorbidities, solitary kidneys or patients who are prone to develop multiple renal tumors as a result of hereditary diseases such as von Hippel-Lindau syndrome.[18] It has been shown that not every patient will benefit from surgical resection of the tumor, and that many factors compete with RCC in relation to patient survival and health.[19-21] For example, advanced age competes with SRMs in survival of elderly patients.[19] Because of this, it is increasingly important to determine which RCC patients are eligible for, and will benefit from, surgical treatment.[21] In the preoperative assessment various factors are important for surgical outcome and prognosis. Besides tumor characteristics (such as stage and grade) these include patient physical status and comorbidities.[20, 22-24] Although comorbidity is taken into account when deciding who is fit for surgery, it had not been objectively validated whether comorbidities actually affect complication rates following nephrectomy using a standardized complication grading system. In **Chapter 5** we investigated the effect of comorbidities on complications following surgical treatment of RCC. We applied the modified Clavien Classification of Surgical Complications (CCSC), which is a standardized classification system for postoperative complications, together with the Charlson comorbidity index.[25-26] The key finding is that major complications occur significantly more often when major comorbidities are present. This shows that comorbidity scores can be used in risk stratification for complications. A future perspective is that comorbidities should be considered, along with other factors as age, during decision-making and counselling of patients before nephrectomy. Furthermore, this study could be repeated for patients with metastatic disease undergoing cytoreductive nephrectomy.

When a malignant SRM has been found in a patient for whom surgical resection is considered inappropriate, other minimally invasive treatments are available. At present, minimally invasive techniques most commonly applied for treatment of small renal tumors are cryoablation (CA) and radiofrequency ablation (RFA). Despite the promising results of these techniques in treatment of SRMs, the clinic is presented with their respective limitations. Local recurrences following both techniques continue to be a problem, particularly in larger tumors. As a consequence, multiple sessions are often necessary.[27] These recurrences appear more frequently compared to partial nephrectomy (PN). **Chapter 7** investigated factors that could affect these higher recurrence rates. Key findings were that incomplete CA and RFA results in an increased proliferation and decreased apoptosis of residual renal tumour cells. Furthermore, we found evidence that the observed hyperproliferation may be caused by stimulatory factors such as hypoxia, HSPs and inflammatory cells. Hyperproliferation of residual tumor cells could facilitate recurrences of renal tumours after

thermal ablation. Based on these observations, it might be recommended to use RFA for smaller lesions or employ larger safety margins around the tumour, although further testing would be required to examine whether the hyperproliferation also occurs in the clinical setting. Even though it is technically easier to perform multiple consecutive RFA procedures compared to CA,[27] our results stress the importance of complete ablation. Our study implies that thermal ablation will remain a beneficial treatment for patients that are surgically unfit. However, whenever possible PN remains the procedure of choice since it induces limited cellular proliferation, it is likely to cause the most complete tumour resection and has the best clinical results.

In the search for an optimal minimally invasive treatment for SRMs, other treatment approaches are being developed.[28] In **Chapter 9** we examined intratumoral administration of holmium-166 acetylacetonate microspheres ([166]HoAcAcMS) as a new treatment for SRMs, using a mouse model. Historically, external beam radiotherapy, another locoregional ablation technique, has not been effective against RCC due to breathing-related movement of the kidneys and the radiosensitivity of adjacent tissue. In contrast to external beam radiation, local administration of radioactive sources is not as limited by the radiosensitivity of the healthy tissue due to selective deposition of radioactivity in the tumor.[29] A key finding consisted of the observation that small amounts of [166]HoAcAcMS were sufficient for a strong anti-tumor effect and simultaneously permit multimodality imaging with CT, SPECT and MRI. These imaging opportunities could lead to an improved intraprocedural therapy evaluation and follow-up and provide a fundamental advantage over existing local therapies such as RFA, where therapy evaluation remains challenging. In **Chapter 10** another minimally invasive treatment option was evaluated. In this translational study renal tumors in mice were locally treated with meso-tetra-hydroxyphenyl-chlorin (mTHPC)-mediated photodynamic therapy (PDT). This technique is regularly applied to patients with superficial skin cancers and head-and neck cancer. With the development of cylindrical lasers and new photosensitizers that allow an increased tissue penetration, the use of PDT can now be extended to treatment of solid tumors.[30] A key finding consisted of the observation that PDT induced necrotic lesions large enough for translation to clinical treatment, and that the effect was most optimal when mTHPC was both present in the blood and tissue. As mTHPC-mediated PDT did not appear to selectively target tumor tissue, and skin photosensitivity remains a problem, a future direction could include the development of mTHPC carriers that solely reach the SRMs. Both techniques are promising new options for minimally invasive treatment of SRMs. However, further clinical studies are necessary to determine their optimal settings and specific clinical value.

As previously described, 25% of RCC patients will develop metastases following initial surgical treatment of the primary tumor with a curative approach. Once metastasized, the only option is palliative treatment. Presently available first line therapy does not prolong survival.[31] The development of treatments that can prevent the formation of metastases and decrease the presence of established metastases is therefore highly important. We postulate that RFA, a therapy currently only used for treatment of SRMs could play a major role in this field of research. **Chapter 8** describes a translational study that determined the effect of RFA of the primary tumor combined with systemic Interleukin-2 (IL-2) therapy on lung metastases. Key findings were that RFA combined with IL-2 induced a tumorspecific immune response that could prevent the formation of metastases and decreased the number of established lung metastases. This antitumor effect was led by cytotoxic T cells and natural killer cells. The future directions of treatment for metastatic RCC (mRCC) may lie in new developments of immunotherapy. In modern research, the search to various ways of inducing a tumorspecific immune response continues.[32] As RFA is capable of inducing such an immune response, its use might be extended to treatment of mRCC patients. Because there is evidence that the antitumor effect of RFA as monotherapy is not strong enough for a clinical response, additional immunostimulatory agents are needed.[33] The systemic IL-2 therapy used in our study proved to be effective, however, in patients this therapy is associated with a high toxicity. It was recently discovered that tyrosine kinase inhibitors have immunoregulatory properties.[34] A future direction of RFA as immunotherapeutic would be combining RFA with these inhibitors. This way a more efficient and practical method can be developed that induces a strong antitumor immune response against RCC.

References

1. Nguyen MM, Gill IS, Ellison LM. The evolving presentation of renal carcinoma in the United States: trends from the Surveillance, Epidemiology, and End Results program. J Urol 2006;176:2397-400; discussion 400.

2. Sun M, Thuret R, Abdollah F, et al. Age-adjusted incidence, mortality, and survival rates of stage-specific renal cell carcinoma in North America: a trend analysis. Eur Urol 2011;59:135-41.

3. Leibovich BC, Han KR, Bui MH, et al. Scoring algorithm to predict survival after nephrectomy and immunotherapy in patients with metastatic renal cell carcinoma: a stratification tool for prospective clinical trials. Cancer 2003;98:2566-75.

4. Lughezzani G, Jeldres C, Isbarn H, et al. Tumor size is a determinant of the rate of stage T1 renal cell cancer synchronous metastasis. J Urol 2009;182:1287-93.

5. Chawla SN, Crispen PL, Hanlon AL, Greenberg RE, Chen DY, Uzzo RG. The natural history of observed enhancing renal masses: meta-analysis and review of the world literature. J Urol 2006;175:425-31.

6. Klatte T, Patard JJ, de Martino M, et al. Tumor size does not predict risk of metastatic disease or prognosis of small renal cell carcinomas. J Urol 2008;179:1719-26.

7. Frank I, Blute ML, Cheville JC, Lohse CM, Weaver AL, Zincke H. Solid renal tumors: an analysis of pathological features related to tumor size. J Urol 2003;170:2217-20.

8. Bosniak MA, Rofsky NM. Problems in the detection and characterization of small renal masses. Radiology 1996;200:286-7.

9. Millet I, Doyon FC, Hoa D, et al. Characterization of small solid renal lesions: can benign and malignant tumors be differentiated with CT? AJR Am J Roentgenol 2011;197:887-96.

10. Laguna MP, Kummerlin I, Rioja J, de la Rosette JJ. Biopsy of a renal mass: where are we now? Curr Opin Urol 2009;19:447-53.

11. Rybicki FJ, Shu KM, Cibas ES, Fielding JR, vanSonnenberg E, Silverman SG. Percutaneous biopsy of renal masses: sensitivity and negative predictive value stratified by clinical setting and size of masses. AJR Am J Roentgenol 2003;180:1281-7.

12. Lechevallier E, Andre M, Barriol D, et al. Fine-needle percutaneous biopsy of renal masses with helical CT guidance. Radiology 2000;216:506-10.

13. Wang R, Wolf JS, Jr., Wood DP, Jr., Higgins EJ, Hafez KS. Accuracy of percutaneous core biopsy in management of small renal masses. Urology 2009;73:586-90; discussion 90-1.

14. Ljungberg B, Cowan NC, Hanbury DC, et al. EAU guidelines on renal cell carcinoma: the 2010 update. Eur Urol 2010;58:398-406.

15. Klatte T, Seligson DB, LaRochelle J, et al. Molecular signatures of localized clear cell renal cell carcinoma to predict disease-free survival after nephrectomy. Cancer Epidemiol Biomarkers Prev 2009;18:894-900.

16. Ficarra V, Brunelli M, Cheng L, et al. Prognostic and therapeutic impact of the histopathologic definition of parenchymal epithelial renal tumors. Eur Urol 2010;58:655-68.

17. Parker AS, Leibovich BC, Lohse CM, et al. Development and evaluation of BioScore: a biomarker panel to enhance prognostic algorithms for clear cell renal cell carcinoma. Cancer 2009;115:2092-103.

18. Hollingsworth JM, Miller DC, Daignault S, Hollenbeck BK. Rising incidence of small renal masses: a need to reassess treatment effect. J Natl Cancer Inst 2006;98:1331-4.

19. Kutikov A, Egleston BL, Wong YN, Uzzo RG. Evaluating overall survival and competing risks of death in patients with localized renal cell carcinoma using a comprehensive nomogram. J Clin Oncol 2010;28:311-7.

20. Santos Arrontes D, Fernandez Acenero MJ, Garcia Gonzalez JI, Martin Munoz M, Paniagua Andres P. Survival analysis of clear cell renal carcinoma according to the Charlson comorbidity index. J Urol 2008;179:857-61.

21. Lane BR, Abouassaly R, Gao T, et al. Active treatment of localized renal tumors may not impact overall survival in patients aged 75 years or older. Cancer 2010;116:3119-26.

22. Bensalah K, Pantuck AJ, Crepel M, et al. Prognostic variables to predict cancer-related death in incidental renal tumours. BJU Int 2008;102:1376-80.

23. de Cassio Zequi S, de Campos EC, Guimaraes GC, Bachega W, Jr., da Fonseca FP, Lopes A. The use of the American Society of Anesthesiology Classification as a prognostic factor in patients with renal cell carcinoma. Urol Int 2010;84:67-72.

24. Heng DY, Xie W, Regan MM, et al. Prognostic factors for overall survival in patients with metastatic renal cell carcinoma treated with vascular endothelial growth factor-targeted agents: results from a large, multicenter study. J Clin Oncol 2009;27:5794-9.

25. Charlson ME, Pompei P, Ales KL, MacKenzie CR. A new method of classifying prognostic comorbidity in longitudinal studies: development and validation. J Chronic Dis 1987;40:373-83.

26. Clavien PA, Barkun J, de Oliveira ML, et al. The Clavien-Dindo classification of surgical complications: five-year experience. Ann Surg 2009;250:187-96.

27. Kunkle DA, Uzzo RG. Cryoablation or radiofrequency ablation of the small renal mass : a meta-analysis. Cancer 2008;113:2671-80.

28. Ritchie RW, Leslie T, Phillips R, et al. Extracorporeal high intensity focused ultrasound for renal tumours: a 3-year follow-up. BJU Int 2010;106:1004-9.

29. Kerkhof EM, Raaymakers BW, van Vulpen M, et al. A new concept for non-invasive renal tumour ablation using real-time MRI-guided radiation therapy. BJU Int 2011;107:63-8.

30. Pinthus JH, Bogaards A, Weersink R, Wilson BC, Trachtenberg J. Photodynamic therapy for urological malignancies: past to current approaches. J Urol 2006;175:1201-7.

31. Coppin C, Kollmannsberger C, Le L, Porzsolt F, Wilt TJ. Targeted therapy for advanced renal cell cancer (RCC): a Cochrane systematic review of published randomised trials. BJU Int 2011;108:1556-63.

32. Van Poppel H, Joniau S, Van Gool SW. Vaccine therapy in patients with renal cell carcinoma. Eur Urol 2009;55:1333-42.

33. den Brok MH, Sutmuller RP, van der Voort R, et al. In situ tumor ablation creates an antigen source for the generation of antitumor immunity. Cancer Res 2004;64:4024-9.

34. Finke JH, Rini B, Ireland J, et al. Sunitinib reverses type-1 immune suppression and decreases T-regulatory cells in renal cell carcinoma patients. Clin Cancer Res 2008;14:6674-82.

Chapter 12: Dutch Summary - Nederlandse Samenvatting

Wereldwijd is het niercelcarcinoom (RCC) met 200.000 nieuwe gevallen per jaar en een sterfte van 102.000 patiënten per jaar de meest voorkomende vorm van nierkanker. Ongeveer 20% van de RCC patiënten heeft uitzaaiingen op het moment van diagnose; een verdere 25% zal uitzaaiingen ontwikkelen na een eerdere behandeling. RCC patiënten met uitzaaiingen hebben een zeer slechte prognose; na 5 jaar leeft nog ongeveer 10%.

In de afgelopen decennia zijn er veranderingen opgetreden op het gebied van RCC. Incidenteel gevonden kleine niertumoren (<4cm) worden toenemend gediagnostiseerd en maken op dit moment 50-60% van alle ontdekte niertumoren uit. Deze tumoren zijn meestal niet agressief en zaaien zelden uit. Ze worden vooral gediagnostiseerd bij ouderen. Doordat deze patiënten vaak comorbiditeiten hebben is chirurgische behandeling niet altijd mogelijk. Ondanks de verschuiving in diagnose naar kleinere niertumoren lijkt het wereldwijde mortaliteitspercentage voor RCC niet af te nemen. Verbeteringen op het gebied van diagnose, behandeling en de voorspelling van de prognose van RCC zijn daarom van groot belang.

In **Deel 1** gaat dit proefschrift in op de nieuwe mogelijkheden wat betreft de diagnostiek en prognostische voorspelling van RCC. Hierbij wordt ingegaan op de rol van preoperatieve diagnostische nierbiopten en het gebruik van diagnostische en prognostische weefselmarkers voor RCC. **Deel 2** behandelt ontwikkelingen in minimaal invasieve therapieën voor het RCC. Hierbij wordt beschreven wat het effect van bestaande technieken als cryoablatie (CA) en radiofrequente ablatie (RFA) op weefselniveau is, en hoe RFA van nut zou kunnen zijn in de ontwikkeling van immunotherapie voor RCC. Daarnaast wordt ingegaan op nieuwe ontwikkelingen voor minimaal invasieve behandeling van het RCC.

Prognostische en diagnostische weefselmarkers voor RCC

Het niercelcarcinoom kan worden onderverdeeld in verschillende subtypen. Hoewel deze typen onder dezelfde groep vallen reageren ze verschillend op behandelingen en bestaan er verschillen in overlevingskansen. In het tumorweefsel zijn markers aanwezig waarmee een indicatie voor de prognose kan worden bepaald, de zogenaamde prognostische weefselmarkers. Hiernaast is het onderscheid in de verschillende subtypen niet altijd goed te bepalen, diagnostische weefselmarkers zijn hierbij waardevol. De meest voorkomende typen RCC zijn het heldercellige RCC (ccRCC, 80%) en het papillaire RCC (pRCC, 11%). **Hoofdstuk 2** geeft een overzicht van alle diagnostische weefselmarkers die een onderscheid kunnen maken tussen ccRCC en pRCC, en van de tot op heden beschreven prognostische weefselmarkers. Hoewel er verscheidene weefselmarkers aanwezig zijn worden ze op dit moment nog niet gebruikt in de kliniek. Redenen hiervoor worden in dit hoofdstuk

beschreven. **Hoofdstuk 3** gaat in op de prognostische waarde van de weefselmarker 'factor inhibiting Hif' (FIH). Deze marker speelt een belangrijke rol in de hypoxia pathway, een onderdeel dat vaak is aangedaan bij het RCC. In dit hoofdstuk komt naar voren dat patiënten welke een tumor hebben met een lage expressie van FIH, een slechtere overleving hebben.

De rol van nierbiopten in diagnostiek van het RCC

Gangbare beeldvormende technieken voor de diagnostiek van RCC zijn contrast-CT, echo en MRI. Beeldvorming alleen blijkt niet altijd in staat onderscheid te maken tussen goedaardige en kwaadaardige tumoren. Ongeveer 20% van de met behulp van deze technieken gevonden verdachte tumoren blijken goedaardig te zijn bij histologische analyse na resectie. Preoperatieve nierbiopten spelen daarom een steeds belangrijkere rol. Naast het feit dat goedaardige tumoren kunnen worden uitgesloten van onnodige behandeling kan het RCC subtype worden bepaald. Hiermee kan een indicatie over de prognose en eventuele respons op therapie worden gegeven. Nierbiopten worden voornamelijk genomen onder echo of CT geleiding. Omdat de nier beweegt tijdens de ademhaling raakt vooral bij de kleine niertumoren de biopsienaald niet altijd de tumor. De huidige beeldvorming-geleide nierbiopten geven daarom niet altijd een accurate diagnose. In **Hoofdstuk 4** wordt een nieuwe 3D beeldvorming-geleide biopsie-techniek beschreven die een verbetering zou kunnen geven in de nauwkeurigheid van de diagnose. Bij deze techniek wordt van te voren het traject van de biopsienaald bepaald, en wordt de naald onder real-time beeldvorming geplaatst, waardoor de kans op een succesvolle biopsie mogelijk toeneemt. Hoewel deze techniek een goed resultaat gaf voor grotere niertumoren, bleek dat de nauwkeurigheid bij tumoren kleiner dan 2.5cm afnam. Ook deze techniek zal daarom verder geoptimaliseerd moeten worden voor biopten van kleine niertumoren.

De impact van comorbiditeiten op postoperatieve complicaties bij RCC

RCC wordt tegenwoordig bovenal gediagnostiseerd in een oudere populatie patiënten die zeer vaak meerdere en soms ook ernstige comorbiditeiten hebben. Het chirurgisch verwijderen van de tumor is hierdoor niet altijd mogelijk, of gewenst. Omdat kleine niertumoren meestal niet agressief zijn, zelden uitzaaien, en er risico's aan een operatie verbonden zijn is uit de literatuur gebleken dat de overleving van patiënten soms beter is als ze niet geopereerd worden. Het is daarom van belang preoperatief te bepalen hoeveel winst de patiënt zal behalen met een operatie. **Hoofdstuk 5** behandelt de impact van comorbiditeit op het ontwikkelen van complicaties na chirurgische behandeling van RCC. Het blijkt dat patiënten met ernstige comorbiditeit een hoger risico hebben op ernstige postoperatieve complicaties. Bij de preoperatieve winstbepaling voor de patiënt is comorbiditeit daarom een belangrijke factor die moet worden meegenomen.

De behandeling van kleine niertumoren

Historisch gezien is radicale nefrectomie de gouden standaard voor behandeling van RCC. Voor kleine niertumoren is de laatste jaren een grote variëteit aan behandelingsmogelijkheden ontstaan. Een deel van de patiënten waarbij een kleine niertumor wordt ontdekt zijn geen kandidaat voor chirurgische behandeling, en zeker niet voor radicale nefrectomie. Redenen hiervoor kunnen zijn dat de patiënt een zeer hoge leeftijd, comorbiditeiten of een mononier heeft. Verder kan de patiënt erfelijke ziekten, zoals de ziekte van Von Hippel-Lindau, hebben. Bij deze ziekte is de kans op meerdere niertumoren groot. Zoals eerder beschreven zijn kleine niertumoren meestal niet agressief en zaaien zelden uit. Het blijkt dat patiënten met vergevorderde leeftijd eerder zullen overlijden aan ouderdom dan aan hun niertumor. Voor patiënten met een kleine niertumor waar chirurgische behandelmogelijkheden beperkt zijn en de levensverwachting laag, is daarom het actief volgen van de tumor een klinisch geaccepteerde mogelijkheid. Wanneer mogelijk zal in deze gevallen eerste een nierbiopt worden genomen om te bepalen om welk type RCC het gaat. Hierna zal de tumorgroei regelmatig worden gevolgd door middel van beeldvorming.

Voor patiënten met een kleine niertumor bij wie chirurgie wel mogelijk is, is een niersparende behandeling de eerste keus. Partiële nefrectomie (PN) is hierbij de standaardbehandeling. Het is aangetoond dat PN dezelfde kanker-specifieke overleving geeft als radicale nefrectomie, en dat hiernaast de nierfunctie wordt gespaard. PN kan worden toegepast met een open, kijkbuis- (laparoscopisch) of robotbenadering. Een belangrijke nieuwe ontwikkeling in niersparende technieken zijn minimaal invasieve therapieën. De meest gebruikte methoden zijn CA en RFA. Deze technieken bevriezen dan wel verhitten de tumor plaatselijk, en kunnen door middel van speciale naalden via de huid (percutaan) of laparoscopisch worden toegepast. Bij RFA wordt via een naald die in de tumor wordt geplaatst een wisselstroom teweeg gebracht. Deze wisselstroom laat de ionen in een tumorcel zo snel trillen dat frictiehitte wordt ontwikkeld. De hoge lokale temperaturen (tussen de 50 en 100°C) die hierbij ontstaan, zorgen ervoor dat de tumorcellen in een gebied rondom de naald sterven. CA veroorzaakt tumorceldood door de tumor lokaal via een naald afwisselend te bevriezen en te ontdooien (<20°C). Sinds de eerste toepassing voor niertumoren van CA in 1995 en RFA in 1997, is het gebruik toegenomen. De eerste lange-termijn resultaten zijn veelbelovend, maar laten ook verbeterpunten zien. Zo zijn de recidiefkansen na CA en RFA aanzienlijk hoger dan na PN. Na eerste behandeling met CA krijgt gemiddeld 1,7-22% een recidief, na RFA 3,2-13% en na PN 0-3,2%. Patiënten die deze behandelingen ondergaan verschillen enigszins van elkaar wat betreft leeftijd en tumorgrootte; patiënten die CA of RFA ondergaan zijn vaak ouder en hebben een kleinere

niertumor. Ook de benadering speelt wellicht een rol in de verschillen in recidief, aangezien RFA meestal percutaan wordt toegepast en CA laparoscopisch, hoewel studies elkaar tegenspreken met betrekking tot het effect van de benadering op de recidiefkans. Ondanks dat deze verschillen een vergelijking bemoeilijken blijkt uit verschillende meta-analyses dat de recidiefkans na CA en RFA significant hoger is dan na PN. Een oorzaak hiervoor kan worden gezocht in stimulatie van tumorgroei door hitte dan wel kou. **Hoofdstuk 7** behandelt de invloed van CA en RFA op de omgevingsfactoren van de tumor. Eerdere studies hebben aangetoond dat resterende tumorcellen na deze behandelingen zich agressiever kunnen gedragen. In de studie beschreven in dit hoofdstuk werd het effect van incomplete CA en RFA op tumorgroei vergeleken met PN in muizen met niertumoren. Inderdaad werd er een toegenomen celgroei en verminderde celdood van overlevende tumorcellen gezien aan de rand van het behandelde gebied. Van invloed bleek een lokaal laag zuurstofgehalte rondom het behandelde gebied. Verder ontstond er een lokale expressie van factoren, zoals eiwitten die een rol spelen in de afweer en 'heat shock proteins', die celgroei en overleving kunnen stimuleren. Hiernaast trad er een invasie van afweercellen op, wat ook van invloed kunnen zijn op de celgroei. De studie in dit hoofdstuk laat zien dat het van belang is de niertumor zo compleet mogelijk te behandelen, en dat de aanwezigheid van deze groeistimulerende factoren moet worden meegenomen in de ontwikkeling van verbeterde behandelingen met CA en RFA.

Immunotherapie als behandeling voor RCC met uitzaaiingen
De behandeling van uitgezaaide RCC (mRCC) bestaat uit 'targeted therapy' bestaande uit tyrosine kinase of mTOR-inhibitors. Deze medicatie gaat de tumorgroei tegen en vermindert de groei van bloedvaten rond de tumor. Hoewel dit de groei van de uitzaaiingen tijdelijk tegen gaat, treedt er na 6 tot 15 maanden resistentie op en verlengt het de overleving niet. Nieuwe behandelstrategieën voor mRCC zijn daarom van groot belang. Vóór het gebruik van targeted therapies was immunotherapie de behandeling van eerste keus. De meest gebruikte middelen waren interleukine-2 (IL-2) en interferon alfa (IFN-α). Hoewel deze ernstige bijwerkingen gaven verdwenen de uitzaaiingen in ongeveer 10% van alle behandelde patiënten. Nieuwe immunotherapeutische benaderingen zijn daarom een interessante ontwikkeling in de behandeling van mRCC. Het doel van immunotherapie is het stimuleren van het afweersysteem zodat het alleen de tumorcellen herkent en vernietigt. Verschillende benaderingen worden op dit moment getest, waarbij vernietigd tumorweefsel zoals bijvoorbeeld door CA of RFA, de beste manier blijkt om het afweersysteem te stimuleren. Dit heeft hetzelfde effect als een vaccinatie, waarbij een afweerreactie optreedt tegen de resten van de dode tumorcellen terwijl de patiënt niet ziek wordt. Het afweersysteem speelt een belangrijke rol bij de groei van een tumor. RFA en CA verstoren

de balans in het lichaam die aanwezig is tussen tumortolerantie en tumorafweer, waardoor een tumor zowel kan worden aangezet tot groei (als beschreven in **Hoofdstuk 7**) of vernietiging. Het is gebleken dat alleen CA of RFA niet in staat zijn een afweerreactie op te wekken die sterk genoeg is om tumorvernietiging volledig tegen te gaan. Hiervoor dient de behandeling met CA of RFA te worden gecombineerd met afweerstimulerende middelen. **Hoofdstuk 8** beschrijft de resultaten van een translationele studie waarin muizen met een niertumor werden behandeld met RFA gecombineerd met IL-2. IL-2 stimuleert het afweersysteem waardoor de combinatie met RFA de balans in het lichaam naar tumorvernietiging kan omzetten. Het bleek dat muizen met deze behandeling significant minder longuitzaaiingen hadden en dat de uitzaaiingen die overbleven kleiner waren. Deze studie is een eerste stap in de richting van een nieuwe behandeling voor mRCC waarbij RFA wordt gecombineerd met afweerstimulerende medicatie.

^{166}HoAcAcMS als nieuwe minimaal invasieve therapie voor RCC

Door de frequente diagnose van kleine niertumoren in oudere patiënten met comorbiditeiten zijn minimaal invasieve therapieën voor kleine niertumoren in volle ontwikkeling. Naast RFA en CA wordt onderzocht of lokale bestraling van de niertumor een effectieve behandeling kan zijn. Historisch gezien was het niet mogelijk niertumoren te bestralen omdat door de beweging van de nier tijdens het ademen er teveel schade aan omliggend gezond weefsel zou ontstaan. **Hoofdstuk 9** beschrijft een nieuwe techniek om de tumor lokaal te bestralen. In dit hoofdstuk worden de resultaten gepresenteerd van een studie naar de effectiviteit van radioactieve bolletjes (holmium-166 acetylacetonate microsferen (^{166}HoAcAcMS)) welke direct in de niertumor worden geïnjecteerd. Als diermodel werd een muis met een niertumor gebruikt. Het bleek dat ^{166}HoAcAcMS adequaat de tumorvorming tegenging. Naast de effectiviteit werden de multimodale beeldvormings-eigenschappen van ^{166}HoAcAcMS onderzocht door SPECT, CT en MRI uit te voeren in speciale proefdierscanners. Hierbij werd aangetoond dat ^{166}HoAcAcMS zichtbaar is met alle drie de beeldvormende technieken en dat bovendien de hoeveelheid aanwezige straling kon worden gekwantificeerd. Deze resultaten tonen de eerste stap in de ontwikkeling van intratumorale injectie van ^{166}HoAcAcMS als mogelijke behandeling van kleine niertumoren.

Fotodynamische therapie als nieuwe minimaal invasieve therapie voor RCC

Een andere minimaal invasieve therapie die van betekenis zou kunnen zijn voor de behandeling van kleine niertumoren is fotodynamische therapie (PDT). Bij PDT wordt een stof toegediend aan de patiënt waardoor cellen gevoelig worden voor licht van een bepaalde golflengte. Zodra een tumorgebied lokaal met dit licht wordt beschenen sterven de tumorcellen. Met het licht wordt zowel het tumorweefsel als de bloedvaten rondom de tumor

beschadigd. PDT wordt op dit moment toegepast in de behandeling van hoofd/hals tumoren en huidtumoren. In de toekomst zullen ook bepaalde gynaecologische en urologische tumoren hiermee worden behandeld. **Hoofdstuk 10** beschrijft de resultaten van de behandeling van kleine niertumoren met PDT in muizen met niertumoren. Muizen met een niertumor kregen de fotosensitizer meso-tetra-hydroxyphenyl-chlorin (mTHPC, Foscan[®]) toegediend. Op verschillende tijdspunten hierna werd de tumor beschenen met licht met een golflengte van 652nm. Hiernaast werden *in vitro* experimenten opgezet met humane RCC cellijnen en een endotheliale cellijn (bloedvaten bestaan grotendeels uit endotheel cellen), waarbij werd onderzocht hoe gevoelig deze niertumor cellen voor PDT waren. De resultaten lieten zien dat de tumoren adequaat werden behandeld door middel van deze techniek. De *in vitro* experimenten lieten zien dat vooral de endotheliale cellijn erg gevoelig was voor PDT, wat aangeeft dat het antitumor effect het meest effectief zal zijn op het moment dat mTHPC zich in het tumorweefsel, maar vooral in de cellen van de bloedvaten bevindt.

mTHPC-gemedieerde PDT lijkt hiermee een mogelijke effectieve minimaal invasieve behandeling voor kleine niertumoren.

Dankwoord

In januari 2008 begon ik aan dit project, nu is het af! Dit proefschrift was nooit tot stand gekomen zonder de hulp van velen.

Allereerst wil ik mijn promotor, Prof. dr. J.L.H.R. Bosch bedanken. Beste Ruud, dank je wel voor het aanbieden van deze promotieplek. Translationeel onderzoek, muizen opereren, het was helemaal nieuw en anders voor ons allemaal. Ik vind het fijn dat je mij de tijd en het vertrouwen hebt gegeven dit project tot een goed einde te brengen. Ik waardeer je brede kennis op het gebied van de urologie, en de manier waarop je deze kennis altijd aan elkaar probeert te linken in onze discussies en brainstorm sessies. Na deze wetenschappelijke jaren kijk ik uit naar onze samenwerking in de kliniek.

Mijn co-promotor, Dr. J.J.M. Jans. Beste Judith, samen een urologisch translationeel lab opzetten, wat een avontuur! Vier jaar geleden begonnen we aan deze lastige taak. In deze tijd heb ik enorm veel van je geleerd door het delen van je kennis en het opzetten en afronden van de studies in dit proefschrift. Dank je wel voor de ruimte die je me gaf om me wetenschappelijk te ontplooien. Je nuchtere kijk op zaken, scherpzinnige feedback op mijn artikelen, vastberadenheid en efficiëntie hielden me goed bij de les. Ik waardeer de manier waarop je naast onze research ook het algemene welzijn in de gaten hield, de gezellige KGB-tjes in Gutenberg waardeer ik zeer. Ik ben trots op wat we in deze jaren hebben weten te bereiken!

De leden van de leescommissie; Prof. dr. M.A.A.J. van den Bosch, Prof. dr. E. E. Voest, Prof. dr. M. van Vulpen, Prof. dr. P.J. van Diest, Prof. dr. R.J.A. van Moorselaar wil ik bedanken voor hun tijd en bereidheid mijn proefschrift te beoordelen. Mijn dank gaat tevens uit naar alle andere leden die zitting hebben willen nemen in de promotiecommissie. Hiernaast wil ik enkele leden van de leescommissie bedanken voor de hulp en begeleiding bij het tot stand doen komen van enige artikelen in het proefschrift. Beste Prof. dr. M.A.A.J. van de Bosch, Maurice, ik wil je bedanken voor de kritische blik en oplossend vermogen bij het schrijven van ons artikel. Je enorme ambitie en de manier van hoe je in korte tijd vele goede zaken hebt opgezet in het UMCU zijn voor mij een inspiratie. Prof.dr. E. E. Voest, beste Emile, dank je wel voor de zeer nuttige feedback en inbreng van alternatieve gezichtspunten tijdens de wekelijkse 'workdiscussions'. Buitengewoon hoe je altijd precies de zaken die van belang zijn uit een presentatie kan uitlichten, en een neus hebt voor 'hot topics'. Prof.dr. P.J. van Diest, beste Paul, tussen de cashewnootjes en colaflessen bij de microscoop zitten was altijd interessant. Bedankt dat je, hoe druk ook, altijd bereid was te

helpen bij het kwantificeren van de meest experimentele kleuringen. Je brede betrokkenheid bij zoveel verschillende projecten is bijzonder.

Veel dank aan het team urologie in het UMCU; Prof.dr. J.L.H.R. Bosch, drs. A. Boeken Kruger, dr. L. de Kort, drs. T. Lock, drs. P. Rosier en dr. E. Kok. Heel veel dank voor de getoonde interesse in mijn onderzoek in de afgelopen jaren en het in mij gestelde vertrouwen om te mogen beginnen met de opleiding urologie binnen cluster Utrecht.

Alle arts-assistenten en arts-onderzoekers urologie die de afgelopen jaren in het UMCU hebben gewerkt: Harm, Joep, Bob, Jacob, Mirjam, Katja, Evelien, Robert, Joanna, Maurits, Jeltje, Annelies, Jetske, Sander, Joost, Raoul, Sybren, Marique, Saskia, Ruben, Sven, Judith, Ruud, Richard, Michelle, Pauline, Boris, Ronald en Pieter. Dank jullie wel voor de gezelligheid, borrels in de Basket en de mooie tijd tijdens de congressen in o.a. Barcelona, Milaan, Stockholm, San Francisco en Washington DC. Harm van Melick, op weg naar de top in het St Antonius, dank je voor de fijne samenwerking en altijd interessante discussies. Ik hoop dat we in de toekomst nog veel studies zullen opzetten.

Mijn grote dank gaat uit naar het Laboratorium van Experimentele Oncologie van het UMCU. De Medema groep; René, Libor, Arne, Monica, Vincentius, Armando, Melinda, Belen, Aniek, Indra, Andre, Livio, Rob, Wytse, Jonne, Judith, Lenno, Claudio, Marvin en anderen. De Voest groep; Emile, Jeanine, Laura, Julia, Ilse, Martijn, Nicolle, Marco, Marlies, Kristy en Joost. De Lens groep; Susanne, Maike, Martijn, Silvie en Rutger. De Kranenburg groep; Onno, Inne, Jamila, Klaas, Danielle, Benjamin, Frederik, Ernst, Lutske, Menno, Maarten, Winan, Nikol en Andre. De Giles groep: Rachel, Sander, Ive en Ellen. En de Derksen groep; Patrick, Miranda, Ron en Eva. Verder dank aan Holger. Heel veel dank voor de ruimte die jullie schepten binnen het lab om ons onderzoek te kunnen ontplooien, en de eindeloos beschikbare kennis en bereidwilligheid te helpen. De ontspannen manier waarop er wordt samengewerkt, de goede sfeer en de talrijke vaak spontane borrels, ijsjes op het bordes en AIO-etentjes zijn goud waard. Bedankt voor de geweldige tijd, zonder jullie had dit proefschrift nooit tot stand kunnen komen.

Prof. dr. G.C. de Gast, beste Bert. Bedankt voor je enthousiasme en enorm goede input bij het opzetten van onze immunotherapie studie. Het was een genoegen met je samen te werken.

De afdeling klinische fysica van het UMCU wil ik bedanken voor de goede samenwerking. Matthijs Grimbergen, dank je voor je altijd positieve instelling en enthousiasme bij het

opzetten en uitvoeren van onze studie. John Klaessens, bedankt voor het altijd beschikbaar zijn voor studies met RFA.

De afdeling nucleaire geneeskunde van het UMCU; Wouter, Frank, Fred, Maarten, Remmert, en Matthijs, en anderen die aan het Holmium project hebben gewerkt; Peter Seevinck, Freek Beekman, Hugo de Jong, Peter Luijten, Jos Kosterink, Wim Hennink, wil ik bedanken voor de kritische blik ten aan zien van het manuscript, fijne samenwerking en goede werksfeer.

Dank aan het Gemeentelijk Dierenlaboratorium voor het beschikbaar stellen van ruimte voor onze experimenten en het verzorgen van de dieren. De pathologie-afdeling in het UMCU wil ik bedanken voor de mogelijkheid in het diagnostisch laboratorium kleuringen te kunnen doen. Petra van der Groep wil ik bedanken voor de extreem goede kennis en hulp op het gebied van succesvolle immunohistochemie. Trudy Jonges, dank voor je geduld bij de beoordeling van de RFA behandelde niertumoren, nog maar 1 patiënt voor inclusie te gaan! Graag wil ik ook de muizenbiobank: Annette, Jan-Willem, Jan, Natalie en Martijn, bedanken voor de hoogstaande kwaliteit en de flexibiliteit als er weer eens last-minute >100 coupes gesneden moesten worden.

Lieve kamergenoten: Jeanine, Laura, Ilse en Julia, ik heb met jullie een mooie tijd gehad in ons altijd te warme dan wel te koude, lawaaierige (hoeveel kunnen ze verbouwen net boven je hoofd), muffige, rommelige kantoortje. Naast het harde werken was er genoeg ruimte voor gezelligheid, goede gesprekken, steun en bespreking van frustraties. Enorm bedankt voor deze waardevolle en leerzame tijd. We weten nog steeds niet wat promoveren nou precies inhoudt, maar…het vormt je!

Lieve paranimfen: Linda en Gisèle. In het begin van onze studententijd in Groningen leerden we elkaar kennen. Als club- en roeiploeggenootjes hebben wij veel samen meegemaakt en het nodige lief en leed gedeeld. Lin, als paranimf naast jou staan in december was bijzonder, ik hoop dat je deze keer minstens zo trots kan zijn! Gis, ik vind het erg leuk dat we ook collega's zijn, wat is urologie toch een mooi vak hè. Beiden bedankt voor alle gezelligheid, leuke uitjes/concerten/festivals en jullie altijd goede adviezen. Met jullie aan mijn zijde zal ik vandaag zeker goed doorkomen!

Zonder steun van mijn lieve vrienden en familie was het mij zeker niet gelukt dit proefschrift te schrijven. Bedankt voor jullie steun en belangstelling, en niet te vergeten de benodigde afleiding! Dear Mike, thank you for showing me what's really important in life!

List of Publications

Intratumoral administration of holmium-166 acetylacetonate microspheres in renal cell carcinoma bearing mice: a novel minimally invasive treatment option. **SGC Kroeze***, W Bult*, M Elschot, PR Seevinck, FJ Beekman, HWAM de Jong, PR Luijten, WE Hennink, AD van het Schip, JLHR Bosch, JFW Nijsen, JJM Jans. (*Authors contributed equally) *PLoS ONE, under review*

Incomplete cryo- of radiofrequente ablatie stimuleert de groei van achterblijvende renale tumorcellen: studie in een muismodel. **SGC Kroeze**, HHE van Melick, MW Nijkamp, F Kruse, LWJ Kruijssen, PJ van Diest, JLHR Bosch, JJM Jans. *TSVU, under review*

Radiofrequente ablatie gecombineerd met Interleukine-2 induceert een antitumor respons tegen het niercelcarcinoom. **SGC Kroeze**, LGM Daenen, MW Nijkamp, JML Roodhart, GC de Gast, JLHR Bosch, JJM Jans. *TSVU, under review*

De follow-up na chirurgische behandeling van het gelokaliseerde niercelcarcinoom: een vragenlijst onder Nederlandse urologen. TJ van Oostenbrugge, **SGC Kroeze**, JLHR Bosch, HHE van Melick. *TSVU, under review*

Incomplete thermal ablation stimulates proliferation of renal carcinoma cells in a murine model. **SGC Kroeze**, HHE van Melick, MW Nijkamp, F. Kruse, LWJ Kruijssen, PJ van Diest, JLHR Bosch, JJM Jans. *BJU Int, pending revisions*

De impact van comorbiditeit op complicaties na tumornefrectomie. PML Hennus, **SGC Kroeze**, JLHR Bosch, JJM Jans. *TSVU, in press*

Examining the "gold standard": A comparative critical analysis of three consecutive decades of monopolar TURP outcomes. **SGC Kroeze***, EK Mayer*, S Chopra, A Bottle, A Patel (*Authors contributed equally) *BJU Int, in press*

Radiofrequency ablation combined with Interleukin-2 induces an anti-tumor immune response to renal cell carcinoma in a murine model. **SGC Kroeze**, LGM Daenen, MW Nijkamp, JML Roodhart, GC de Gast, JLHR Bosch, JJM Jans. *J Urol, in press*

Photodynamic therapy as novel nephron-sparing treatment option for small renal masses. **SGC Kroeze**, MCM Grimbergen, H Rehmann, JLHR Bosch, JJM Jans. *J Urol 2012;187(1):289-95*

The impact of comorbidity on complications following nephrectomy: use of the Clavien Classification of Surgical Complications. **SGC Kroeze***, PML Hennus*, JLHR Bosch, JJM Jans. (*Authors contributed equally). *BJU Int, in press*

Real-time 3D fluoroscopy guided large core needle biopsy of renal masses: a critical early evaluation according to the IDEAL recommendations. **SGC Kroeze**, M Huisman, HM Verkooijen, PJ van Diest, JLHR Bosch, MAAJ van den Bosch. *Cardiovasc Intervent Radiol, Epub. ahead of print Aug 6, 2011*

Diagnostic and prognostic tissuemarkers in clear cell and papillary renal cell carcinoma. **SGC Kroeze***, AM Bijenhof*, JLHR Bosch, JJM Jans. (*Authors contributed equally). *Cancer Biomark 2010;7(6):261-8.*

Expression of nuclear FIH independently predicts overall survival of clear cell renal cell carcinoma patients. **SGC Kroeze**, JS Vermaat, A van Brussel, HHE van Melick, EE Voest, TG Jonges, PJ van Diest, J Hinrichs, JLHR Bosch, JJM Jans. *Eur J Cancer 2010;46(18):3375-82*

Weefselmarkers voor prognose bepaling bij patiënten met niercelcarcinoom. **SGC Kroeze**, JLHR Bosch, JJM Jans. *TSVU 2010:5;122-128*

Assessment of Laparoscopic Suturing Skills of Urology Residents: a Pan European Study. **SGC Kroeze**, EK Mayer, S Chopra, R Aggarwal, A Darzi, A Patel. *Eur Urol 2009;56(5):865-73*

Resident's laparoscopic training exposure still limited. **SGC Kroeze**, EK Mayer, R Aggarwal, A Patel. *Eur Urol Today 2008;20(2):37*

Curriculum vitae

Stephanie Kroeze was born on the 20th of May 1983 in Emmen, the Netherlands. After graduating at the Esdal College in Emmen in 2001 she studied Medicine at the University of Groningen from 2001 to 2007. She first expressed interest in research in 2005 by joining the Gips International School of Hepatology and Tropical Medicine (GISH-T) under supervision of Prof.dr. C.H. Gips. That year she performed a research project at the Department of Malaria Biology at the Queensland Institute of Medical Research in Brisbane, Australia (Dr. D.L. Gardiner). During her internship at the Deventer Hospital she developed an enthusiasm for urology; therefore, she joined the Department of Urology at the St. Lucas Andreas Hospital, Amsterdam, the Netherlands (Dr. E.A. Heldeweg) for her final clinical elective. After obtaining her medical degree in 2007 she worked as an Honorary Doctor at the Department of Urology at St. Mary's Hospital, London, UK (Dr. A. Patel), following which she was able to complete a PhD programme at the Department of Urology at the University Medical Center Utrecht, the Netherlands (Prof.dr. J.L.H.R. Bosch). During her time as a PhD student she presented her work at several international medical congresses for which she received two prices for best poster presentations. In January 2012 she started her residency program in urology at the Department of general surgery at the St. Antonius Hospital in Nieuwegein, the Netherlands under supervision of Dr. P.M.N.Y.H. Go.